HELSINGIN YLIOPISTO
HELSINGFORS UNIVERSITET
UNIVERSITY OF HELSINKI

# GEOCHEMICAL STUDY OF THE KUMPULA CAMPUS DRILL CORE AND OUTCROPS: APPLYING A PORTABLE XRF DEVICE FOR WHOLE ROCK ANALYSIS

Milja Räisänen
May 2018
Master's Thesis
Department of Geosciences and Geography
Division of Geology
University of Helsinki

HELSINGIN YLIOPISTO
HELSINGFORS UNIVERSITET
UNIVERSITY OF HELSINKI

| Tiedekunta/Osasto Fakultet/Sektion – Faculty<br>Faculty of Science | Laitos/Institution– Department<br>Department of Geosciences and Geography |
|---|---|

Tekijä/Författare – Author
Milja Räisänen

Työn nimi / Arbetets titel – Title
Geochemical study of the Kumpula Campus drill core and outcrops: Applying a portable XRF device for whole rock analysis

Oppiaine /Läroämne – Subject
Geology

| Työn laji/Arbetets art – Level<br>Master's Thesis | Aika/Datum – Month and year<br>May/2018 | Sivumäärä/ Sidoantal – Number of pages<br>54+22 |
|---|---|---|


Tiivistelmä/Referat – Abstract

As a part of Kumpula Campus Drill Hole Project, a 370 m deep drill hole was drilled on the University of Helsinki, Kumpula campus area in December 2015. Drilling took place on an amphibolitic outcrop, which is the main rock type of the area and part of the 1.9 Ga old Svecofennian orogenic belt.

In this work, the geochemistry of the campus bedrock is analyzed, focusing on the amphibolite. Granite, actinolite rock and diopside-actinolite skarn are additional rock types described from the core in this work. The geochemical methods utilized are a portable X-ray fluorescence (P-XRF) spectrometer Niton XL3t GOLDD+ by Thermo Scientific and a laboratory wavelength dispersive X-ray fluorescence (WD-XRF) spectrometer PANAlytical Axios mAX 4kW. WD-XRF device is utilized in quantitative analysis and semi-quantitative Omnian scans. In addition to geochemical interpretation of the bedrock, feasibility of the P-XRF device in outcrop and drill core related studies is evaluated by comparing the methods.

The surface of the drill core was analyzed with the P-XRF device. Representative samples of each rock type were sawed of the core and analyzed with both P-XRF and WD-XRF Omnian scans. In addition to surface analyses, a fused bead was prepared from one representative amphibolite sample and analyzed with WD-XRF quantitative method. Outcrop studies focused on the feasibility of the P-XRF device in *in situ* analyses.

Compared to nearest temporally related amphibolite units, the amphibolite of the campus bedrock seems to be more felsic on average. All described rock types are connected to former petrogenetic interpretations of the local bedrock. However, further geochemical analyses are required to verify the interpretations. WD-XRF quantitative method and Omnian scans suggest almost similar results for fused bead of the amphibolite. Changing the sample type to solid rock surface introduces heterogeneity related problems to the quantitative determination of Omnian scans and quality of the results decreases almost to the level of P-XRF. Yet, the advantage of the Omnian scans method in rock surface analyses compared to P-XRF is better detection of light elements. For example, P-XRF device detects Mg, Al and K poorly and Na is not detected at all. On the other hand, $SiO_2$ is on average detected quite accurately from rock surface with P-XRF when compared to WD-XRF quantitative method for fused bead. WD-XRF Omnian scans and quantitative application results of fused bead do not seem to differ remarkably. Broad rock type classification can be made with P-XRF device for drill core, but results cannot be considered quantitative. It should also be noticed, that the major element oxide sum values of P-XRF drill core surface analyses are quite low on average (84.00 wt.%). In outcrop analyses, different features lower the quality of the rock surfaces, resulting in even lower major element oxide sum values in analysis. Although major oxide sum values are very low on outcrops, relatively high amounts of for example Cl, S and P are detected for unknown reasons.

Major advantages of the P-XRF device are the ease of use, light weight and rather good detection of for example $SiO_2$. Developing the quantitativeness of the device would make it more comparable to laboratory XRF devices but it already has multiple features that are highly beneficial in a wide range of scientific fields.



Avainsanat – Nyckelord – Keywords
Portable XRF, Helsinki, geochemistry, Kumpula campus, Svecofennian, amphibolite

Säilytyspaikka – Förvaringställe – Where deposited
University of Helsinki


Muita tietoja – Övriga uppgifter – Additional information

HELSINGIN YLIOPISTO
HELSINGFORS UNIVERSITET
UNIVERSITY OF HELSINKI

| Tiedekunta/Osasto Fakultet/Sektion – Faculty<br>Matemaattis-luonnontieteellinen tiedekunta | Laitos/Institution– Department<br>Geotieteiden ja maantieteen laitos | |
|---|---|---|
| Tekijä/Författare – Author<br>Milja Räisänen | | |
| Työn nimi / Arbetets titel – Title<br>Kumpulan kampuksen kairasydämen ja paljastumien geokemiallinen tutkimus: kannettavan XRF-laitteen käyttö kokokivianalytiikassa | | |
| Oppiaine /Läroämne – Subject<br>Geologia | | |
| Työn laji/Arbetets art – Level<br>Pro Gradu | Aika/Datum – Month and year<br>Toukokuu/2018 | Sivumäärä/ Sidoantal – Number of pages<br>54+22 |


Tiivistelmä/Referat – Abstract

Osana Helsingin yliopiston Kampusreikä projektia, vuonna 2015 Kumpulan kampuksen kallioperään porattiin 370 m syvä kairareikä opetustarkoitukseen. Kampuksen kallioperän pääkivilaji on paleoproterotsooinen, n. 1.9 Ga vanha amfiboliitti. Tässä työssä amfiboliitin geokemiaa selvitetään Thermo Scientificin Niton XL3t GOLDD+ kannettavan röntgenfluoresenssi laitteen (P-XRF), sekä laboratoriokäyttöisen aallonpituusdispersiivisen röntgenfluoresenssilaitteen (WD-XRF) avulla. WD-XRF-analysaattorista hyödynnetään kvantitatiivista metodia sekä semi-kvantitatiivista Omnian menetelmää. Geokemian ohella P-XRF-laitteen käyttöä arvioidaan XRF menetelmiä vertaillen. Amfiboliitin lisäksi kairasydämestä kuvailtiin graniitti, aktinoliitti kivi ja diopsidi-aktinoliitti karsi.

Kampusreiästä saadun kairasydämen pintaa analysoitiin P-XRF-laitteella. Lisäksi siitä sahattiin edustavat näytteet jokaisesta kuvaillusta kivilajista ja näytteiden pinnat analysoitiin sekä P-XRF, että WD-XRF Omnian-metodeilla. Yhdestä edustavasta amfiboliittinäytteestä analysoitiin pinta P-XRF-laitteella sekä WD-XRF Omnian-menetelmällä. ja lisäksi siitä valmistettiin fluksinappi, joka analysoitiin sekä WD-XRF Omnian-menetelmällä, että kvantitatiivisella WD-XRF-menetelmällä. Paljastuma-analyysien avulla tutkittiin lähinnä *in situ* P-XRF-mittausten onnistumista vallitsevissa olosuhteissa.

Amfiboliitti on tulostensa perusteella felsisempi kuin läheiset saman ikäiset amfiboliittiyksiköt. Kaikkien kivilajien tarkempi kuvailu vaatii kuitenkin lisää geokemiallisia analyysejä. Eri XRF-menetelmien tuloksia vertailtaessa todetaan näytetyypin valinnalla olevan huomattava vaikutus tuloksiin. Sahattujen näytteiden pinta-analyyseissä WD-XRF Omnian-menetelmän etuna on parempi kevyiden alkuaineiden (Mg, K ja Al) rekisteröityminen verrattuna P-XRF-menetelmään. Natriumia P-XRF-laite ei rekisteröi ollenkaan. P-XRF-menetelmä kiven pinnasta antaa keskimäärin melko oikean pitoisuuden $SiO_2$:lle, kun verrataan kvantitatiivisen analyysin tulokseen fluksinapista. WD-XRF Omnian-menetelmän ja WD-XRF kvantitatiivisen menetelmän tuloksilla ei ole juurikaan eroa fluksinappianalyyseissä. Karkeita kivilajivaihteluita pystytään havaitsemaan P-XRF-laitteella kairasydämestä, eikä WD-XRF Omnian-menetelmä välttämättä tuo tämän tyyppiseen tutkimukseen lisäarvoa. P-XRF-menetelmää ei kuitenkaan voi pitää kvantitatiivisena. Huomioitava seikka on myös se, että P-XRF-menetelmän pääalkuaineoksidien summat jäävät alhaisiksi kairasydämen pinnan analyyseissä (k.a. 84.00 p.%). Paljastumilla arvo putoaa entisestään, ja pintojen huono laatu osoittautuu suurimmaksi ongelmaksi. Vaikka pääalkuaineoksidien summa on hyvin alhainen, niin esimerkiksi Cl, S ja P esiintyvät suhteellisen korkeina pitoisuuksina paljastumilla, toistaiseksi tuntemattomista syistä.

P-XRF menetelmän eduiksi voidaan todeta erityisesti sen helppokäyttöisyys, liikuteltavuus ja esimerkiksi $SiO_2$ pitoisuuden melko todenmukainen rekisteröityminen. Laitteen kvantitatiivisuuden kehittäminen nostaisi sen kilpailukykyä tarkkojen laboratoriolaitteiden rinnalla, mutta tähän asti saavutetuista ominaisuuksista on jo nyt paljon hyötyä esimerkiksi kairasydäntutkimuksissa.



Avainsanat – Nyckelord – Keywords
Helsinki, geokemia, amfiboliitti, XRF, Kumpula, svekofenninen orogenia

Säilytyspaikka – Förvaringställe – Where deposited
Helsingin yliopisto

Muita tietoja – Övriga uppgifter – Additional information

## CONTENTS


1. INTRODUCTION ..... 5
   1.1 Kumpula Campus Drill Hole Project ..... 5
   1.2 Geological setting ..... 7
   1.3 Aim of the study ..... 8
2. METHODS ..... 9
   2.1 WD-XRF ..... 9
      *2.1.1 Quantitative application* ..... *9*
      *2.1.2 Omnian scans* ..... *10*
   2.2 P-XRF ..... 10
3. MATERIALS AND SAMPLE PREPARATION ..... 11
   3.1 Drill core ..... 11
      *3.1.1 P-XRF core surface analyses* ..... *13*
      *3.1.2 Sawed pieces* ..... *13*
      *3.1.3 Fused bead* ..... *14*
   3.2 Outcrops ..... 15
4. PETROGRAPHY ..... 16
   4.1 Amphibolite ..... 17
   4.2 Granite ..... 18
   4.3 Actinolite rock ..... 19
   4.4 Diopside-actinolite skarn ..... 20
6. RESULTS ..... 21
   6.1 Whole rock geochemistry of the rock types ..... 22
   6.2 Comparison of the XRF methods ..... 26
      *6.2.1 Amphibolite sample A1* ..... *26*
      *6.2.2 Sawed amphibolite pieces: P-XRF and Omnian scans comparison* ..... *29*
   6.3 Whole drill core analysis with the P-XRF device ..... 32
   6.4 Outcrops: effects of surface quality and field circumstances ..... 36
7. DISCUSSION ..... 39
   7.1 Error and contamination sources of the analyses ..... 39
      *7.1.1 Sample preparation* ..... *39*
      *7.1.2 Analysis* ..... *40*
      *7.1.3 Outcrop notes* ..... *41*
   7.2 Feasibility of the introduced methods in field and drill core analyses ..... 41
   7.3 Improvements and possible future studies regarding the P-XRF ..... 44
   7.4 Drill core geochemistry: Omnian scans and P-XRF analyses ..... 45
   7.5 Considerations of petrology and a comparison to local geology ..... 46
      *7.5.1 Amphibolite* ..... *47*
      *7.5.2 Other rock types* ..... *49*

8. CONCLUSIONS ..... 50
8. ACKNOWLEDGEMENTS ..... 51
9. REFERENCES ..... 52
APPENDIX I: Sawed surface P-XRF data of the amphibolite sample A1 ..... 55
APPENDIX II: Curved surface P-XRF data of the amphibolite sample A1 ..... 55
APPENDIX III: WD-XRF Omnian scans data of the drill core samples ..... 56
APPENDIX IV: P-XRF data of the drill core samples ..... 57
APPENDIX V: P-XRF data of the whole drill core analyses ..... 58
APPENDIX VI: P-XRF data of the outcrop analyses ..... 68
APPENDIX VII: Geochemical data of the temporally related amphibolite units ..... 76

# 1. INTRODUCTION

## 1.1 Kumpula Campus Drill Hole Project

In 2015, an opportunity to take a closer look of the Kumpula campus bedrock (Fig. 1) occurred, when the Kumpula Campus Drill Hole Project started. The Project aims to produce scientific data of the bedrock and serve as an environment for pre-graduate drill hole and core related education in geosciences in the Kumpula campus (Kukkonen et al. 2016). The drilling contractor Suomen Malmi Oy operated the diamond core drilling in December 2015, on an outcrop south of Dynamicum building (Fig. 1.C). The drill hole is 370 meters long and dips towards northeast with a dip of 70 degrees (Kukkonen et al. 2016). The diameter of the core is 56 mm and that of the drill hole 76 mm.

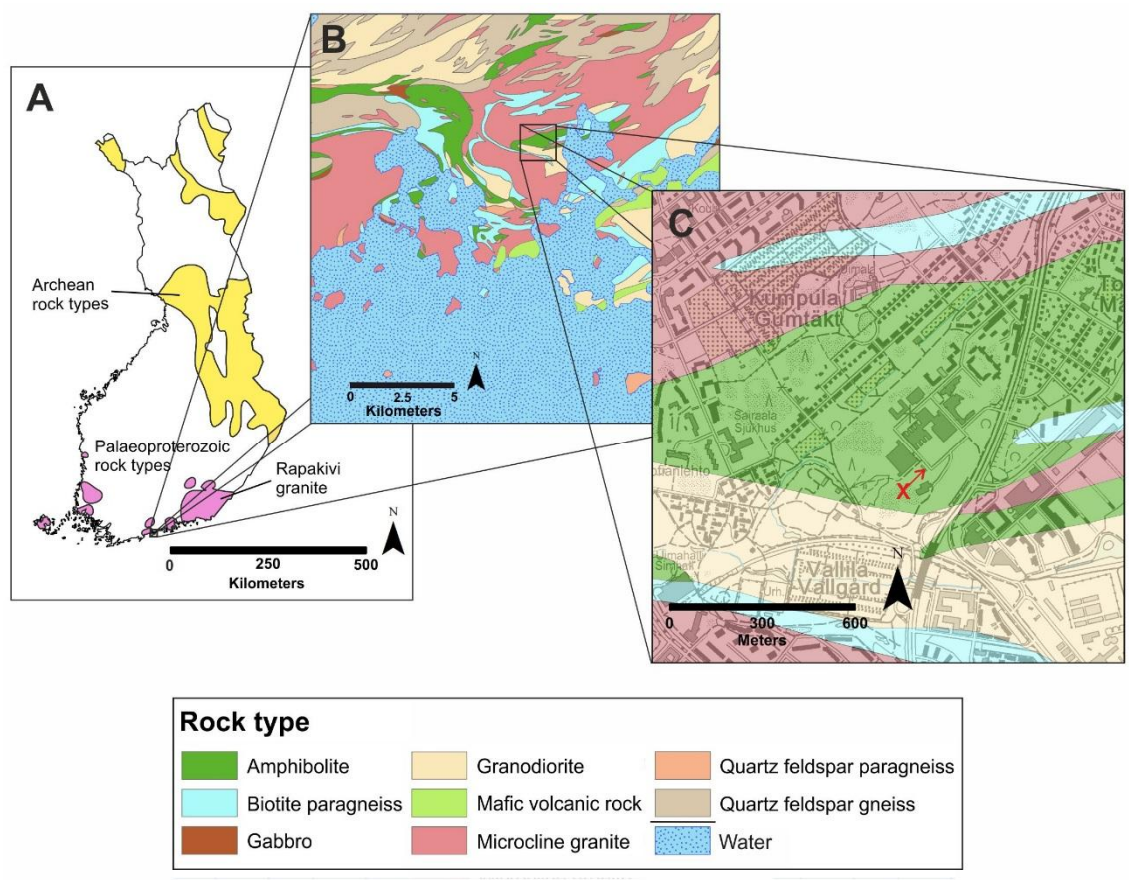


Figure 1.A: Location of Helsinki and major bedrock units of Finland (after Korsman and Koistinen 1998). B: Versatile bedrock of the Helsinki coast. C: Kumpula campus area bedrock. Dark gray campus buildings can be seen in the center of the map. Red X and arrow mark the drilling site and surface projection. B and C bedrock maps modified after Geological survey of Finland, abbr. GTK. Basemap of Finland in A and B © National land survey of Finland, abbr. NLS. City map of Helsinki in C © NLS.

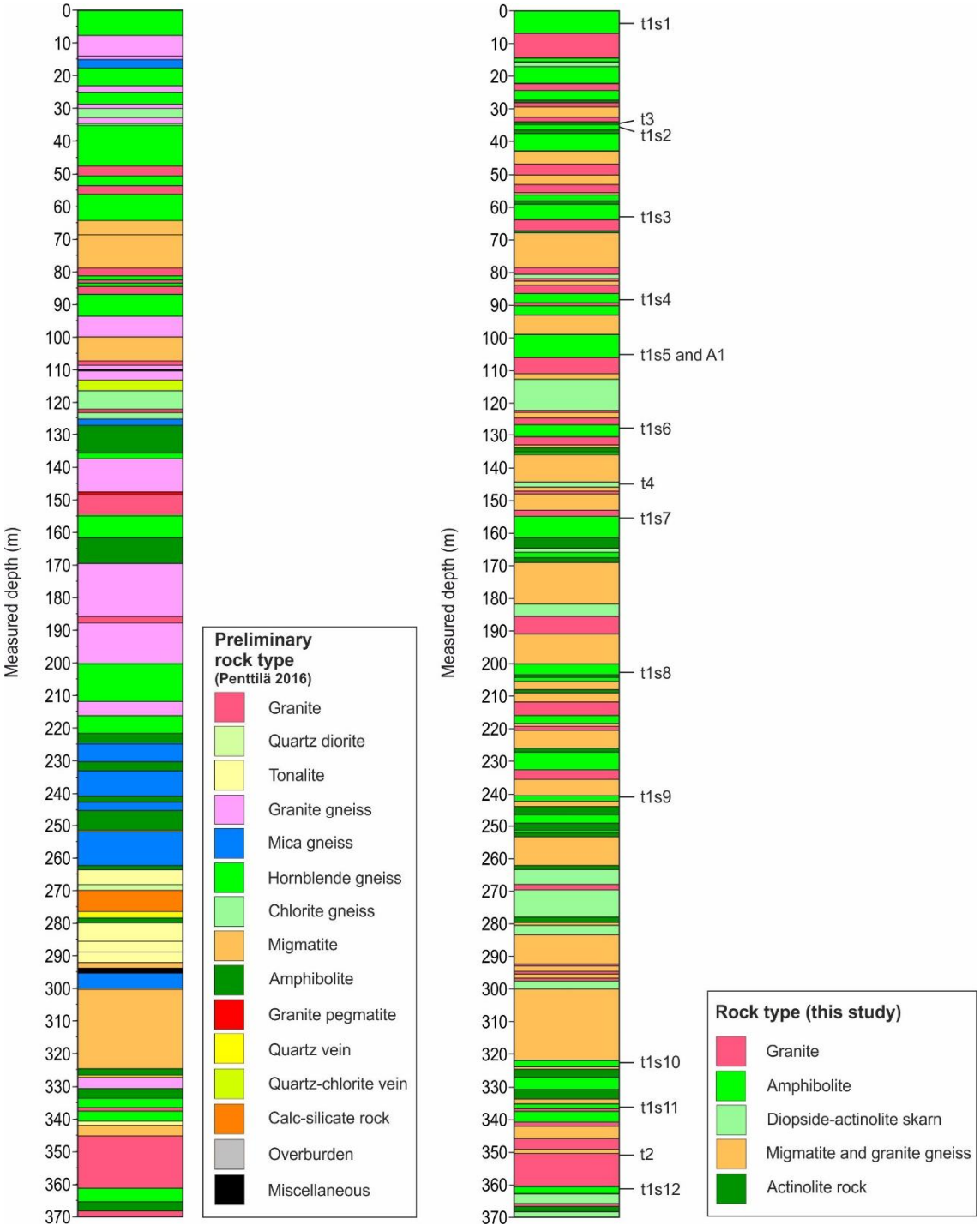


Figure 2. Preliminary rock type classification of the drill core according to Penttilä (2016) and a simplified classification used in this work. Depths of WD-XRF analysis spots are marked next to the core. WD-XRF Omnian scans IDs: Amphibolite t1s1–t1s12, granite t2, actinolite rock t3 and diopside-actinolite skarn t4. WD-XRF quantitative application analysis of the amphibolite marked as A1.

Preliminary master's thesis studies in geology utilized the drill core and hole in fracture mapping and 3D-modeling (Valtonen in prep.), petrology (Penttilä in prep.) and

geochemistry. Figure 2 shows the preliminary division of the drill core rock types (Penttilä 2016) and a simplified classification used in this work.

In addition to drill core, an extensive set of wireline geophysical logs ran by GRM-Services Oy are available to support geological studies. The geophysical parameters include optical imaging, acoustic imaging, rock resistivity (several methods), self-potential, IP effect, magnetic susceptibility, gamma ray spectroscopy (U, Th and K), total gamma, gamma-gamma density, fluid temperature and fluid electrical conductivity (salinity) (Kivinen 2016).

### 1.2 Geological setting

Kumpula campus, University of Helsinki is situated in southern Finland (Fig. 1.A). The bedrock of Helsinki and the whole southern and western Finland are composed of the roots of a mountain range belonging to Palaeoproterozoic Svecofennian orogenic belt, which had its peak point of orogeny at about 1.9 Ga (Laitala 1991).

The orogeny was a result of an active Svecofennian island arc system obliquely colliding against the Archaean continent. Because of the complexity of the collision, Pajunen et al. (2008) have divided it to multiple geotectonic events, deformation phases and related rock series. Simplifying, the evolution of the Svecofennian orogeny 1.90–1.87 Ga consists of a N–S trending compression and a southward migrating, local extension (Pajunen et al. 2008).

The extension events caused strong vertical shortening and prograde high-T/low-P metamorphosis resulting in some of the originally sedimentary and volcanic rocks metamorphosing to mica-bearing gneisses, hornblende gneisses and amphibolites. Plutonic rocks of Svecofennian age usually conform to the structures of volcanic rocks. The late-orogenic granites intruded the pre-existing bedrock and are usually mixed with other rock types thus forming gneisses, migmatites and breccias (Laitala 1991, Nironen 1998, Pajunen et al. 2008).

The Kumpula campus buildings are situated on a Proterozoic amphibolite unit with a minor part of the outcrop south of the buildings belonging to a granodiorite unit (Fig. 1.B and 1.C).

### 1.3 Aim of the study

During the previous decades, the increasing interest towards the portable X-ray fluorescence (P-XRF) spectrometer has resulted in fast technological development. The non-destructiveness and fastness of the analyses are advantageous properties in a wide variety of scientific fields. P-XRF devices have already been tested and utilized in e.g. detecting metals in pre-concentrated aqueous samples (Marguí et al. 2012), detecting hazardous substances in soils (Markey et al. 2008, Parsons et al. 2013, Hatakka et al. 2016), mineral exploration (Sarala et al. 2014), chemostratigraphy (Rowe et al. 2012), archaeology (Liritzis and Zacharias 2011), industrial quality control (Shrivastava et al. 2005), and in the future will also be utilized in planetary surface explorations (Young et al. 2016).

As the Niton XL3t GOLDD+ P-XRF spectrometer by Thermo Scientific is a quite new (2015) purchase in the Department of Geosciences and Geography, major part of this work aims to evaluate the feasibility of the P-XRF device in *in situ* outcrop studies and drill core related studies. With the help of drill core and outcrop data, the geochemical characteristics of especially the amphibolite of the campus bedrock are examined. In the process the P-XRF method is compared to laboratory wavelength dispersive X-ray fluorescence (WD-XRF) spectrometer PANAlytical Axios mAX 4kW.

Thus, the geochemical data obtained with different XRF methods serve, not only as a window to the geochemical composition of the bedrock, but as a ground for P-XRF – WD-XRF comparisons. Major element oxide results were selected as the most reliable data for identifying the differences between the XRF methods. Together with fracture information (Valtonen in prep.) and an extensive petrology interpretation (Penttilä in prep.) the ongoing master's thesis projects form a comprehensive survey of the Kumpula campus bedrock.

## 2. METHODS

The X-ray fluorescence spectroscopy is based on non-destructive exciting and detecting of characteristic secondary X-rays (*fluorescence*) of different elements in a sample (Norrish and Chappell 1967). By detecting the fluorescence intensities, it is possible to identify the elements and evaluate their proportions. Fluorescence is excited by radiating the sample with high intensity X-rays (Norrish and Chappell 1967, Potts and Webb 1992). Main differences of the two methods used in this work are related to fluorescence detection and are described in the following chapters.

Both spectrometers belong to the Department of Geosciences and Geography, University of Helsinki. In addition to XRF analyses, a brief petrography work was done for each described rock type to get a better picture of the mineral compositions.

### 2.1 WD-XRF

WD-XRF devices are wavelength dispersive, which means that the emitted sample fluorescence is directed to the detector via a synthetic analyzing crystal, which disperses the fluorescence spectrum (Norrish and Chappell 1967). Adjusting the angle between crystal and detector, multiple wavelengths can be detected, individually. Collimators are placed between the X-ray tube and the sample and between the sample and the detector to direct the primary X-rays and fluorescence (Marguí 2013). The diffraction and collimation weakens the fluorescence intensity and analysis is also much slower than with P-XRF device, but resolution remains high (Marguí 2013). High resolution allows lower detection limits and thus better identification of trace elements than with P-XRF device (e.g. Potts and Webb 1992). WD-XRF analyzer used in this work is PANAlytical Axios mAX 4kW.

#### *2.1.1 Quantitative application*

The quantitative WD-XRF application was utilized for one fused bead analysis. The quantitative calibration uses international certified reference samples of 19 different natural compositions for detecting the elements (Heikkilä 2015) and has also a fixed

fundamental parameters (FP) model that corrects matrix effects calculated for on an average granodioritic composition (Pasi Heikkilä, pers.comm. 2018). FP model considers fluorescence of all orders, physical constants and multiple instrumental features (Marguí 2013).

### *2.1.2 Omnian scans*

Along with quantitative application, PANalytical's semi-quantitative method called Omnian was utilized for all sawed rock surface analyses and for the fused bead analysis. The standardless Omnian scans method is calibrated using matrix independent setup samples (PANalytical 2018). Elements from O to U can be detected using multiple analyzing crystals. The quantification uses a software that has advanced FP model algorithms compared to quantitative application (PANalytical 2018). The model has variable features that are calculated individually for each setup sample and unknown sample (Pasi Heikkilä, pers.comm. 2018). Background profile fitting and peak search is based on theoretical peak database (Heikkilä 2015). In the end, the software converts elemental peak intensities to elemental concentrations and thus theoretical composition is obtained. Omnian method also allows the user to correct the kV-kcps spectrums received from the analysis, if necessary.

## 2.2 P-XRF

Portable XRF devices exploit energy dispersion (ED) directly by simultaneously detecting all wavelengths of the fluorescence (e.g. Kramar 1997). Comparing to collimated fluorescence obtained with WD-XRF, ED-XRF detector views a wider range of polychromatic fluorescence (Potts and Webb 1992). The resolution especially in the lower energies of the spectrum is poor (Potts and Webb 1992), and the method is thus at best semi-quantitative for most elements. However, simpler instrument with less delicate parts compared to WD-XRF makes fast qualitative (elemental range from Mg to U) and semi-quantitative analyses possible with a miniaturized apparatus (Marguí 2013). Depending on the sample type to be analyzed, there are multiple different kinds of P-XRF devices optimized for different purposes. Different softwares also expand the use of the device as new calibrations are added.

The portable XRF device used in this work is Niton XL3t GOLDD+ (50kV) by Thermo Scientific with a round analysis window diameter of 8mm. In all the analyses the analysis mode was set to “Mining Cu/Zn” and the analysis time was fixed to 100 seconds to optimize the detection time required for different elements. The device was held in hand during all analyses.

## 3. MATERIALS AND SAMPLE PREPARATION

### 3.1 Drill core

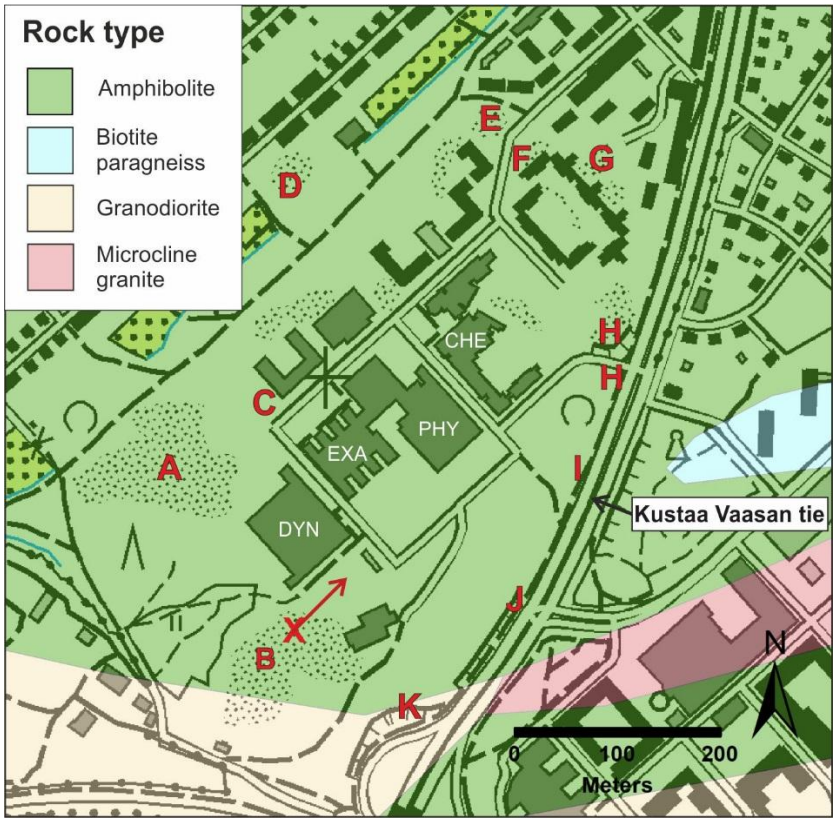


Figure 3. Locations of the selected outcrops in relation to Kumpula campus buildings. The selected outcrops are named with letters A–K. Red X and arrow mark the drilling site and surface projection of N-E trending drill hole. Abbreviations: DYN=Dynamicum, EXA=Exactum, PHY=Physicum and CHE= Chemicum. Bedrock map after GTK and basemap © NLS.

The drilling took place in the Kumpula campus area, on an amphibolite outcrop (Outcrop B, Fig. 3) south of Dynamicum building. The complete set of 82 boxes containing the 370 meter long drill core is stored in the basement of Physicum building.

All referenced depths regarding the drill core in this work are measured depths along the core and not precise vertical depths.

Before geochemical analyses, the core was visually examined to preliminarily define different rock types and other features like fractures. There were two major fracture zones in depths 108.80–110.20 m and 294.40–295.20 m. Other than that, the core is rated excellent in rock quality designation (RQD) (Valtonen in prep.).

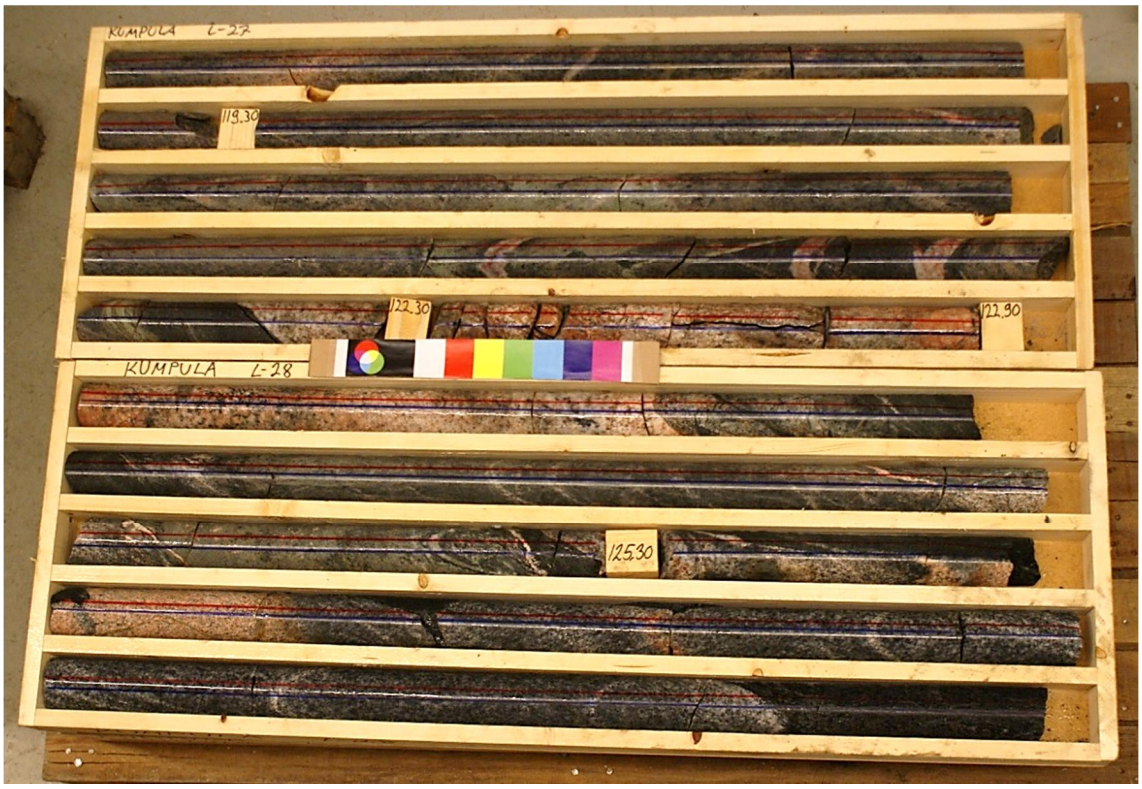


Figure 4. An example of the drill core from depth ~118–127 m. Wet drill core shows high variation in rock type. The core in this figure has for example skarn, granitic veins, granitic gneiss, amphibolite and actinolite rock.

Four different main rock types were determined by simplified visual estimations: amphibolite, granite, actinolite rock and diopside-actinolite skarn (Fig. 4). Details of these rock types are presented in Chapter 4. Closer description of the core is presented in petrology studies by Penttilä (in prep.). Despite the relatively high amount of variation in rock type (Fig. 2 and Fig. 4), amphibolite was chosen to be in the center of attention in the present study. The relatively small grainsize of the amphibolite was considered to increase the suitability for direct XRF analyses and therefore most of the analyses are focused on it (Table 1).

In addition to the four rock types described above, large part of the core is migmatite and gneiss of various compositions. Their wider examination was not considered meaningful for this work, however.

Table 1. Total number of core analyses with each method of each rock type.

| | Amphibolite | Granite | Actinolite rock | Diopside-actinolite skarn |
|---|---|---|---|---|
| **Core surface, whole length** | | | | |
| P-XRF | 38 | 46 | 27 | 29 |
| **Sawed core pieces** | | | | |
| Rock surface: | | | | |
| P-XRF | 12 | 1 | 1 | 1 |
| WD-XRF Omnian scans | 12 | 1 | 1 | 1 |
| **Amphibolite sample A1** | | | | |
| Rock surface: | | | | |
| P-XRF | 20 | | | |
| WD-XRF Omnian scans | 1 | | | |
| Fused bead: | | | | |
| WD-XRF quant.app. | 1 | | | |
| WD-XRF Omnian scans | 1 | | | |

### *3.1.1 P-XRF core surface analyses*

Every major rock type unit was analyzed with P-XRF at least once, depending on the thickness of the unit. Best way to perform the analyses turned out to be to place the analysis window tightly against the curved surface of the core. This way the distance between the apparatus and rock surface was minimized and escaping of the X-ray beam and fluorescence best avoided. The core was analyzed without removing it from the containers. Based on drill core results, variation in geochemistry and rock type with depth are later evaluated.

### *3.1.2 Sawed pieces*

To compare the P-XRF and WD-XRF methods, fiveteen representative, round pieces (each ~2 cm thick) were sawed out of the drill core: twelve amphibolites, one granite, one actinolite rock and one diopside-actinolite skarn. Sample pieces did not require additional preparations as the diameter of the core was already small enough to fit in the sample holder of the WD-XRF device. Sawed surfaces of the pieces were analyzed first

with P-XRF and then utilizing WD-XRF Omnian scans. Before WD-XRF analyses, sample pieces were cleansed with VWR Ultrasonic Cleaner that uses ultra sound. Pieces were placed in distilled water at room temperature for 20 minutes. In WD-XRF device, the power was set to 3kW and analysis surface to 27 mm in diameter. Sample type was selected as “Solid compounds”.

One extra piece of amphibolite (sample A1) from depth 105.35 m was sawed in half parallel to the core length and analyzed multiple times with the P-XRF device: ten times from the curved core surface and ten times from the straight sawed surface. This way the heterogeneity of the amphibolite sample and the effect of surface curvature were examined. The remaining half of the piece was melted into fused bead and analyzed with WD-XRF quantitative method and Omnian scans.

*3.1.3 Fused bead*

Sample preparation and WD-XRF studies were carried out at the Mineralogy laboratory of Kumpula campus, University of Helsinki. Preparing the fused bead started with crushing the sample with a jaw crusher (Suomen Teräsrakenne Oy MKH press, model CMT 100/150, 4kW). The previous rock type in the crusher had been granodiorite. After crushing, the sample pieces were heated in a Teflon cup at 105 °C for about 24 hours to remove volatiles. Then 30 g of representative fractions were picked and pulverized with Fritsch PULVERISETTE 6 ball mill. Sample fractions were pulverized in a tungsten carbide pan, with three tungsten bullets and few droplets of ethanol for 15 minutes, at around 350 rpm.

The process continued then with measuring 0.6 g of pulverized sample in a Au-Pt crucible. Then the flux was added: total of 6.0 g ± 0.001 g of $Li_2B_4O_7$ (49.75 %), $LiBO_2$ (49.75%) and LiBr (0.50%). After adding the fluxing agent, total weight of the sample was 6.6 g. The sample was then melted with Claisse M4 burner at 1000 °C for 1700 seconds and after that poured into Au-Pt mold to cool. Throughout the preparation of the fused bead the Mineralogy Laboratory Manual (Heikkilä 2015) instructions were followed.

### 3.2 Outcrops

The surroundings of the campus were explored by selecting a total of eleven representative outcrops around the campus during the summer of 2016. In the Figure 3 the selected outcrops are named with letters A–K. The most important factor, when deciding which outcrops were to be analyzed, was finding surfaces that qualify for the P-XRF analyses. The success of each analysis was evaluated directly with the help of major element oxides sum.

Features increasing the surface suitability were considered to be for example cleanness, small grain size, solidity and smoothness. The impact of these features on the results are further examined by comparing good quality and poor quality surfaces occurring next to each other. Poor quality surfaces were covered in lichen, moss or pollution and/or were weathered. Without further biological or chemical examination, poor quality surfaces were not classified by detail and were treated as one group.

According to the GTK bedrock map, the campus area is situated in an amphibolitic lithological unit with granite, biotite paragneiss and granodiorite units nearby. Field observations support the GTK interpretation. Major rock type was found to be amphibolite with grain size of ~2 mm in diameter, but varying even inside one outcrop. Usually mafic minerals were notably elongated. In addition to varying grain size, composition and color varied as well and thus deciding the name between granitic gneiss/hornblende gneiss/migmatite/amphibolite was not straightforward.

Pink granitic veins crossing amphibolite were coarse and of various thicknesses, thickest being ~1 m in diameter (found on Outcrop D, Fig. 3). Fine grained, mafic dike crossed part of outcrop H and was not found on any other outcrop.

The representativeness of different rock types in the outcrop analyses was completely dependent on the applicability of the P-XRF method. The purpose of the outcrop analyses was to analyze the surfaces *in situ* without any sample preparation, other than removing the most notable debris off the surfaces. In few cases, a fresh surface was chipped with a hammer. This was easiest along Kustaa Vaasan tie (Fig. 3), where the outcrops are vertical road cuttings. Depending on each outcrop size and suitability for

the P-XRF analyses, one or more analyses on each and a total of 114 analyses were conducted in the surroundings of the campus with the P-XRF device.

## 4. PETROGRAPHY

The petrographic examinations were done for four thin sections prepared from the drill core. The selection of these particular samples were determined by their representativeness of each different main rock type described for the drill core. The 30 µm thick, polished thin sections were examined with Nikon Labophot-2 Pol polarizing microscope.

The following description of each sample includes macroscopic description, microscopic description, mineral assemblage listed and possible special features. Photographs and photomicrographs of the samples are presented with individual descriptions for each rock type. Photographs include a picture of the hand sample and magnified pictures of the thin sections in plane-polarized light (PPL) and cross-polarized light (XPL).

Mineral abbreviations in photomicrographs after Kretz (1983):

Act = actinolite
Ap = apatite
Bt = biotite
Pl = plagioclase
Hbl = hornblende
Qtz = quartz
Kfs = K-feldspar
Ttn = sphene (titanite)
Zo = zoisite
Tr = tremolite
Ep = epidote

### 4.1 Amphibolite

Representative sample of the area's main rock type, amphibolite, is from the depth of 36 m. Hand specimen seems quite dark and even-grained, grain size being about 1 mm in diameter (Fig. 5.A). With naked eye, a preferred orientation is clearly visible in thin section. One light colored vein crosscuts the sample.

Main minerals include abundant hornblende (~50%), plagioclase (~25%) and quartz (~15%) (Fig 5). Biotite occurs as an accessory mineral, along with zircon and apatite (together ~10%). Plagioclase has multiple twinning and is partly altered to sericite (Fig. 5.B and 5.C). Such secondary alteration can be seen especially around the vein.

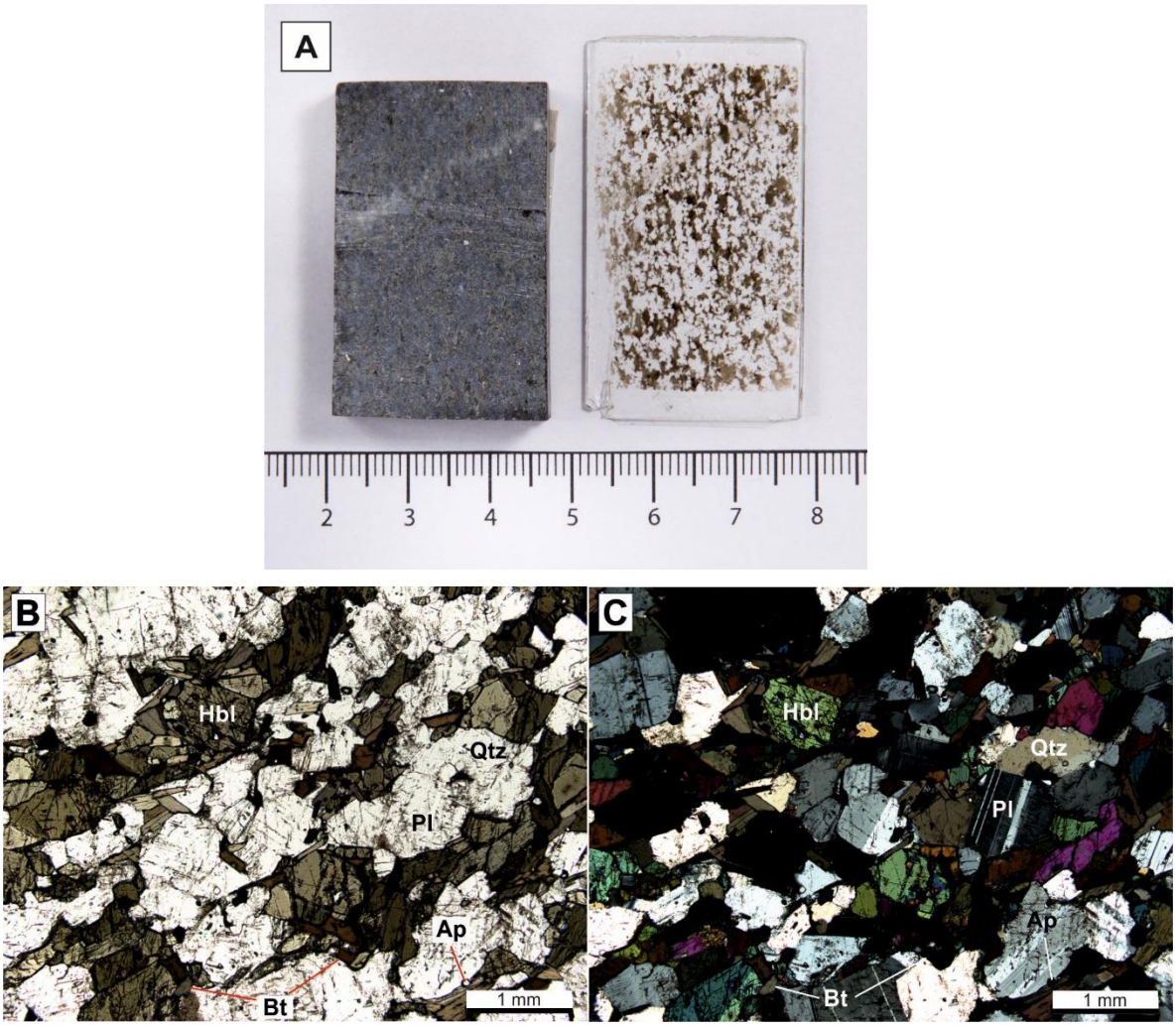


Figure 5.A: Hand specimen is even-grained and dark gray in color with grain size about 1 mm in diam. Light colored vein crosscuts the sample. Thin section shows clearly the dark green amphibole. B: Thin section with 2.5X magnification in PPL: Transparent grains are mainly plagioclase and quartz. Green minerals are amphibole and also some biotite is present. C: XPL: Amphibole shows first order colors and plagioclase multiple twinning.

## 4.2 Granite

Granite sample is from the depth of 351.50 m. Hand specimen is reddish and even-grained with grain size of ~2mm in diameter (Fig. 6.A). With naked eye, thin section seems felsic and without a preferred orientation.

Quartz (~35%) exhibits undulating crystal boundaries and some of the crystals show undulose extinction. Plagioclase (~25%) is partly altered to sericite. Potassium feldspar (~30%) shows cross-hatched microcline twinning and perthite. Accessory minerals include biotite that is in some places altered to chlorite. Epidote is also present in minor amounts and is always associated with biotite (together ~10%) (Fig. 6).

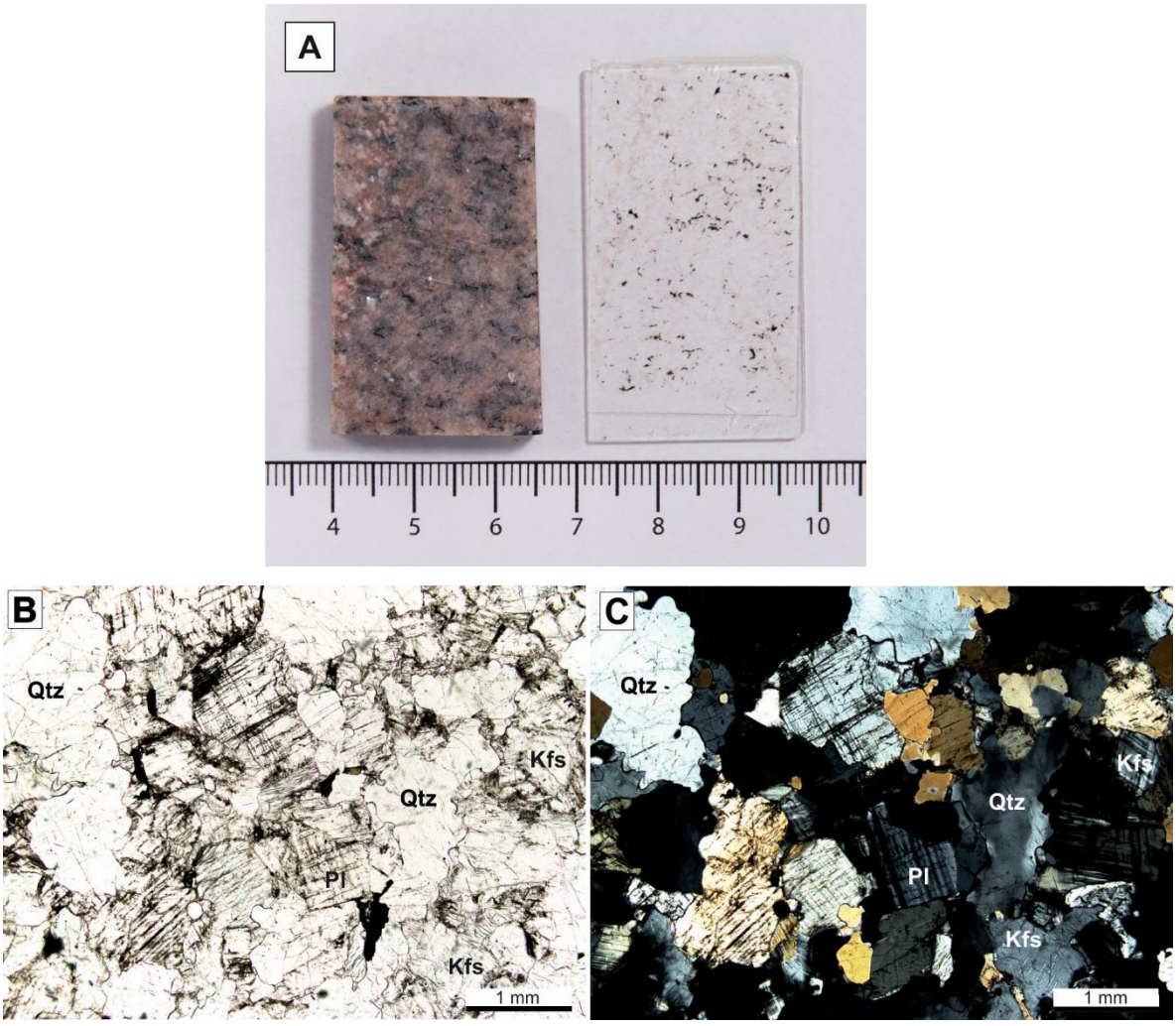


Figure 6.A: Hand specimen of the granite sample seems reddish with a grainsize of 1–2 mm. B: 2.5X magnification in PPL: the abundance of felsic minerals is clear. Sericite dims the feldspar crystals. C: In XPL only first order colors are visible. Quartz shows undulose extinction and undulating crystal boundaries.

### 4.3 Actinolite rock

Actinolite rock sample is from the depth of 35 m. Rock has a clear preferred orientation. Clusters of biotite crystals are clearly visible with naked eye in thin section. The material between the clusters is light green in color (Fig. 7.A).

Biotite (~40%) shows very faint light brown pleochroism (Fig. 7.B). Largest crystals are 0.5 cm in diameter. Crystal boundaries have strings of high relief crystals with halos. These are too tiny to be recognized. Between biotite crystals and crystal clusters, there are actinolite crystals (~60%) that are slightly pleochroic from pale green to white. Actinolite crystals are anhedral and <0.5 mm in diameter. No other minerals are present and this rock is probably of metasomatic origin (Fig. 7).

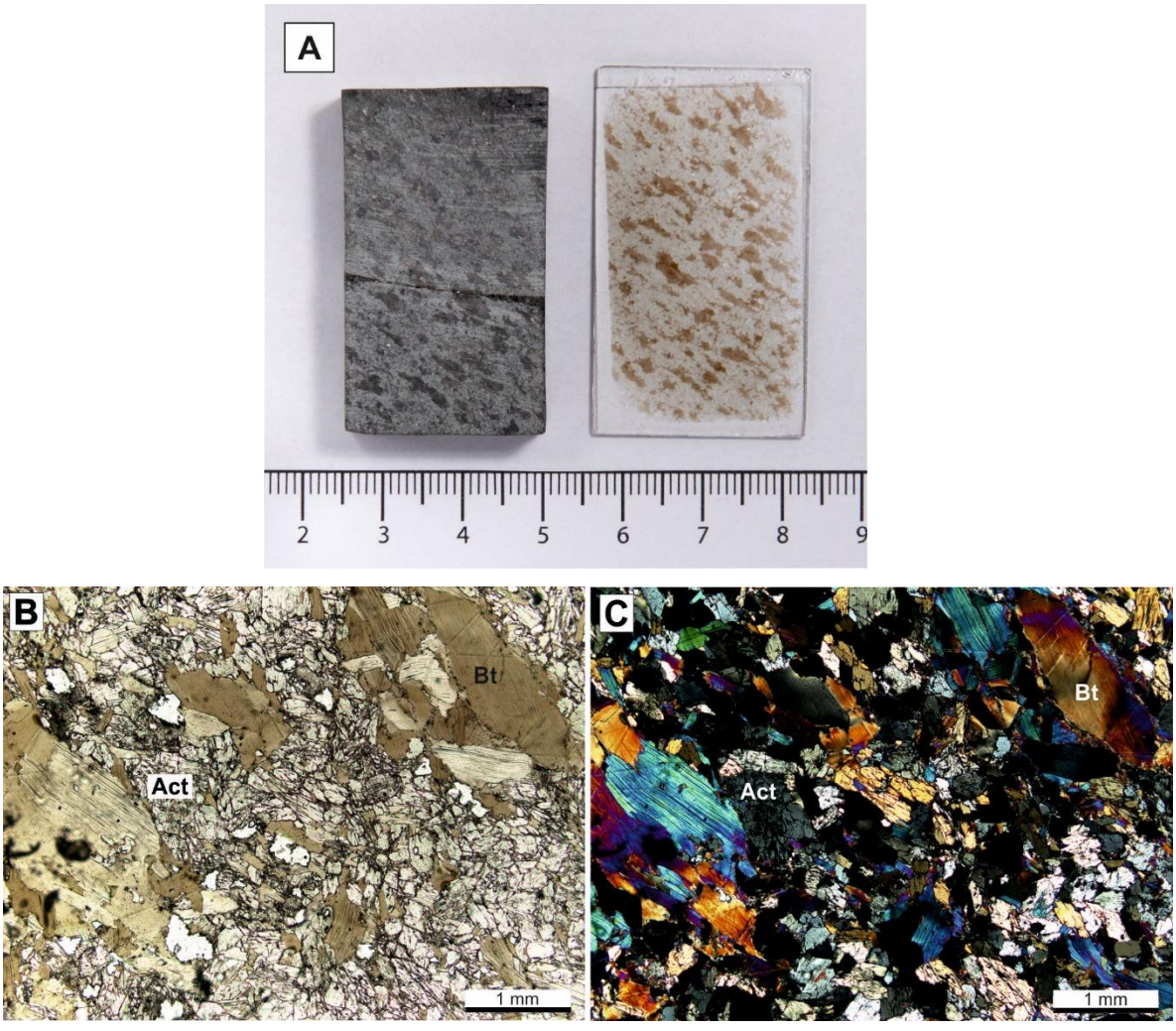


Figure 7.A: Hand specimen of actinolite rock is dark green and clearly oriented. Thin section shows the brownish pleochroism of biotite clusters. B: PPL and C: XPL 2.5X magnification reveals the variation in grainsizes: biotite grains are even multiple mm long, and smaller actinolite crystals fill the spaces between biotite clusters.

### 4.4 Diopside-actinolite skarn

Diopside-actinolite skarn is from the depth of 145.70 m. Hand specimen is greenish gray in color (Fig. 8.A). Grain size is about 1 mm in diameter and the rock is even-grained. One dark green filled fracture crosscuts the sample. Minerals have no preferred orientation. Thin section looks almost completely colorless with an unaided eye.

Plagioclase (~50%) is strongly altered to sericite in some parts, especially around the filled fracture crosscutting the sample (Fig. 8.F, 8.G). Plagioclase composition is andesitic in unaltered crystals and albitic in altered crystals on the basis of the extinction angle of the twinning. Diopside (~30%) is present as subhedral crystals. Actinolite (~10%) occurs as euhedral/subhedral crystals with slightly yellow/light green color in PPL. Sphene (~5%) occurs as an accessory mineral throughout the sample as small subhedral crystals. The fracture crosscutting the sample hosts tremolite, subhedral epidote and subhedral zoisite (together ~5%) (Fig. 8.B–8.G).


Figure 8.A. Hand sample and a thin section of diopside-actinolite skarn are quite faded in color and grain size is about 1 mm. The thin fracture crosscutting the sample has whiter colored, altered surroundings and a dark filling.

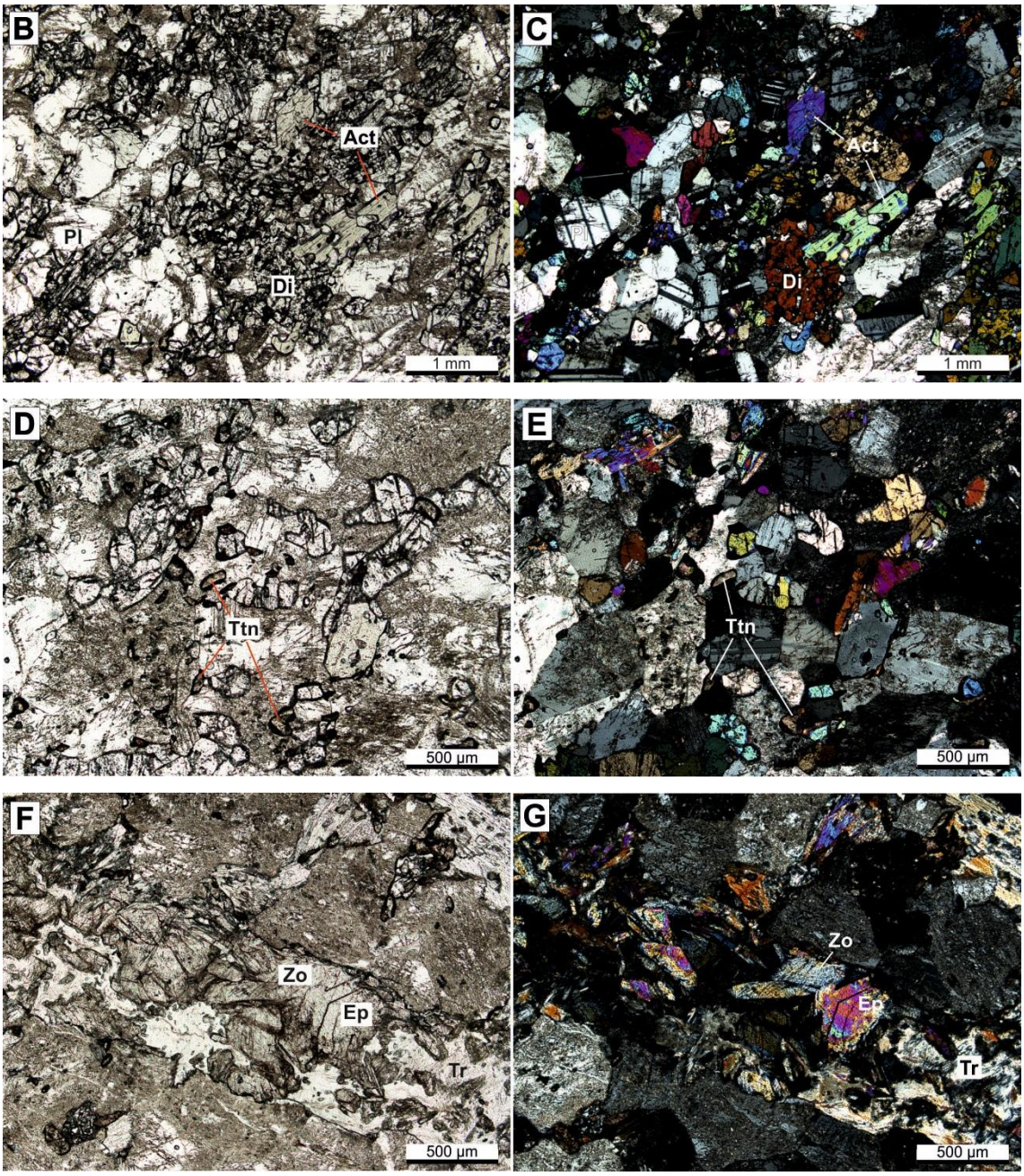


Figure 8.B and C: 2.5X magnification of the thin section shows slightly angular actinolite crystals, rounded diopside crystals and twinning in plagioclase. D and E: 5X magnification focuses on dark reddish brown sphene crystals that occur throughout the sample. F and G: 5X magnification of the fracture crosscutting the sample. Fracture hosts e.g. zoisite, epidote and tremolite.

## 6. RESULTS

Granite, actinolite rock and diopside-actinolite skarn whole rock geochemistry are fully based on WD-XRF Omnian scans from sawed rock surface analyses. The most quantitative result of the amphibolite with major element oxide sum of 98.13 wt.% was obtained with WD-XRF quantitative method of fused bead. These results together with

petrographic observations are considered first to interpret the petrology and petrogenesis of the Kumpula campus bedrock, focusing on the amphibolite. All presented values are untreated. Complete set of the results is tabulated in the appendices.

### 6.1 Whole rock geochemistry of the rock types

$SiO_2$ content of the selected rock types is highest in granite (72.04 wt.%) (Table 2). Granite has also relatively high $K_2O$ content (4.23 wt.%) but less e.g. $TiO_2$ (0.08 wt.%), $FeO_t$ (0.72 wt.%), MgO (0.35 wt.%) and CaO (1.20 wt.%) than other rock types. Actinolite rock has $FeO_t$ (8.87 wt.%) and MgO (17.73 wt.%) contents that are distinctively high compared to other rock types. On the other hand, $SiO_2$ is only 43.19 wt.% and $Na_2O$ 0.30 wt.%. Diopside-actinolite skarn shows high $Al_2O_3$ (18.15 wt.%) and CaO (10.59 wt.%) contents.

$SiO_2$ content of amphibolite is 57.41 wt.% (Table 2), which is equivalent to andesitic composition (Fig. 9) (Le Bas et al. 1986). $K_2O$ wt.% together with $Na_2O$ wt.% is 5.58 wt.%, which specifies the composition to andesite area, near the boundary of basaltic andesite (Fig. 9). More precise plotting of the WD-XRF quantitative result sets the rock type as an alkali basalt area according to the diagram by Pearce (1996), that uses Nb/Y and Zr/Ti ratios (Fig. 10) and thus eliminates the effects of alkali mobilization typical to metamorphic rocks. Amphibolite's TAS ratio plots to the sub-alkaline field and more precisely to medium-K field, which indicates calc-alkaline suite (Ewart 1982).

Degree of silica-saturation (Equation [1]) suggest the rock to be silica-oversaturated and Mg-number (Equation [2]) is less than that of primary magmas. Due to the lack of additional samples and more precise trace element and isotope data, further geochemical interpretation for amphibolite is not presented in this work.

Table 2. Whole-rock geochemical compositions of the four rock types of the Kumpula campus bedrock based on single analyses. Depths of the samples can be seen in Figure 2.

| Rock type | Amhibolite | Granite | Actinolite rock | Diopside-actinolite skarn |
|---|---|---|---|---|
| Sample ID | A1 | t2 | t3 | t4 |
| Method | WD-XRF | WD-XRF | WD-XRF | WD-XRF |
| Sample type | Quantitative app. fused bead | Omnian scans rock surface | Omnian scans rock surface | Omnian scans rock surface |
| $SiO_2$ (wt.%) | 57.41 | 72.04 | 43.19 | 51.91 |
| $TiO_2$ | 0.97 | 0.08 | 0.58 | 0.68 |
| $Al_2O_3$ | 15.37 | 13.75 | 8.20 | 18.15 |
| FeOt | 7.50 | 0.72 | 8.87 | 1.35 |
| MnO | 0.12 | 0.02 | 0.17 | 0.04 |
| MgO | 4.93 | 0.35 | 17.73 | 5.33 |
| CaO | 6.06 | 1.20 | 7.30 | 10.59 |
| $Na_2O$ | 3.93 | 4.08 | 0.30 | 4.30 |
| $K_2O$ | 1.65 | 4.23 | 3.81 | 0.92 |
| $P_2O_5$ | 0.19 | 0.05 | 0.17 | 0.26 |
| Sum | 98.13 | 96.53 | 90.30 | 93.52 |
| Ba (ppm) | 415 | 360 | 140 | 200 |
| Cl | n.a. | 190 | 140 | 80 |
| F | n.a. | n.d. | 1390 | n.d. |
| S | n.a. | 60 | 60 | 50 |
| Ce | 48 | n.d. | n.d. | n.d. |
| Co | n.a. | n.d. | 70 | n.d. |
| Cr | 154 | n.d. | 2530 | 170 |
| Cu | 8 | 20 | 30 | 30 |
| Ga | n.a. | 20 | 20 | 20 |
| La | 19 | n.d. | n.d. | n.d. |
| Nb | 14 | n.d. | n.d. | 10 |
| Ni | 23 | 40 | 880 | 60 |
| Pb | n.a. | 40 | n.d. | n.d. |
| Rb | 72 | 180 | 270 | 40 |
| Sr | 292 | 80 | 10 | 320 |
| U | 4 | n.d. | n.d. | n.d. |
| V | 157 | n.d. | 150 | 180 |
| Y | 17 | n.d. | n.d. | n.d. |
| Zn | 65 | 10 | 100 | 30 |
| Zr | 78 | 70 | 50 | 90 |

n.a.= not analysed
n.d.= not detected

Degree of silica saturation is calculated as following:

$$\frac{\left(\frac{SiO_2 wt.\%}{60.08}\right)}{\left(\frac{Na_2O\ wt.\%}{61.98}\right)} \quad [1]$$

=15.07 (> 6, rock is silica-oversaturated) for the representative amphibolite sample A1.

Magnesium number:

$$\frac{100*\left(\frac{MgO\ wt.\%}{40.30}\right)}{\left(\frac{MgO\ wt.\%}{40.30}+\frac{FeO_t\ wt.\%}{71.85}\right)} \quad [2]$$

= 53.95 (< 68–75 for primary magmas) for the representative amphibolite sample A1.

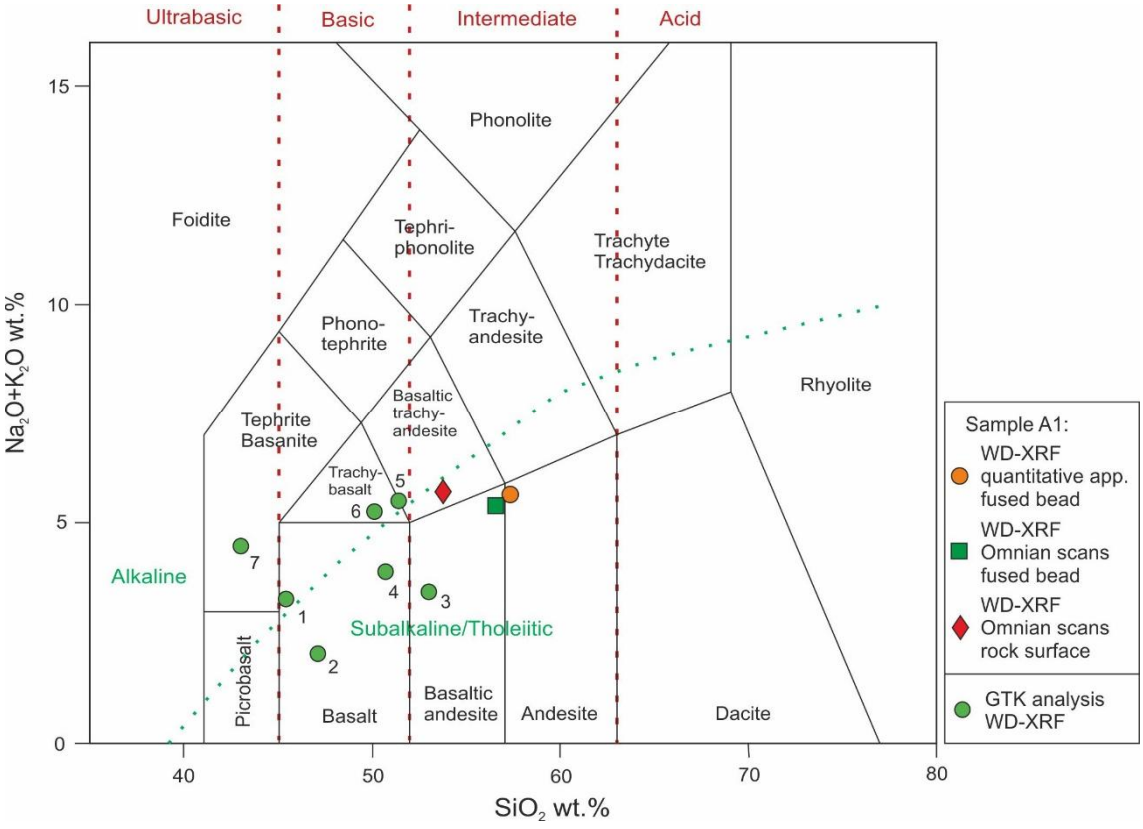


Figure 9. Results of three different WD-XRF analyses conducted for amphibolite sample A1 plotted in TAS diagram. Quantitative method sets the composition to the andesite field, close to basaltic andesite field. Selected values from GTK rock geochemical database of Finland of temporally related amphibolite units for reference (Fig. 16 and Appendix VII). Redrawn from Le Bas et al. (1986).

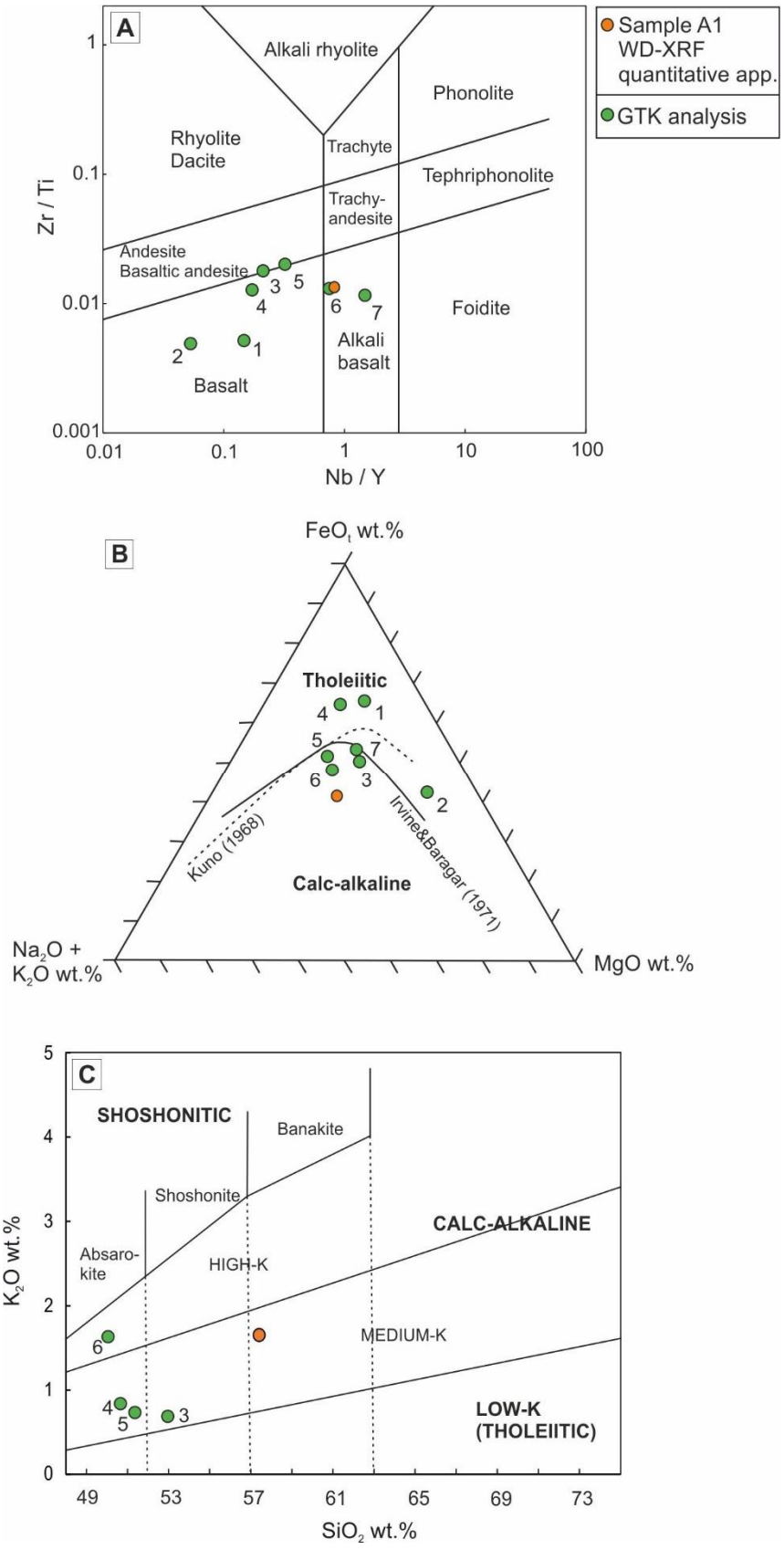


Figure 10 A: WD-XRF quantitative result falls in alkali basalt field in Zr/Ti v. Nb/Y diagram. Redrawn from Pearce (1996; revised from Winchester & Floyd 1977). B and C: Quantitative WD-XRF result plotted on AFM diagram and K-field diagram (redrawn from Ewart 1982), both indicating calc-alkaline series. Selected values from GTK rock geochemical database of Finland of temporally related amphibolite units for reference (Fig. 16 and Appendix VII).

## 6.2 Comparison of the XRF methods

### *6.2.1 Amphibolite sample A1*

The amphibolite sample A1 was used to compare and evaluate the different XRF analysis methods (Table 3). It seems that values gained from fused bead especially in terms of major element oxides are quite similar whether they were obtained with Omnian scans or quantitative application (Table 3, Fig. 11).

Table 3. Whole-rock chemical composition of amphibolite sample A1 obtained with different XRF methods. All results of the ten P-XRF analyses are tabulated in Appendix I.

| Method | WD-XRF quantitative fused bead | WD-XRF Omnian scans fused bead | WD-XRF Omnian scans rock surface | P-XRF* mining mode rock surface |
|---|---|---|---|---|
| n | 1 | 1 | 1 | 10 |
| $SiO_2$ (wt.%) | 57.41 | 56.60 | 53.97 | 57.94 |
| $TiO_2$ | 0.97 | 0.95 | 0.85 | 0.80 |
| $Al_2O_3$ | 15.37 | 15.55 | 15.76 | 10.93 |
| FeOt | 7.50 | 7.69 | 5.72 | 6.19 |
| MnO | 0.12 | 0.13 | 0.11 | 0.12 |
| MgO | 4.93 | 4.91 | 3.69 | 1.71 |
| CaO | 6.06 | 5.87 | 5.68 | 6.32 |
| $Na_2O$ | 3.93 | 3.69 | 4.17 | n.a. |
| $K_2O$ | 1.65 | 1.68 | 1.50 | 1.19 |
| $P_2O_5$ | 0.19 | 0.20 | 0.21 | 0.18 |
| Sum | 98.13 | 97.27 | 91.65 | 85.37 |
| Ba (ppm) | 415 | 360 | 340 | 520 |
| Cl | n.a. | n.d. | 670 | 210[7] |
| S | n.a. | 70 | 100 | 220[8] |
| Ce | 48 | n.d. | n.d. | n.a. |
| Cr | 154 | 240 | 120 | 240 |
| Cu | 8 | n.d. | n.d. | n.d. |
| La | 19 | n.d. | n.d. | n.a. |
| Nb | 14 | n.d. | 10 | n.d. |
| Ni | 23 | 230 | 60 | 60[2] |
| Rb | 72 | 150 | 40 | 20 |
| Sn | n.a. | n.d. | n.d. | 40[2] |
| Sr | 292 | 350 | 320 | 230 |
| U | 4 | n.d. | n.d. | n.a. |
| V | 157 | 190 | 120 | 240 |
| Y | 17 | n.d. | 10 | n.a. |
| Zn | 65 | n.d. | 40 | n.a. |
| Zr | 78 | 110 | 90 | 70 |

*= P-XRF results are averages of ten sawed surface analyses.
Superscripted numbers indicate the number of values included in the average value if all are not included.

n= number of analyses

n.a.= not analyzed

n.d.= not detected

Comparing the Omnian scans results suggests, that changing the sample type from fused bead to sawed rock surface, has a notable negative effect on the results. Major oxide sum value drops from 97.27 wt.% to 91.65 wt.%. Most of the major element oxide values are lower than the ones obtained with Omnian scans on fused bead or quantitative application. Oxide values that are higher in Omnian rock surface results are $Al_2O_3$ with 15.76 wt.%, $Na_2O$ with 4.17 wt.% and $P_2O_5$ with 0.21 wt.%. The effect of changing from fused bead to rock surface is visible in Figure 11, where Omnian scans and quantitative application results from fused bead do not differ remarkably, but Omnian scans results from rock surface are clearly different from these two.

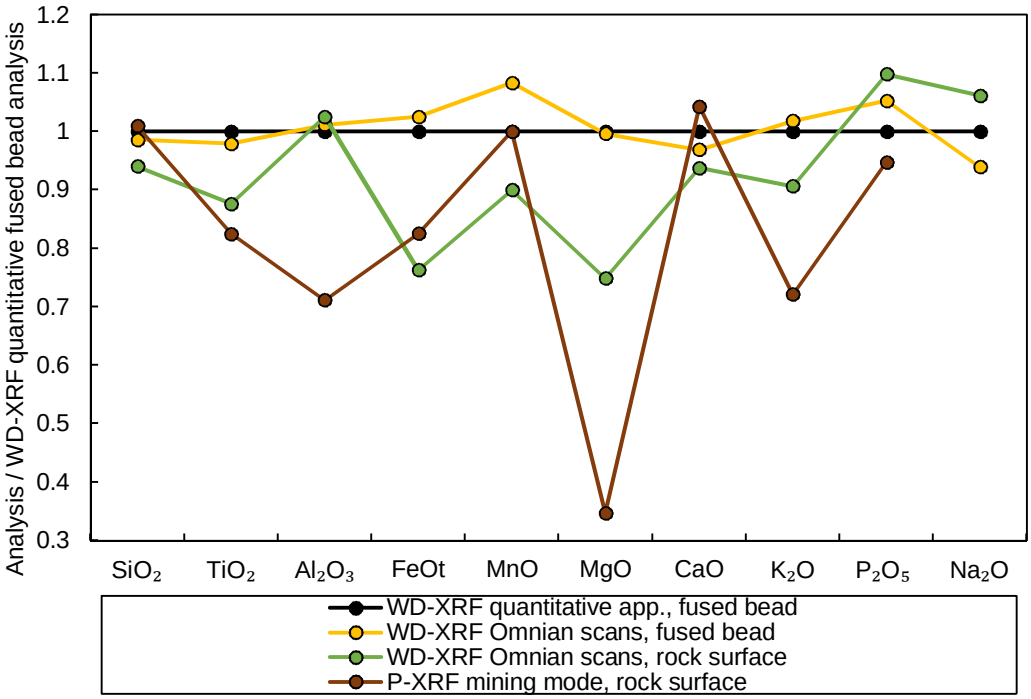


Fig 11. Amphibolite sample A1 XRF results of major element oxides as ratios compared to quantitative application results. P-XRF results are averages of ten sawed surface analyses and do not include $Na_2O$. All results of the ten P-XRF analyses are tabulated in Appendix I.

P-XRF major oxide values are notably lower on average than values obtained with WD-XRF quantitative application or Omnian scans from fused bead, $SiO_2$ (57.94 wt%), MnO (0.12 wt.%), CaO (6.32 wt%) and P2O5 (0.18 wt.%) being the exceptions. MgO value (1.71 wt.%) is undoubtedly too low and not reflecting the real rock composition.

Taking a closer look on the ten individual P-XRF sawed surface values and comparing them to WD-XRF quantitative application values (Fig. 12), it is revealed how

amphibolite sample heterogeneity scatters the P-XRF results. Comparison to quantitative application also shows which major element oxide values are altogether, heterogeneity considered, erroneous in P-XRF results.

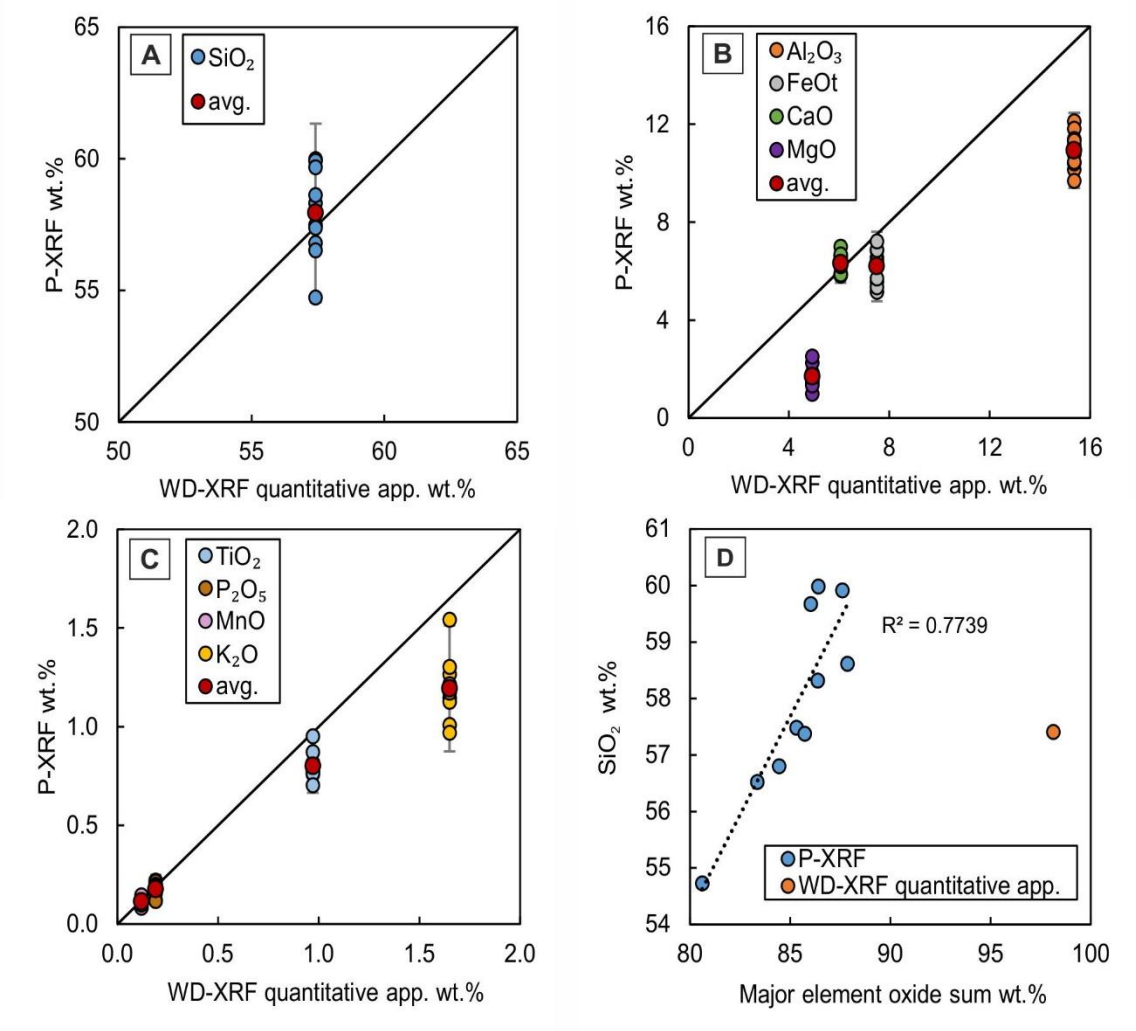


Figure 12. A, B and C: Ten P-XRF results of the sawed surface of amphibolite sample A1 compared to quantitative application values of the fused bead. Major element oxides are divided in three diagrams depending on their weight percent range. 2 x standard deviation (2σ) bars and average values are included. D: P-XRF $SiO_2$ wt.% values correlation to major element oxide sum wt.% values, with R squared value of 0.7739 indicating relatively high correlation.

Tabulated results of the ten P-XRF analyses, both on sawed and curved rock surfaces can be seen in Appendix I and II. Values in Fig. 12 are untreated; thus, the sum of major element oxides is not constant between the methods. Correlation between P-XRF $SiO_2$ values (that range between 54.73–59.98 wt.%) and major element oxide sum values (80.61–87.86 wt.%) is clearly visible, with R squared value of about 0.77. Quantitative application $SiO_2$ value is 57.41 wt.% with major element oxide sum value of 98.13

wt.%. This observation suggests that if the P-XRF oxide sum would hypothetically be 100 wt.%, $SiO_2$ would probably be overrepresented in P-XRF results. However, the average of P-XRF $SiO_2$ values is very close to quantitative value (Fig. 12.A), which is a quite promising result for P-XRF device.

P-XRF values of $Al_2O_3$ (range between 9.69–12.12 wt.%), MgO (0.99–2.52 wt.%) and $K_2O$ (0.97–1.54 wt.%) values are all clearly lower than quantitative application values (15.37 wt.%, 4.93 wt% and 1.65 wt% respectively). $FeO_t$ (5.15–7.21 wt.%) and $TiO_2$ (0.70–0.95 wt.%) are just slightly lower than quantitative application values (7.50 wt.% and 0.97 wt.% respectively).

*6.2.2 Sawed amphibolite pieces: P-XRF and Omnian scans comparison*

Widening the comparison from sample A1 to twelve sawed amphibolite pieces from different depths (3.90, 36.00, 63.35, 88.95, 105.35, 128.30, 156.00, 203.00, 241.55, 323.20, 336.70 and 361.60 m, Fig. 2) of the core, the heterogeneity of the amphibolite can be studied on a wider scale. All major element oxide values seem to be scattered (Fig. 13, notice the scales) with both methods. Presented values are once again untreated so major element oxide sum is not constant between the methods. Major element oxide sums vary between 84.37–90.72 wt.%, averaging at 88.11 wt.% with P-XRF device and between 89.29–94.42 wt.%, averaging at 92.29 wt.% with Omnian scans (Appendix III and IV).

$SiO_2$ values, that are scattered between 54.13–64.51 wt.% with P-XRF, are all higher than corresponding Omnian scans values (48.22–59.32 wt.%), whereas $Al_2O_3$ (varying between 11.04–14.01 wt.%) and MgO (0.53–2.61 wt.%) with P-XRF are all higher with Omnian scans (14.89–18.07 wt% $Al_2O_3$ and 3.36–7.45 wt.% MgO) (Fig. 13 and Fig. 14). Especially in the case of MgO, the range is wider in Omnian scans than P-XRF. CaO results seem to correlate quite well and $K_2O$ is rather close to 1:1 correlation as well. Other oxide results are scattered without a clear trend.

Omnian scans method and P-XRF were previously observed to give values for rock surface that are on average lower than quantitative method results of fused bead (Fig. 11). Major relations between P-XRF and Omnian scans from rock surface shown in Fig.

11 (e.g. MgO and $Al_2O_3$ ratios) are clear in twelve sample comparisons as well, but all differences between the methods are clearly not constant.

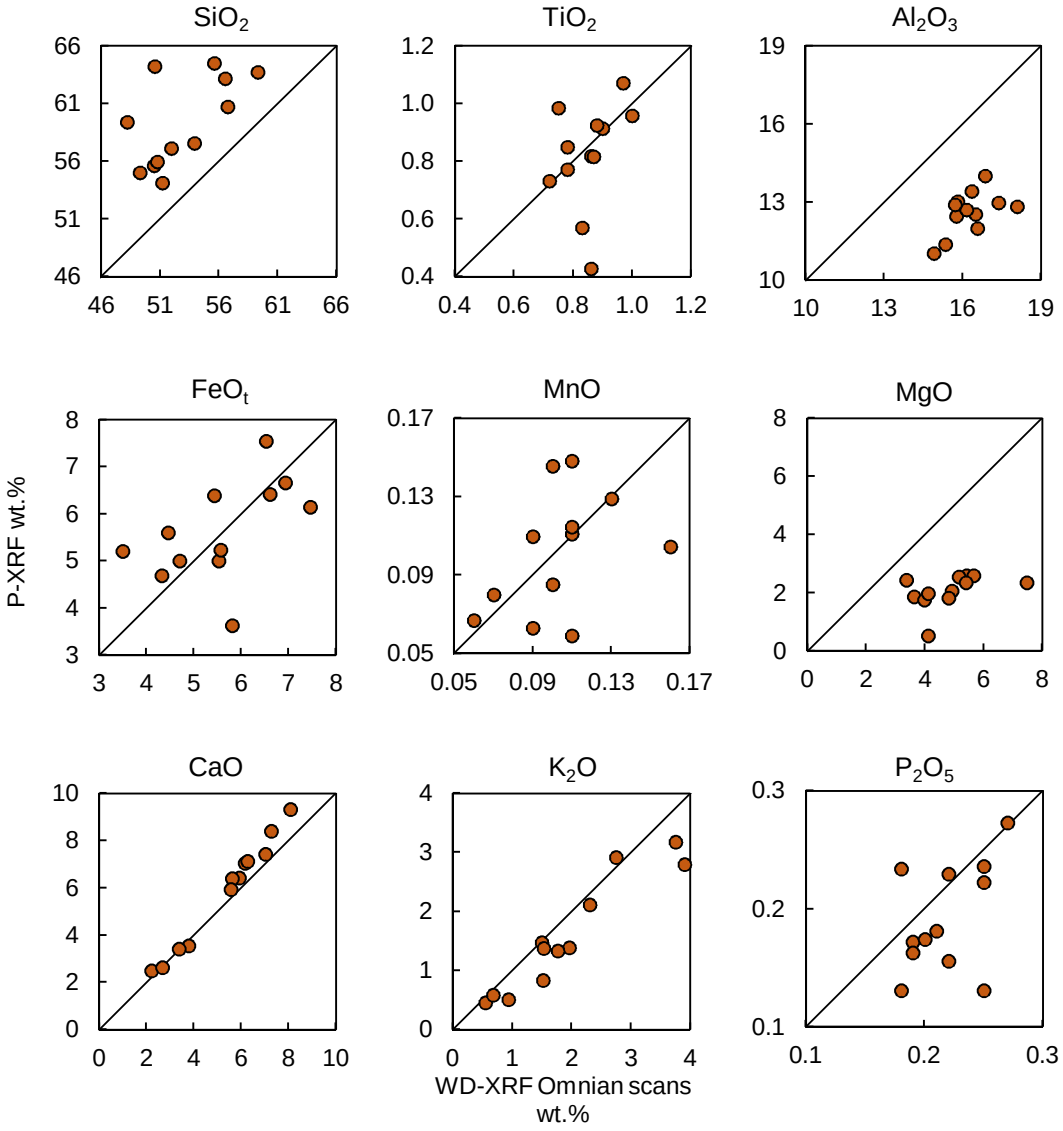


Figure 13. P-XRF and Omnian scans results of the twelve amphibolite samples. Black line from lower left corner to upper right corner represents 1:1 correlation between the methods. $Na_2O$ is excluded.

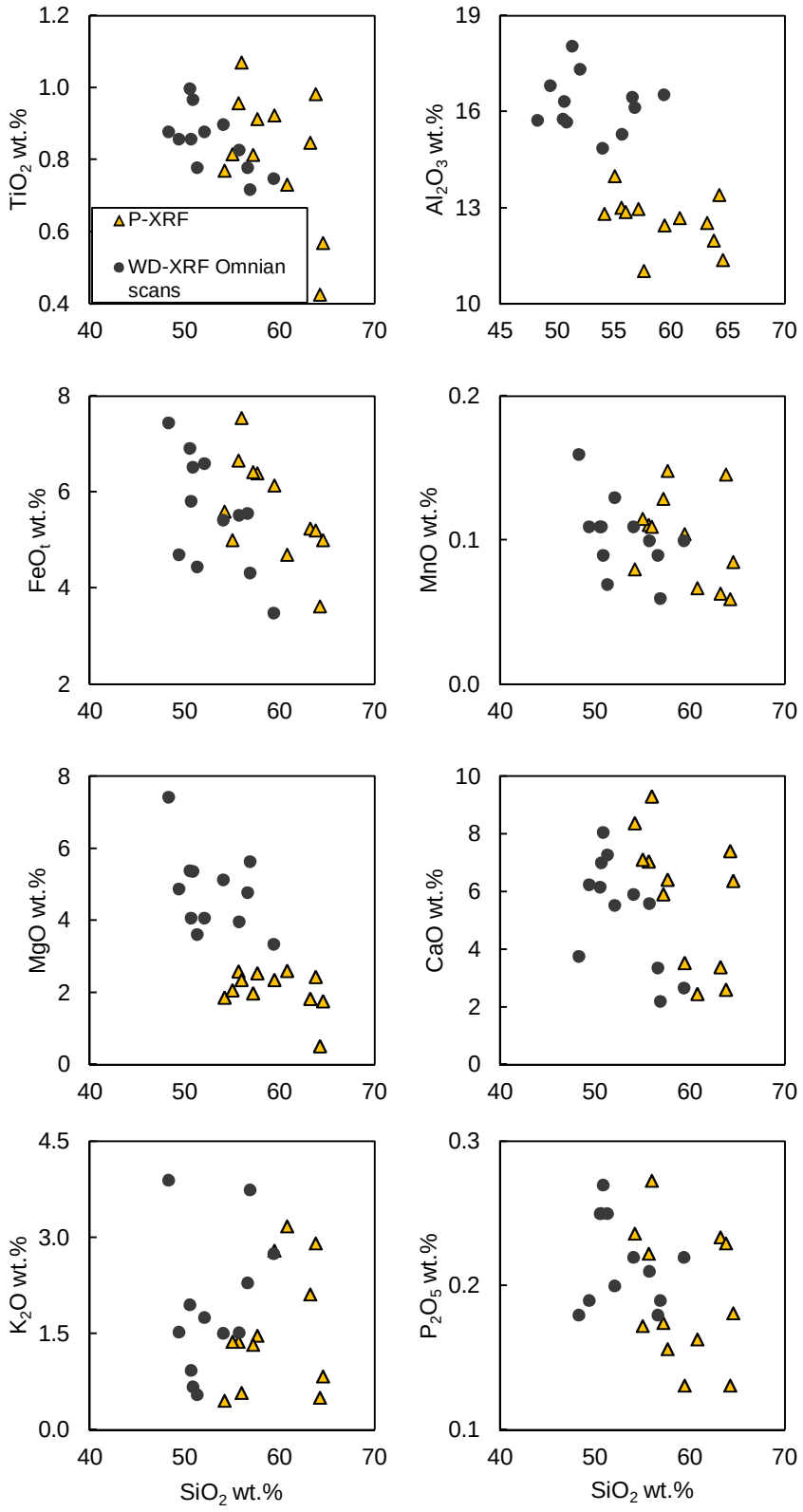


Figure 14. Harker diagrams of P-XRF and WD-XRF Omnian scans values for the twelve amphibolite samples.

### 6.3 Whole drill core analysis with the P-XRF device

To evaluate the feasibility of P-XRF during drill core logging, the curvature of the core was first considered. In addition to ten repeated P-XRF analyses of the sawed surface of amphibolite sample A1, curved core surface of the same piece was also analyzed repeatedly.

Compared to the sawed surface results (Fig. 15), curved surface values seem to have a bit wider range, with average values of e.g. $SiO_2$ (57.14 wt.%), $TiO_2$ (0.90 wt.%) and $K_2O$ (1.45 wt.%) (Appendix I and II) that are even closer to quantitative application values than sawed surface P-XRF values (57.94 wt.%, 0.80 wt.% and 1.19 wt.% respectively). Sawed surface has major element sum values varying between 80.61 wt.% and 87.86 wt.% averaging at 85.37 wt.% and curved surface between 80.08 wt.% and 89.26 averaging at 84.63 wt.%. Differences in the values between the surfaces are however relatively minor in general.

Major element oxide sum values for the whole length of the core range between 74.70 wt.% and 92.63 wt.%, averaging at 84.00 wt.%. Main element oxide sums and other tabulated P-XRF results for the whole length of the core can be seen in Appendix V.

Comparing the selected oxides P-XRF results to depth and lithology (Fig. 16), variation in major element oxide values between different rock types can be observed. Changes in $SiO_2$ content alone clearly indicate changes from mafic amphibolitic and actinolite-rock units to felsic granitoid units. Between 170 m and 220 m, $SiO_2$ and $Al_2O_3$ values seem quite constant but $FeO_t$ values show relatively high variation. Relatively high $FeO_t$ and CaO values of actinolite rock (Table 2) is visible between 250–300 m with quite thin actinolite rock sections.

Although relative variation in major element oxide values can be observed between the rock types, possible changes in the geochemistry of the amphibolite along the length of the drill core is not distinguished. Omnian scans values of twelve amphibolite pieces do not seem to correlate with depth either, but higher values of $Al_2O_3$ compared to P-XRF is once again observed (Fig. 16).

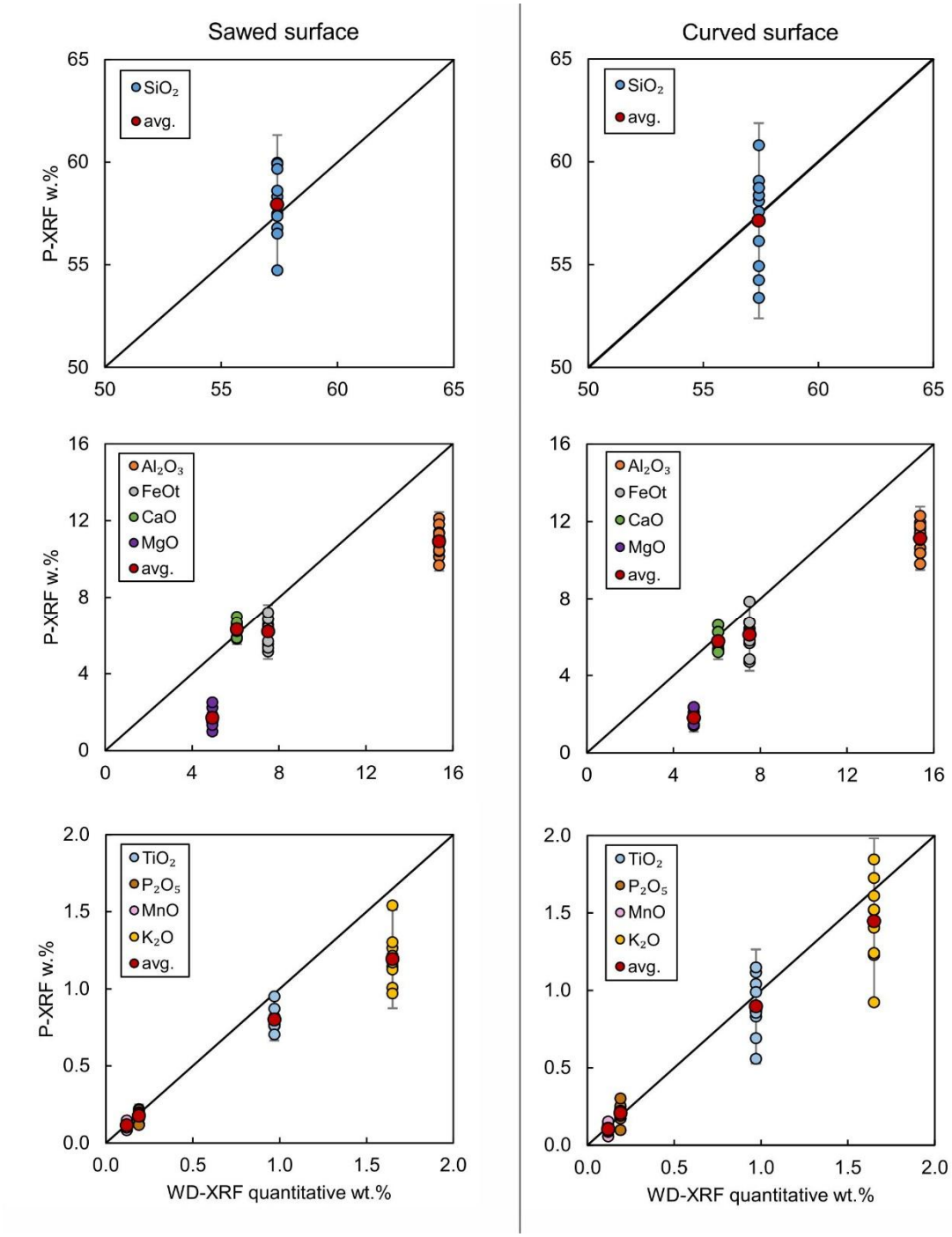


Figure 15. Ten P-XRF analyses of sawed and curved drill core surfaces of the amphibolite sample A1 compared to quantitative WD-XRF values.

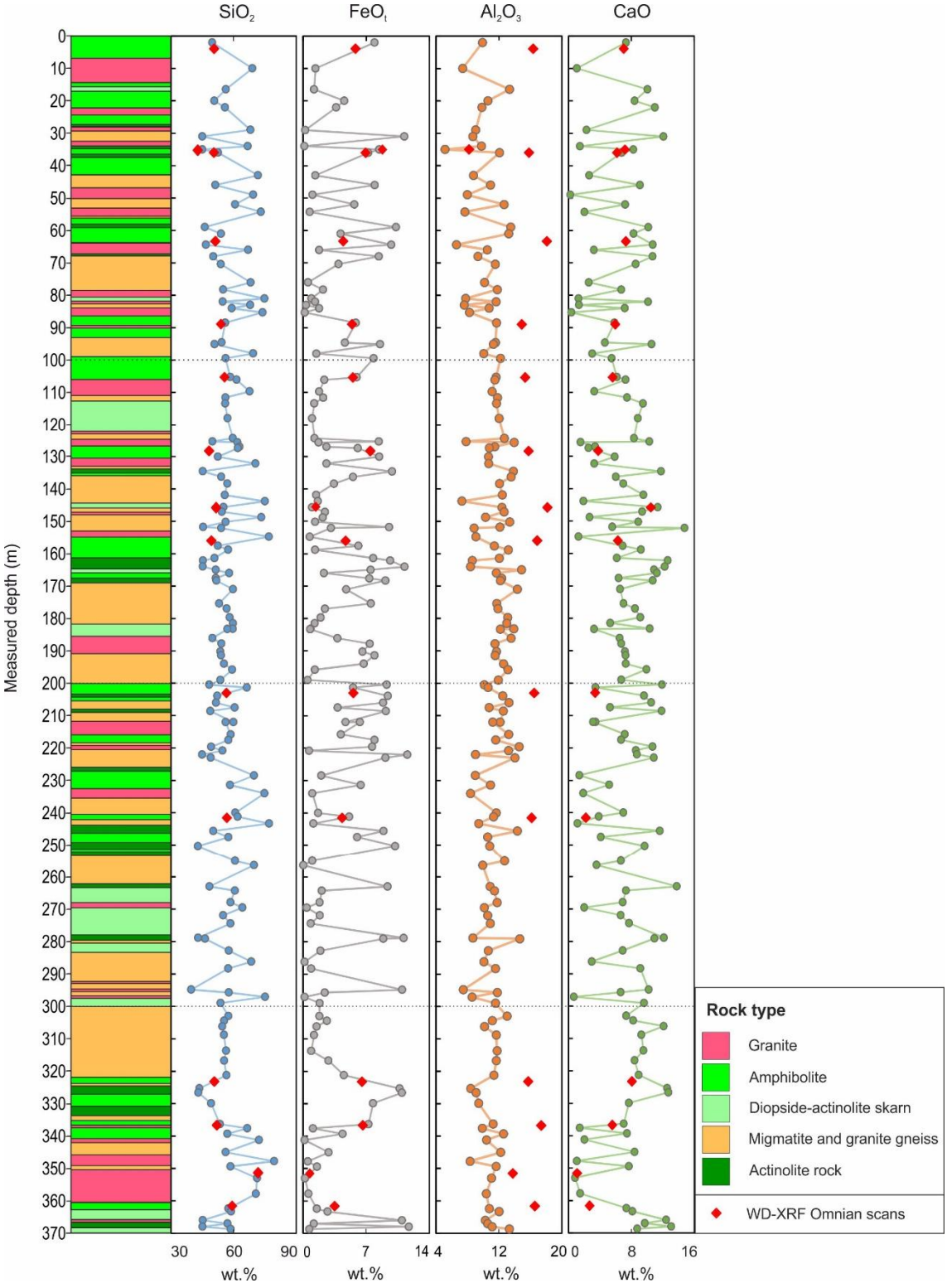


Figure 16. Rock types and P-XRF values of selected major element oxides compared to depth. Omnian scan values of twelve amphibolite samples and granite, actinolite rock and diopside-actinolite skarn are marked as red spots. Variation in geochemistry can clearly be observed between the rock types.

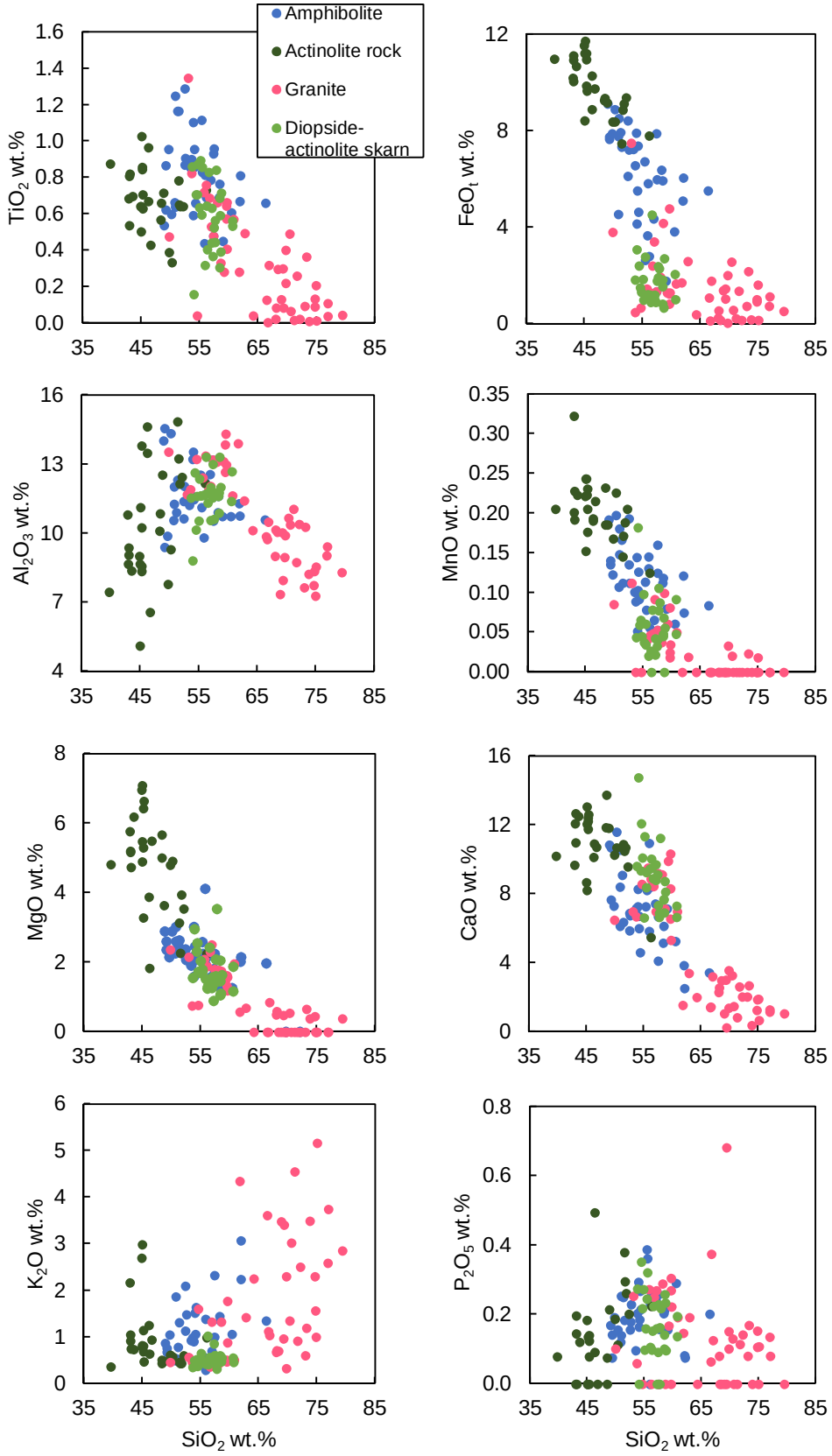


Figure 17. Harker diagrams of all P-XRF results of the drill core color coded by initially determined rock types.

Illustrating the P-XRF core results according to initially determined rock type classes (Fig. 17), major element oxide results show some trends and groups. Comparing to $SiO_2$ wt.% values in Harker diagrams, $TiO_2$, $FeO_t$, MnO, MgO and CaO wt.% clearly decrease as $SiO_2$ wt.% increase. $K_2O$ and $P_2O_5$ do not seem to show any trends, but some value ranges are favored over others. $Al_2O_3$ is the only major element oxide that seems to have completely different trendline depending on rock type: actinolite rock has positive trend and granite negative, changing at about 55 wt.% $SiO_2$, which is possibly caused by the fractioning of feldspars.

Indeed, broad classes of different rock types can be distinguished from the P-XRF results alone without visual examination or previous lithological logging, especially from $FeO_t$, $SiO_2$, MgO and MnO results. Some ranges for major element oxides can also be derived from the results, although P-XRF results cannot be considered quantitative. Comparisons between quantitative WD-XRF values and P-XRF values of sample A1 (Fig. 15) clarify that untreated P-XRF results from the rock surface concerning for example $SiO_2$, CaO and MnO are quite close to the most accurate quantitative application results. The accuracy of the P-XRF results needs to be considered when examining the results of the whole drill core. Additional consideration is needed with major element sum values that are not very high (84.00 wt.% on average).

### 6.4 Outcrops: effects of surface quality and field circumstances

In the case of outcrops, quality of the analysis surface became highly important factor for the analysis to be successful, since no sample preparation was done. Outcrops were varyingly rough, weathered, altered and usually covered in e.g. lichen, moss and pollution, which seemed to dramatically affect the detection of underlying bulk rock elements. These surfaces are later called “poor quality surfaces”. “Good quality surfaces” are grouped as being as clean as possible, considering the circumstances, but weathering and roughness could not be completely avoided. Results of the outcrop analyses show variation in success of the analyses from outcrop to another (Appendix VI) and from good quality surface to poor quality surface (Table 4).

Table 4. Geochemical comparison of good quality and poor quality amphibolite outcrop surfaces. Results obtained with P-XRF.

| | Good quality surface | Poor quality surface |
|---|---|---|
| n | 47 | 45 |
| $SiO_2$ (wt.%) | 49.79 | 25.34 |
| $TiO_2$ | 0.73 | 0.42 |
| $Al_2O_3$ | 7.91 | 3.40 |
| $FeO_t$ | 3.37 | 3.45 |
| MnO | 0.06 [38] | 0.05 [35] |
| MgO | 0.95 [43] | 0.20 [10] |
| CaO | 4.50 | 2.51 |
| $K_2O$ | 1.10 | 1.44 |
| $P_2O_5$ | 0.23 [45] | 0.58 |
| Total | 68.64 | 37.39 |
| Ba (ppm) | 370 | 410 |
| Cl | 130 [9] | 520 [38] |
| S | 1300 [45] | 5950 |
| Co | n.d. | 180 [2] |
| Cr | 170 [46] | 180 |
| Cu | 60 [1] | 50 [16] |
| Ni | 210 [1] | 130 [2] |
| Pb | 30 [30] | 50 [38] |
| Rb | 40 [16] | 30 [24] |
| Sn | 40 [3] | 40 [2] |
| Sr | 190 | 170 |
| V | 170 [44] | 150 [42] |
| W | 100 [1] | 90 [2] |
| Zn | 50 [38] | 100 |
| Zr | 100 | 90 |

n = number of analyses
n.d.= not detected
Superscripted numbers indicate the number of values included in the avg. value if all are not included

Distinguishing different rock types was challenging from weathered and covered surfaces. Therefore, the amphibolite average values presented in Table 4 are probably of compositionally more variable amphibolite than in the drill core. Major element oxide sum of amphibolite from all outcrop analyses (good + poor surfaces) is only 53.35 wt.% on average (Table 5). Major oxide sum value is notably low on average regardless of whether the surfaces were clean or not (Table 4), yet poor quality surfaces have an average oxide sum value of almost half of that of the good quality surfaces.

Although having very low major oxide sum values, poor quality surface results show remarkably high amounts of $P_2O_5$ (0.58 wt.%), S (5950 ppm) and Cl (520 ppm) compared to clean surface results (0.23 wt.%, 1300 ppm and 130 ppm respectively). Also, $FeO_t$ (3.45 wt.%), $K_2O$ (1.44 wt.%), Ba (410 ppm), Cr (180 ppm) Pb (50 ppm), and Zn (100 ppm) are higher on covered surfaces. Good quality surface results are 3.37 wt.%, 1.10 wt.%, 370 ppm, 170 ppm, 30 ppm and 50 ppm respectively. Poor detection of light elements is visible in outcrop results as well with 0.95 wt.% MgO and 7.91 wt.% $Al_2O_3$ values for good quality surfaces on average. Cu was detected more likely from poor quality surfaces (Table 4).

Table 5. All amphibolite results and average results obtained with different XRF methods.

| | Core | | | | | | | Outcrops |
|---|---|---|---|---|---|---|---|---|
| Sample type | Piece A1 | | | | Sawed pieces | | Core surface | Rock surface |
| n | 1 | 1 | 1 | 10 | 12 | 12 | 38 | 92 |
| Method | WD-XRF quantitative fused bead | WD-XRF Omnian scans fused bead | WD-XRF Omnian scans rock surface | P-XRF* mining mode sawed rock surface | WD-XRF* Omnian scans rock surface | P-XRF* miningmode rock surface | P-XRF* mining mode rock surface | P-XRF* mining mode rock surface |
| $SiO_2$ (wt.%) | 57.41 | 56.60 | 53.97 | 57.94 | 52.90 | 59.26 | 55.63 | 37.83 |
| $TiO_2$ | 0.97 | 0.95 | 0.85 | 0.80 | 0.85 | 0.82 | 0.78 | 0.58 |
| $Al_2O_3$ | 15.37 | 15.55 | 15.76 | 10.93 | 16.27 | 12.61 | 11.56 | 5.70 |
| FeOt | 7.50 | 7.69 | 5.72 | 6.19 | 5.57 | 5.64 | 5.82 | 3.41 |
| MnO | 0.12 | 0.13 | 0.11 | 0.12 | 0.10 | 0.10 | 0.11 | $0.05^{73}$ |
| MgO | 4.93 | 4.91 | 3.69 | 1.71 | 4.82 | 2.08 | 2.12 | $0.58^{53}$ |
| CaO | 6.06 | 5.87 | 5.68 | 6.32 | 5.34 | 5.84 | 6.86 | 3.53 |
| $Na_2O$ | 3.93 | 3.69 | 4.17 | n.a. | 4.28 | n.a. | n.a. | n.a. |
| $K_2O$ | 1.65 | 1.68 | 1.50 | 1.19 | 1.93 | 1.57 | 1.18 | 1.27 |
| $P_2O_5$ | 0.19 | 0.20 | 0.21 | 0.18 | 0.22 | 0.19 | 0.19 | $0.40^{90}$ |
| Sum | 98.13 | 97.27 | 91.65 | 85.37 | 92.28 | 88.11 | 84.25 | 53.35 |
| Ba (ppm) | 415 | 360 | 340 | 520 | 250 | 410 | 430 | 390 |
| Cl | n.a. | n.d. | 670 | $210^{7}$ | 180 | $130^{2}$ | $130^{3}$ | $450^{47}$ |
| S | n.a. | 70 | 100 | $220^{8}$ | 150 | $760^{6}$ | $420^{31}$ | $3630^{90}$ |
| Ag | n.a. | n.d. | n.d. | n.d. | n.d. | 100 | n.d. | n.d. |
| Bi | n.a. | n.d. | n.d. | n.d. | n.d. | $10^{2}$ | n.d. | n.d. |
| Ce | 48 | n.d. | n.d. | n.a. | n.d | n.a. | n.a. | n.a. |
| Co | n.a. | n.d. | n.d. | n.d. | $60^{1}$ | n.d. | n.d. | $180^{2}$ |
| Cr | 154 | 240 | 120 | 240 | 200 | 290 | 280 | $170^{91}$ |
| Cu | 8 | n.d. | n.d. | n.d. | $30^{11}$ | $60^{1}$ | $110^{5}$ | $50^{17}$ |
| F | n.a. | n.d. | n.d. | n.a. | $1620^{7}$ | n.a. | n.a. | n.a. |
| Ga | n.a. | n.d. | n.d. | n.a. | 20 | n.a. | n.a. | n.a. |
| La | 19 | n.d. | n.d. | n.a. | n.d | n.a. | n.a. | n.a. |
| Nb | 14 | n.d. | 10 | n.d. | 10 | 10 | n.d. | n.d. |
| Ni | 23 | 230 | 60 | $60^{2}$ | 60 | $60^{2}$ | $80^{5}$ | n.d. |
| Pb | n.a. | n.d. | n.d. | n.d. | $20^{8}$ | 10 | $20^{11}$ | $40^{68}$ |
| Rb | 72 | 150 | 40 | 20 | 100 | $50^{10}$ | $30^{24}$ | $35^{40}$ |
| Sn | n.a. | n.d. | n.d. | $40^{2}$ | n.d | $30^{4}$ | $40^{4}$ | $40^{5}$ |
| Sr | 292 | 350 | 320 | 230 | 300 | 220 | 220 | 180 |
| U | 4 | n.d. | n.d. | n.a. | n.d | n.a. | n.a. | n.a. |
| V | 157 | 190 | 120 | 240 | 190 | 250 | 260 | $160^{86}$ |
| W | n.a. | n.d. | n.d. | n.d. | n.d. | $60^{2}$ | n.d. | $90^{3}$ |
| Y | 17 | n.d. | 10 | n.a. | $20^{1}$ | n.a. | n.a. | n.a. |
| Zn | 65 | n.d. | 40 | n.a. | 70 | 50 | $50^{36}$ | $70^{83}$ |
| Zr | 78 | 110 | 90 | 70 | 110 | 60 | 70 | 100 |

*= Results are averages, superscripted numbers indicate the number of values included in the avg. value if all are not included
n= number of analyses
n.a.= not analyzed
n.d.= not detected

# 7. DISCUSSION

## 7.1 Error and contamination sources of the analyses

### *7.1.1 Sample preparation*

For the XRF results to actually represent the source rock composition, especially unprepared samples need to be selected with care and keeping the requirements of the analysis surface diameters of the devices in mind. The round detection area of P-XRF is only 8 mm in diameter and that of WD-XRF 27 mm, which limits the representativeness of the results, especially in the case of coarse-grained samples. When analyzing with P-XRF without any sample preparation, rock types with smaller grainsize probably give more exact results of the geochemistry than rock types that are coarser. Coarseness of the rock type can be compensated by taking multiple analyses of the sample from different spots, so every mineral is definitely represented in the average results.

Aforementioned problems related with heterogeneity are minimized by preparing a fused bead with highly homogeneous composition. However, multiple stages of the preparation increase the possibility of contamination. In this work, unknown contamination starts in the drilling process with possible contamination from the diamond drill and initial handling of the core. Possible contamination on sample surface can be avoided, when picking the fragments for melting of fused bead, but when analyzing the core surface directly with P-XRF device, detecting the possible surface contamination is unavoidable.

During the powdering of picked fragments of sample A1, the most notable contamination sources were the tungsten carbide pan, the bullets and the Co binder. In the melting process, the Pt-Au alloy crucible and Li, B and Br of the fluxing agent were sources of contamination. Any kind of skin contact with the sample during the whole preparation was avoided for minimizing the skin contamination of e.g. K, Cl and S (Worley et al. 2006). Even thicknesses of the prepared samples for surface analyses and smoothness of the sample surfaces were also paid attention to, because of possible

effect later in analysis on the intensity of the emitted fluorescence (Potts et al. 1997a, Marguí 2013).

*7.1.2 Analysis*

The error sources related to the analysis process can be examined in two groups: instrumental errors and errors caused by the sample composition, known as matrix effects.

XRF spectrometers produce characteristic X-rays from Be-window and Rh-anode (in WD-XRF device) or Ag-anode (in P-XRF device) of the X-ray tube, which can be minimized by placing different filters between the tube and the sample (e.g. Potts and Webb 1992). Fluorescence might also be emitted from analyzing crystal and detector gas of WD-XRF device (Marguí 2013). Major problems with the energy dispersive detection style of P-XRF are related to the reduced resolution compared to WD-XRF (Young et al. 2016). Adding the miniaturized technology of a portable size, the detection of light elements become difficult (e.g. Mg and Al) or impossible (Na and lighter). In general, the detection limits are higher than with WD-XRF. The power of the X-ray tube of the portable device is clearly lower than that of laboratory apparatus and the rechargeable batteries slowly run down during long analysis series. This might negatively affect the success of P-XRF analyses.

In the sample itself, matrix effects are the biggest challenge. This means that other elements cause a distraction in the analysis process. In the energy spectrum, the neighboring elements might absorb or enhance each other, which is a problem in a sample with great compositional variability such as geological samples (Norrish and Hutton 1968). In WD-XRF analysis, the relatively good resolution decreases the elemental peak overlaps in the spectrum (Marguí 2013).

In addition to characteristic fluorescence of an element, secondary and even tertiary fluorescence, that all pile up in the results, are excited in the sample and detected. Also, Auger-emission, Compton scattering and Rayleigh scattering are caused by the incoming X-ray beam in the sample. Multiple correction methods such as FP in WD-XRF automatically correct previously mentioned error sources (Marguí 2013).

Quantitative correction might be done by the user with WD-XRF Omnian scans with manually modifying the Omnian spectrums, which can be considered as an error source as well.

*7.1.3 Outcrop notes*

When working in field and analyzing outcrops without sample preparation, the surface features become highly important factors affecting the success of the analyses. The reasons for notable amounts of e.g. Cl, P and especially S in the outcrop analyses (Table 4) are beyond the range of this work, but it can be concluded that different kinds of coverings are to be taken into account when working in field.

In addition to coverings and weathering, surface smoothness and grain size affect the outcrop analyses. Hardly ever is the outcrop so smooth that P-XRF device can be pressed tightly against the rock during the analysis. Uneven surface makes it harder for the emitted X-rays to “hit the target” and they might escape during the analysis (Potts et al. 1997b). Also, all the fluorescence might not get detected when there is space between the sample and the apparatus (Potts et al. 1997b). Curviness of the drill core surface causes the same problem although surface is smooth. Many error sources mentioned above can be eliminated or at least minimized with the attentiveness of the user, which is a remarkable part of working with P-XRF.

## 7.2 Feasibility of the introduced methods in field and drill core analyses

Table 6 summarizes the major differences regarding the use of the introduced methods. Whether conducting outcrop or drill core analyses, required quality of the results usually direct the decision when choosing between the methods available. Both qualitative and quantitative results are obtained only with WD-XRF quantitative application that utilizes calibrations with certified reference materials. WD-XRF Omnian scans reach to the level of being semi-quantitative and the actions of the user are in important role when evaluating the results. Good quality results are obtained with Omnian scans especially when fused bead is used as a sample type. Changing the sample type to rock surface has a remarkable effect on the results and quantitativeness

of the method decreases (Table 3, Fig. 11). Instrumental complexity increases the resolution of WD-XRF making it more quantitative but challenging to fit in a portable model.

P-XRF is as well semi-quantitative at the most. As suggested before (Fig. 12), depending on the element, P-XRF can give on average quite accurate results, e.g. for $SiO_2$ at least in the case of amphibolite. The relatively low price when compared to complex laboratory apparatus lowers the bar for choosing P-XRF as the method for at least preliminary analysis. P-XRF cannot replace accurate, quantitative methods, but in cases when sample cannot be detached, destroyed or modified, P-XRF might be the best choice also in semi-quantitative laboratory analyses. Therefore, when the most accurate whole rock geochemical results are not required, but broad classification is the target, Omnian scans for the sawed pieces of the core might not give significant further information compared to P-XRF, which might be considered more cost-effective method to obtain the wanted information.

Detecting hazardous substances in soils, sediments and pre-concentrated waters, or doing other scientific research, where collecting samples is restricted, semi-quantitative *in situ* analyses conductible with P-XRF spectrometer will absolutely be beneficial. Especially in field circumstances the fastness and ease of use are desirable properties. Holding the device in hand provides flexibility for indoor analyses also when for example drill core does not need to be removed from its container.

However, if quantitative results are required, the sample needs more preparation which is time-consuming and thus underlines the importance of careful selection of the most representative sample. Choosing the Omnian scans application for WD-XRF analysis, instead of WD-XRF quantitative application, stretches the sample type requirement. Time-consuming sample preparation of fused bead or pressed powder pellet can be skipped, if wanted, and a representative solid rock piece can be analyzed instead. However, chipped sample from an outcrop with altered or covered surface probably needs more preparation than drill core sample that may also already have the correct diameter to fit in the sample holder of the WD-XRF spectrometer. Polishing the analysis surfaces of the samples would easily eliminate any error sources related to surface topography.

In consequence, depending on the chosen method, preparation or lack of preparation cause multiple points of consideration for the evaluation of the results: representativeness, heterogeneity and contamination. User is also in an active role in every XRF method, whether during the sample preparation (WD-XRF) and/or during the analysis itself (P-XRF) or in correcting the received spectrums (WD-XRF Omnian scans). Utilizing portable XRF device does not require expertise and the procedure is quite straightforward. Yet, handheld device requires much more attention from the user during the analysis for the analyses to be successful than laboratory devices. On the other hand, laboratory WD-XRF devices require expertise during the whole analysis process from sample preparation to results evaluation. The professionality of the user need to be taken into account in the evaluation of error sources and contamination.

Table 6. Main differences regarding the use of XRF methods introduced in this work.

| Method | Axios mAX<br>WD-XRF<br>quantitative app. | Axios mAX<br>WD-XRF<br>Omnian scans | Niton XL3t GOLDD+<br>portable ED-XRF<br>mining mode |
|---|---|---|---|
| Data quality | qualitative +<br>quantitative | qualitative+<br>semi-quantitative | qualitative+<br>semi-quantitative |
| Detectible elemental range | O–U | O–U | Mg–U |
| Sample type | fused bead | fused bead<br>powder pellet<br>solid rock surface | almost any kind |
| Contamination from | sample prep. | sample prep. | sample prep.<br>coverings in outcrops |
| Error sources | matrix effects<br>instrumental errors | matrix effects<br>instrumental errors<br>heterogeneity<br>surface topography<br>spectrum modification | matrix effects<br>instrumental errors<br>heterogeneity<br>surface topography |
| User activity | sample prep.<br>application options | sample prep.<br>spectrum modification | holding the apparatus |
| Expensiveness of the device<br>(to purchase and maintain) | relatively<br>expensive | relatively expensive | relatively inexpensive |
| Required expertise | high | high | low |
| Fastness | relatively slow | relatively slow | relatively fast |

### 7.3 Improvements and possible future studies regarding the P-XRF

The effect of weathering and contamination on the analysis surfaces of the outcrops was not studied very extensively in this work. The major conclusions were that the major element oxide sums were on average notably lower compared to drill core results. Although clean surfaces can be favored over the covered ones in field, the surfaces are always uneven which has a huge impact on the success of the analysis. In addition to unevenness, different coverings have a remarkable effect on the results. For example S, Cl and P are more abundant on the outcrop surfaces for unknown reasons. It would require more examining and expertise of different scientific fields to reveal the effects of different coverings.

Potts et al. (2006) examined the weathering effects on the P-XRF results and based on surface concentrations and bulk rock compositions calculated ratios for correcting the weathering effects for different elements in rhyolite and dolerite samples. Corrected values were compared to accurate WD-XRF results of the rocks and corrections were found to improve some element values and worsen others. However, weathering effects were also found to be very complex and dependent on multiple factors and generalizations were therefore not recommended. When examining the quantitative geochemistry of a rock type, analyzing weathered, or in other ways poor quality, surface should be avoided at least for the fact that XRF spectrometer excited fluorescence has been detected to originate mostly from depths of 0.01–5 mm (Potts et al. 1997a).

The problem with outcrop surface roughness and curviness of the drill core, both leaving a layer of air between the device and sample was also noticed to be part of the problem of low sum values in P-XRF analyses. Potts et al. (1997b) noticed that an air layer as thin as 1–2 mm is enough to cause major errors in the results, but with the help of scatter peak normalization a correction function for neutralizing surface roughness effects could be derived at least for elements with a higher atomic number. With further XRF outcrop studies and detailed descriptions of the coverings, it would be interesting to try and improve the corrections with Kumpula campus area outcrop and drill core materials.

On the base of this work, future studies regarding the improvement of P-XRF device should include problem solving of user effects by developing a portable light weight stand of some kind. Working in field would also benefit of a method for easily erasing weathered and contaminated surface layer thus also improving the surface smoothness. It would also be important to improve the detection limits and ability of detecting light elements, so that quantitative P-XRF analysis would become more accurate.

### 7.4 Drill core geochemistry: Omnian scans and P-XRF analyses

Taking the formerly mentioned weaknesses of P-XRF device into account, the decision of analyzing on average only one spot of each rock type unit in the drill core with P-XRF did not give reliable enough information about the geochemistry of the rock types. It would have been reasonable, but more time-consuming, to take multiple analyses of each unit and calculate average values.

Multiple P-XRF analyses from amphibolite sample A1 revealed the small-scale heterogeneity of the amphibolite. The P-XRF–WD-XRF quantitative application comparison suggests that $SiO_2$, CaO, $P_2O_5$ and MnO concentrations of the drill core obtained with P-XRF can be examined quite confidently on average, although major element oxide sums are only 84.63 wt.% on average in ten amphibolite curved surface analyses.

In future studies, it would be interesting to include multiple P-XRF analyses and accurate WD-XRF quantitative analyses of the other rock types present in the drill core as well. This would bring more information and test the interpretations drawn so far based only on amphibolite about the accuracy of P-XRF.

Twelve sawed pieces of the amphibolite were supposed to give an idea of the possible change in geochemistry of amphibolite in relation to depth (Fig. 16). Study was conducted with WD-XRF Omnian scans and P-XRF, so that comparison between the methods could also be done, and double results were considered to provide more reliable information. The results did give a fairly wide geochemical range for the amphibolite, but correlation in relation to depth was not observed in this scale. On the other hand, the uncertainties of the analysis methods were in such a big role that

possible change in geochemistry in relation to depth might not even get detected this way.

WD-XRF Omnian scans from rock surfaces did not prove to be more accurate than P-XRF on average, but the major advantage of the method is the ability to detect light elements (Na, Al and Mg) better (Fig. 11). The relatively high correlation in CaO and $K_2O$ analyses according to the method comparison based on 12 samples (Fig. 13) does not mean that the results are accurate, however. In case of $K_2O$, both methods give too low results when compared to WD-XRF quantitative application. It is also clear that P-XRF gives lower values for $Al_2O_3$ and MgO when compared to either Omnian scans or quantitative application. $Al_2O_3$ result obtained with Omnian scans from rock surface is quite accurate, but MgO is too low. Harker diagrams of the P-XRF results (Fig. 14) reveal the shortcomings of the initial rock type classification. Rock type identification of some analysis points would require revising.

Although the P-XRF results cannot be considered quantitative in general, relative abundances of the major element oxides (e.g. $SiO_2$, $FeO_t$, MgO) give adequate hints of the lithological changes in the core and a broad felsic-mafic discrimination could be made even without any visual logging data.

### 7.5 Considerations of petrology and a comparison to local geology

The rocks of Helsinki area show very little original or pre-orogeny features or textures (Laitala 1991, Kähkönen 1998). Only some sparse striping suggests a layered, probably a tuffaceous rock for the protolith, and Laitala (1991) thus assumes that areas amphibolites and hornblende gneisses were originally tuffaceous sediments, alkaline volcanic rocks and in some areas possibly alkaline plutonic rocks. During the collision of island arc and old Archean bedrock, low pressure greenschist/amphibolite facies metamorphism took place and shaped most of the rock types visible in Kumpula campus drill core today. Metamorphosis is thought to have happened in 15–20 km depth, at 500–700 °C (Laitala 1991, Kähkönen 1998).

The obtained geochemical and petrographic data was successfully connected to former presentation of the Helsinki and southern Finland geology by, e.g., Laitala (1991) and

Korsman and Koistinen (1998). However, the accurate petrology of the amphibolite is based on only one quantitative WD-XRF analysis and one thin section. More reliable interpretation would require multiple analyses and more quantitative trace element studies. Other three rock types presented are described only by their petrographical features and single Omnian scans results and thus have even more uncertain petrogenesis. More profound thin section works with samples from the whole length of the drill core would bring wider knowledge about the mineral compositions and heterogeneities of the described rock types. Future studies will bring more information and test the conclusions drawn below.

### *7.5.1 Amphibolite*

Calc-alkaline magmas, that produce rock types typical of mature arcs, have high silica (see Equation [1]) and alkali contents (Best 2003). This kind of magma development was favored when Archean crust and an active island arc system collided and related continental growth was increasingly thickening the crust (Korsman and Koistinen 1998, Best 2003). Mg number (see Equation [2]), suggests the magma not to be primary.

Increasing temperature and the presence of fluids during the metamorphosis changed the texture of the amphibolite to more granoblastic. Ca-Al-silicates, albite and aluminous chlorite together probably formed hornblende and more Ca-rich plagioclase (Best 2003).

TAS diagram (Fig. 9) and Zr/Ti–Nb/Y diagram (Fig. 10.A) give different results for the protolith of the amphibolite, which underlines the importance of considering the alkali mobilization when studying the petrogenesis of metamorphic rocks. It would be interesting to see more precise plotting of the amphibolite in the Zr/Ti – Nb/Y diagram with better trace element results obtained e.g. with inductively coupled mass spectrometry (ICP-MS).

Comparing to whole rock analyses of nearest temporally related amphibolite units (Fig. 10, Fig. 16, Table 7), $SiO_2$ wt.% seems to be higher in quantitative WD-XRF analysis of the sample A1 in this work (57.41 wt.%) than in the other amphibolite units on average (48.67 wt.%). Sample A1 values for $Al_2O_3$ (15.37 wt.%), $Na_2O$ (3.93 wt.%) and $K_2O$

(1.65 wt.%) are also higher than average values of the nearest units (14.83 wt%, 3.11 wt.% and 0.86 wt.% respectively). The rest of the major element oxide values are lower. This indicates the amphibolite sample A1 chosen for this work to be more felsic than the selected samples of GTK. Utilizing the ICP-MS results of the same analysis points (Appendix VII) and plotting the results in Zr/Ti–Nb/Y diagram (Fig. 10.A) set the values is basaltic, basaltic-andesite and alkali basalt areas. Sample number 6 from Sääksjärvi plots very close to sample A1. GTK samples are from quite a large area (Fig. 16), each being quite far from Kumpula campus drill hole.

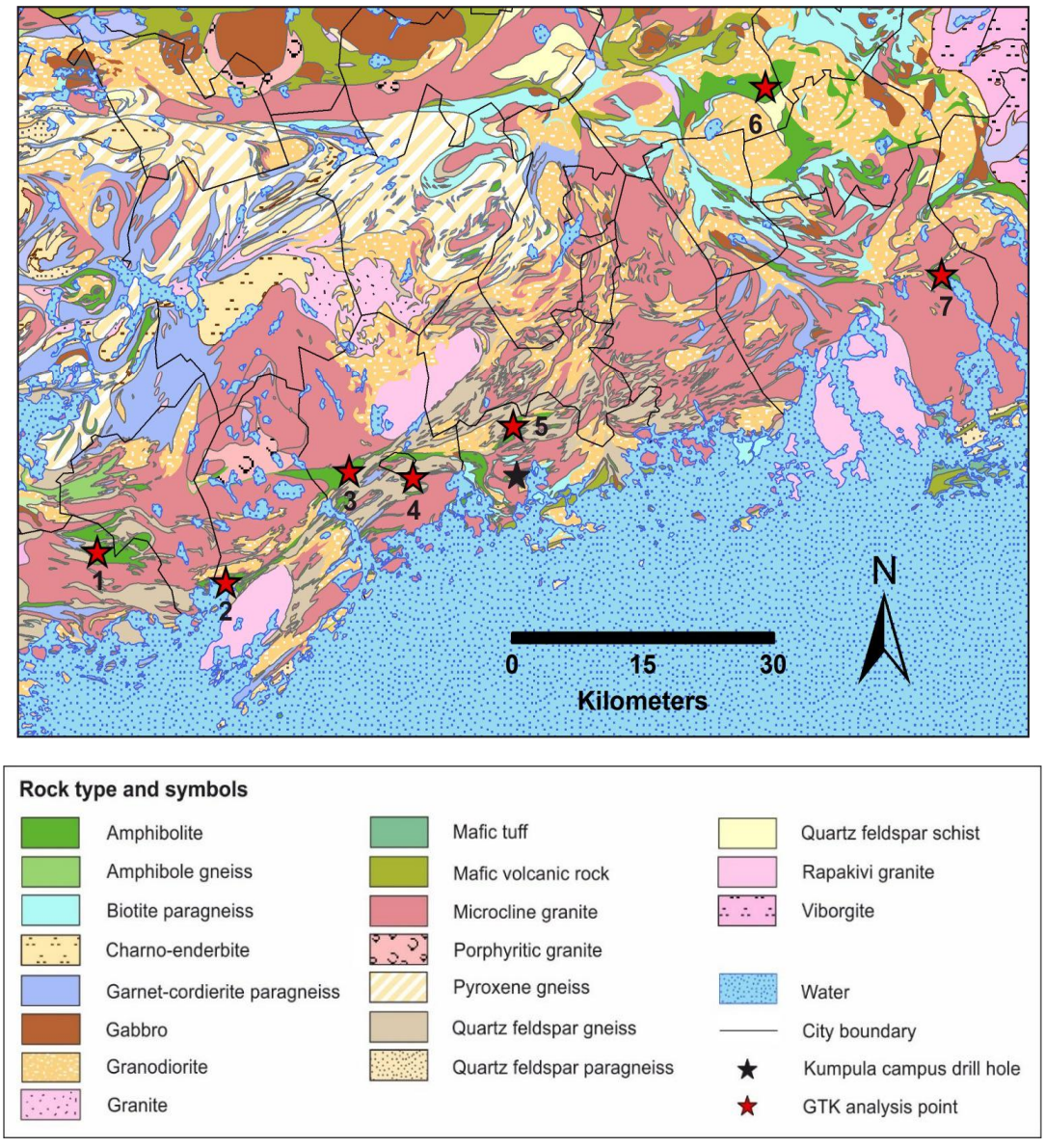


Figure 16. Locations of the seven closest analysis points of GTK The rock geochemical database of Finland from temporally related amphibolite units in relation to Kumpula campus drill hole. Bedrock map after GTK. Basemap of Finland and city boundaries © NLS.

Table 7. Whole-rock geochemistry of selected temporally related amphibolite units. Results are obtained with Phillips PW1480 WD-XRF with pressed powder pellets. Data from GTK rock geochemical database of Finland (Rasilainen et al. 2007).

| Point ID | 1 | 2 | 3 | 4 | 5 | 6 | 7 | |
|---|---|---|---|---|---|---|---|---|
| Location | Inkoo | Kirkkonummi | Espoo | Espoo | Helsinki | Sääksjärvi | Porvoo | |
| Rock type | Amp. | Amp. | Amp. | Amp. | M.volc. | Amp. | M.volc. | avg. |
| $SiO_2$ (wt.%) | 45.40 | 47.10 | 53.00 | 50.70 | 51.40 | 50.10 | 43.00 | 48.67 |
| $TiO_2$ | 2.70 | 0.64 | 0.62 | 2.38 | 0.96 | 1.77 | 2.44 | 1.64 |
| $Al_2O_3$ | 12.10 | 15.60 | 16.70 | 13.80 | 16.70 | 15.90 | 13.00 | 14.83 |
| FeOt | 15.93 | 7.77 | 7.76 | 13.32 | 9.90 | 8.73 | 11.25 | 10.66 |
| MnO | 0.26 | 0.16 | 0.16 | 0.24 | 0.19 | 0.15 | 0.17 | 0.19 |
| MgO | 5.24 | 8.57 | 4.36 | 3.41 | 3.96 | 4.24 | 5.53 | 5.04 |
| CaO | 8.22 | 11.60 | 8.09 | 7.16 | 6.62 | 7.69 | 11.40 | 8.68 |
| $Na_2O$ | 2.19 | 1.74 | 2.75 | 3.06 | 4.77 | 3.63 | 3.62 | 3.11 |
| $K_2O$ | 1.07 | 0.28 | 0.68 | 0.83 | 0.72 | 1.62 | 0.85 | 0.86 |
| $P_2O_5$ | 0.12 | 0.03 | 0.10 | 0.24 | 0.20 | 0.93 | 0.30 | 0.27 |
| Sum | 93.23 | 93.48 | 94.21 | 95.13 | 95.42 | 94.76 | 91.55 | 93.97 |
| Ba (ppm) | 163 | 61.8 | 213 | 179 | 392 | 596 | 459 | |
| Cl | 741 | 141 | 261 | 483 | 80.1 | 505 | 146 | |
| S | 220 | 737 | 114 | 591 | 78 | 2270 | 1500 | |
| | | | | | | | | |
| Cr | <19 | 491 | 47.1 | 27 | 24 | 27 | 96.1 | |
| Cu | 30.1 | 72 | 17 | 33.9 | <17 | 129 | 188 | |
| Ga | 22 | 19 | 23.2 | 23.7 | 29 | 29.8 | 31.4 | |
| Nb | <7 | <7 | <7 | 7.6 | <7 | 22.5 | 45.9 | |
| Ni | <14 | 103 | <14 | 15 | <14 | 38.4 | 122 | |
| Pb | 16 | <14 | 22 | 23 | 27 | 16 | 15 | |
| Rb | 66.1 | 14.6 | 15.3 | 20.7 | 33.1 | 141 | 29 | |
| Sr | 121 | 153 | 272 | 149 | 224 | 1200 | 323 | |
| V | 974 | 185 | 184 | 459 | 209 | 221 | 395 | |
| Y | 30.6 | 9.1 | 16 | 46.7 | 17.4 | 20.3 | 21.3 | |
| Zn | 175 | 77 | 92.3 | 135 | 131 | 141 | 121 | |
| Zr | 84.8 | 21 | 70.5 | 194 | 115 | 186 | 195 | |

Mo excluded (all values <LOD)
Amp.= amphibolite
M.volc.= mafic volcanite

### *7.5.2 Other rock types*

Diopside-actinolite skarn indicates low temperature metamorphic conditions with active metasomatism. Laitala (1991) states that metasomatism between the impure limestones, gneissic layers and gneissic surrounding rocks of the area formed skarn. Diopside has partly altered to actinolite, plagioclase has albitized and released Ca and Al that served as building material for epidote and zoisite. Free Ca together with Ti-oxides probably formed sphenes (Best 2003).

Low-temperature metamorphic conditions formed also actinolite rocks with high MgO content. All the clinopyroxenes altered to actinolite and some chlorite (Best 2003). The grain size is smaller than that of amphibolites and mineral grains are subhedral or anhedral. Granite has probably formed later during the orogeny and intruded the

metamorphic rocks following their structural control (Laitala 1991, Korsman and Koistinen 1998).

## 8. CONCLUSIONS

Amphibolite, granite, actinolite rock and diopside-actinolite skarn among with migmatite and gneiss are found in Kumpula campus bedrock. Variation in rock types is wider than bedrock map suggests but all can be connected to former geological interpretations of the Helsinki area. The amphibolite of Kumpula seems more felsic than nearest temporally related amphibolite units. To specify the petrogenesis of amphibolite and other described rock types, would it require more extensive thin section and trace element studies.

WD-XRF Omnian scans and quantitative application suggest almost similar results for fused bead of amphibolite sample A1. Changing the sample type to solid rock surface of sample A1 introduces heterogeneity related problems to the quantitative determination of Omnian scans. Omnian scans and P-XRF analyses of twelve sawed pieces of the amphibolite from different depths of the drill core suggest quite wide compositional range for the amphibolite. The cause is probably a combination of amphibolite heterogeneity and methodology caused variation. Correlation along depth cannot be observed. Omnian scans and P-XRF results seem to correlate best with CaO and $K_2O$. MgO and $Al_2O_3$ values are always lower with P-XRF.

Analyzing the drill core surface with P-XRF was found to be useful, fast and easy method for detecting broad geochemical changes although major element oxide sum is only 84.00 wt.% on average. Comparing ten P-XRF analyses of sample A1 to WD-XRF quantitative application analysis of fused bead revealed that P-XRF $SiO_2$ wt.% value is quite accurate on average. Other relatively accurate P-XRF results on average are for CaO and MnO. On the other hand, MgO, $K_2O$ and $Al_2O_3$ are poorly detected with P-XRF device.

Outcrop studies conclude that the quality of the analysis surface has a major impact on the success of P-XRF analyses. Considerable factors are smoothness, grain size,

weathering, pollution, alteration and organisms such as lichen and moss. Major oxide sum values of outcrop studies are very low, yet enhanced concentrations of Cl, P and S are detected especially on poor quality surfaces. The reasons for enhancements would require further research.

Comparing to other introduced methods, utilizing P-XRF requires much more attention from the user during the analyses. However, WD-XRF quantitative method, WD-XRF Omnian scans and P-XRF were all proven to be useful methods in different contexts. Selection depends on the study and the need for further analyses should be evaluated in each case.

## 8. ACKNOWLEDGEMENTS

I would like to express my gratitude to my supervisors Jussi Heinonen and Ilmo Kukkonen for helping me develop as a geologist during this master's thesis project. Special appreciation goes to Pasi Heikkilä for patient guidance with everything related to complex XRF methods. I also wish to acknowledge the help provided by Helena Korkka for preparing the thin sections and Matti Poutiainen for helping me with the thin section interpretations. Finally, for never ending support and encouragement, my gratitude belongs to my family and friends.

## 9. REFERENCES


Best, M.G. 2003. Igneous and Metamorphic petrology. 2nd edition. Blackwell Science Ltd, Malden, 729 p.

Ewart, A. 1982. The mineralogy and petrology of Tertiary-Recent orogenic volcanic rocks with special reference to the andesitic-basaltic compositional range. In: Thorpe, R.S. (Eds.), Andesites: Orogenic Andesites and Related Rocks.

Geological survey of Finland, 2017. Bedrock map of Finland scale-free, version 2.1.

Hatakka, T., Nuottimäki, K., Sarala, P., Taivalkoski, A. and Tarvainen, T. 2016. Kenttä-XRF-analysaattorin soveltuvuus geokemiallisiin taustapitoisuustutkimuksiin. Geological survey of Finland, Espoo, archive report 97/2015, 115 p.

Heikkilä, P. 2015. Mineralogy laboratory manual. Department of Geosciences and Geography, University of Helsinki, 18 p.

Irvine, T.N. and Baragar, W.R.A. 1971. A Guide to the Chemical Classification of the Common Volcanic Rocks. Canadian Journal of Earth Sciences, 8, 523–548.

Kivinen, A. (GRM-Services Oy) 2016. Kampusreikä: Geofysikaaliset reikämittaukset, work report, 13 p.

Korsman, K. and Koistinen, T. Suomen kallioperän yleispiirteet. 1998. In Lehtinen, M., Nurmi, P. and Rämö, T. (Eds.). Suomen kallioperä: 3000 vuosimiljoonaa. The Geological Society of Finland, Helsinki, 93–104.

Kramar, U. 1997. Advances in energy-dispersive X-ray fluorescence. Journal of Geochemical Exploration 58, 73–80.

Kretz, R. 1983. Symbols for rock-forming minerals. American Mineralogist 68, 277–279.

Kukkonen, I.T., Koivisto, E. and Whipp, D. 2016. Helsinki University Kumpula campus drillhole project. In: Kukkonen et al. (Eds.), Lithosphere 2016 – Ninth Symposium on the Structure, Composition and Evolution of the Lithosphere in Finland. Programme and Extended Abstracts, Espoo, Finland, November 9–11, 2016. Institute of Seismology, University of Helsinki, Report S-65, 166 p.

Kuno, H. 1986. Differentiation of basalt magmas. In: Hess, H.H and Poldervaart, A. (Eds.) Basalts: The Poldervaart treatise on rocks of basaltic composition, 2, Interscience, New York, 623–688.

Kähkönen, Y. Svekofenniset liuskealueet. 1998. In: Lehtinen, M., Nurmi, P. and Rämö, T. (Eds.). Suomen kallioperä: 3000 vuosimiljoonaa. The Geological Society of Finland, Helsinki, 199–227.

Laitala, M. 1991. Pre-Quaternary rocks of the Helsinki map-sheet area. Explanation to the maps of pre-quaternary rocks. Geological survey of Finland. Sheet 2034.

Le Bas, M.J., Le Maitre, R.W., Streckeisen, A. and Zanettin, B. 1986. A Chemical Classification of Volcanic Rocks Based on the Total Alkali-Silica Diagram. Journal of Petrology 27, part 3, 745–750.

Liritzis, I. and Zacharias, N. 2011. Portable XRF of Archaeological Artifacts: Current Research, Potentials and Limitations. In: Shackley, M.S. (Eds.). X-Ray Fluorescence Spectrometry (XRF) in Geoarchaeology, 109–142.

Marguí, E., Grieken, R. van, 2013. X-Ray Fluorescence Spectrometry and Related Techniques: An Introduction. Momentum Press, New York, 142 p.

Marguí, E., Hidalgo, M., Queralt, I., Meel, K. van and Fontàs, C. 2012. Analytical capabilities of laboratory, benchtop and handheld X-ray fluorescence systems for detection of metals in aqueous samples pre-concentrated with solid-phase extraction disks. Spectrochimica Acta Part B 67, 17–23.

Markey, A.M., Clark, C.S., Succop, P.A. and Roda, S. 2008. Determination of the Feasibility of Using a Portable X-Ray Fluorescence (XRF) Analyzer in the Field for Measurement of Lead Content of Sieved Soil. Journal of Environmental Health 70, 24–29.

National Land Survey of Finland. 2016. General map of Finland, 1: 1 000 000.

National Land Survey of Finland. 2016. Basemap of Helsinki, sheet L4133L.

Nironen, M., Proterotsooiset orogeeniset syväkivet. In: Martti Lehtinen, Pekka Nurmi and Tapani Rämö (Eds.) 1998. Suomen kallioperä: 3000 vuosimiljoonaa. The Geological society of Finland, Helsinki 375 p.

Norrish, K. and Chappell, B.W. 1967. X-ray Fluorescence Spectroscopy. In: Zussman, J. (Eds.) Physical methods in determinative mineralogy. Academic Press, London, 161–214.

Norrish, K. and Hutton, J.T. 1968. An accurate X-ray spectrographic method for the analysis of a wide range of geological samples. Geochimica et Cosmochimica Acta, 33, 431–453.

Pajunen, M., Airo, M.-L., Elminen, T., Mänttäri, I., Niemelä, R., Vaarma, M., Wasenius, P. and Wennerström, M. 2008. Tectonic evolution of the Svecofennian crust in southern Finland. In: Pajunen, M. (Eds.). Tectonic evolution of the Svecofennian crust in southern Finland – a basis for characterizing bedrock technical properties. Geological Survey of Finland, Special Paper 47, 15–160.

PANalytical. 2018. Omnian method. Page visited 5.4.2018. http://www.panalytical.com/Xray-fluorescence-software/Omnian.htm

Parsons, C., Grabulosa, E.M., Pili, E., Floor, G.H., Roman-Ross, G. and Charlet, L. 2013. Quantification of trace arsenic in soils by field-portable X-ray fluorescence spectrometry: Considerations for sample preparation and measurement conditions. Journal of Hazardous Materials 262, 1213–1222.

Pearce, J.A. 1996. A User's guide to Basalt Discrimination Diagrams. In: Wyman, D.A. (Eds.) Trace Element Geochemistry of Volcanic Rocks: Applications for Massive Sulphide Exploration. Geological Association of Canada, Short Couse Notes 12, 79–113.

Penttilä, K., Kukkonen, I., Heinonen, J.S., Räisänen, M. and Valtonen, R. 2016. Logging and lithology of the Kumpula Campus drill hole. Poster presentation in: Lithosphere 2016 – Ninth Symposium on the Structure, Composition and Evolution of the Lithosphere in Finland. Espoo, Finland, November 9-11.

Potts, P. J., Williams-Thorpe, O. and Webb, P.C. 1997a. The Bulk Analysis of Silicate Rocks by Portable X-Ray Fluorescence: Effect of Sample Mineralogy in Relation to the Size of the Excited Volume. Geostandard Newsletter, 21, 29–41.

Potts, P. J., Webb, P. C. and Williams-Thorpe, O. 1997b. Investigation of a Correction Procedure for Surface Irregularity Effects Based on Scatter Peak Intensities in the Field Analysis of Geological and Archaeological Rock Samples by Portable X-ray Fluorescence Spectrometry. Journal of Analytical Atomic Spectrometry, 12, 769–776.

Potts, P.J. and Webb, P.C. 1992. X-ray fluorescence spectrometry. Journal of Geochemical Exploration 44, 251–296.

Potts, P.J., Bernardini, F., Jones, M.C., Williams-Thorpe, O. and Webb, P.C. 2006. Effects of weathering on *in situ* portable X-ray fluorescence analyses of geological outcrops: dolerite and rhyolite outcrops from the Preseli Mountains, South Wales. X-Ray Spectrometry 35, 8–18.

Rasilainen, K., Lahtinen, R. and Bornhorst, T.J. 2007. The Rock Geochemical Database of Finland. Geological survey of Finland. Report of Investigation 164.

Rowe, H., Hughes, N. and Robinson, K. 2012. The quantification and application of handheld energy-dispersive x-ray fluorescence (ED-XRF) in mudrock chemostratigraphy and geochemistry. Chemical Geology 324–325, 122–131.

Sarala, P., Taivalkoski, A. and Valkama, J. 2014. Kannettavan XRF-analysaattorin käyttö moreenigeokemiallisessa tutkimuksessa. Geological survey of Finland, Rovaniemi, archive report 120/2014, 22 p.

Shrivastava, P., O'Connell, S. and Whitley, A. 2005. Handheld X-Ray Fluorescence: Practical Application as a Screening Tool to Detect the Presence of Environmentally-Sensitive Substances in Electronic Equipment. Proceedings of the 2005 IEEE International Symposium on Electronics and the Environment, New Orleans, LA, USA, May 16–19, 2005, 157–162.

Winchester, J.A. and Floyd. P.A. 1977. Geochemical discrimination of different magma series and their differentiation products using immobile elements. Chemical Geology, 20, 325–343.

Worley, C.G., Wiltshire, S.S., Miller, T.C., Havrilla, G.J and Majidi, V. 2006. Detection of visible and latent fingerprints by micro-X-ray fluorescence. Advances in X-ray Analysis, 49, 363–368.

Young, K.E., Evans, C.A., Hodges, K.V., Bleacher, J.E. and Graff, T.G. 2016. A review of the handheld X-ray fluorescence spectrometer as a tool for field geologic investigations on Earth and in planetary surface exploration. Applied Geochemistry 72, 77–87.

## APPENDIX I: Sawed surface P-XRF data of the amphibolite sample A1

| ID | 1 | 2 | 3 | 4 | 5 | 6 | 7 | 8 | 9 | 10 |
|---|---|---|---|---|---|---|---|---|---|---|
| $SiO_2$ (wt.%) | 59.98 | 59.91 | 59.67 | 56.80 | 57.48 | 56.52 | 54.73 | 58.32 | 57.37 | 58.62 |
| $TiO_2$ | 0.77 | 0.79 | 0.77 | 0.82 | 0.95 | 0.76 | 0.76 | 0.70 | 0.82 | 0.87 |
| $Al_2O_3$ | 12.12 | 11.81 | 11.40 | 10.14 | 10.76 | 11.13 | 9.69 | 11.33 | 10.41 | 10.47 |
| $FeO_t$ | 5.15 | 5.56 | 5.35 | 6.84 | 6.55 | 5.70 | 6.28 | 6.42 | 6.87 | 7.21 |
| MnO | 0.09 | 0.09 | 0.08 | 0.14 | 0.11 | 0.10 | 0.13 | 0.13 | 0.14 | 0.15 |
| MgO | 0.99 | 1.83 | 1.46 | 1.81 | 1.84 | 1.52 | 1.53 | 1.33 | 2.25 | 2.52 |
| CaO | 5.91 | 6.18 | 5.82 | 6.63 | 5.86 | 6.21 | 6.37 | 6.99 | 6.54 | 6.68 |
| $K_2O$ | 1.19 | 1.26 | 1.30 | 1.15 | 1.54 | 1.22 | 1.01 | 0.97 | 1.13 | 1.17 |
| $P_2O_5$ | 0.20 | 0.16 | 0.18 | 0.12 | 0.22 | 0.22 | 0.12 | 0.17 | 0.20 | 0.19 |
| Sum | 86.41 | 87.61 | 86.03 | 84.44 | 85.32 | 83.37 | 80.61 | 86.37 | 85.72 | 87.86 |
| Ba (ppm) | 510 | 540 | 530 | 530 | 490 | 500 | 520 | 520 | 530 | 560 |
| Cl | n.d. | 230 | 180 | n.d. | 80 | 480 | n.d. | 150 | 70 | 270 |
| S | n.d. | 400 | 150 | 270 | 230 | n.d. | 150 | 180 | 170 | 220 |
| Cr | 200 | 240 | 210 | 260 | 250 | 210 | 210 | 200 | 260 | 320 |
| Ni | n.d. | n.d. | n.d. | n.d. | n.d. | n.d. | n.d. | n.d. | 50 | 60 |
| Rb | 20 | 20 | 20 | 20 | 30 | 20 | 20 | 20 | 20 | 20 |
| Sn | 30 | n.d. | n.d. | n.d. | n.d. | n.d. | n.d. | n.d. | n.d. | 40 |
| Sr | 250 | 240 | 260 | 220 | 230 | 240 | 220 | 240 | 210 | 200 |
| V | 200 | 200 | 200 | 260 | 270 | 250 | 230 | 280 | 250 | 250 |
| Zn | 30 | 40 | 30 | 40 | 40 | 30 | 40 | 30 | 40 | 50 |
| Zr | 150 | 30 | 40 | 50 | 50 | 30 | 80 | 140 | 60 | 40 |

Excluded elements (all values <LOD): Cu,Nb,Co,As,Se,Mo,Pd,Ag,Cd,Sb,W,Au,Pb,Bi

## APPENDIX II: Curved surface P-XRF data of the amphibolite sample A1

| ID | 1 | 2 | 3 | 4 | 5 | 6 | 7 | 8 | 9 | 10 |
|---|---|---|---|---|---|---|---|---|---|---|
| $SiO_2$ (wt.%) | 56.14 | 58.09 | 58.37 | 57.58 | 59.08 | 54.93 | 53.38 | 54.25 | 58.74 | 60.81 |
| $TiO_2$ | 0.83 | 0.87 | 0.69 | 0.87 | 0.56 | 1.04 | 0.99 | 1.12 | 1.15 | 0.86 |
| $Al_2O_3$ | 11.66 | 10.63 | 11.95 | 10.36 | 11.41 | 9.81 | 10.37 | 11.04 | 11.79 | 12.30 |
| $FeO_t$ | 6.76 | 6.06 | 4.70 | 5.67 | 4.84 | 7.87 | 6.42 | 6.27 | 6.75 | 5.80 |
| MnO | 0.13 | 0.10 | 0.06 | 0.10 | 0.09 | 0.15 | 0.10 | 0.11 | 0.11 | 0.10 |
| MgO | 2.35 | 1.39 | 1.43 | 1.71 | 1.71 | 1.74 | 1.47 | 2.08 | 2.37 | 1.86 |
| CaO | 6.63 | 5.62 | 5.69 | 5.26 | 6.27 | 6.25 | 5.36 | 5.68 | 5.21 | 5.83 |
| $K_2O$ | 1.23 | 1.40 | 1.24 | 1.52 | 0.92 | 1.46 | 1.73 | 1.61 | 1.85 | 1.52 |
| $P_2O_5$ | 0.18 | 0.20 | 0.17 | 0.10 | 0.23 | 0.24 | 0.25 | 0.30 | 0.22 | 0.19 |
| Sum | 85.91 | 84.36 | 84.30 | 83.17 | 85.11 | 83.48 | 80.08 | 82.47 | 88.17 | 89.26 |
| Ba (ppm) | 580 | 520 | 440 | 560 | 470 | 570 | 550 | 580 | 630 | 510 |
| Cl | 250 | 330 | 210 | 1020 | 490 | 350 | 290 | 460 | 380 | 100 |
| S | 370 | 240 | 390 | 300 | 370 | 290 | 230 | 330 | 380 | 240 |
| Cr | 260 | 250 | 210 | 230 | 170 | 340 | 220 | 240 | 290 | 220 |
| Ni | n.d. | n.d. | n.d. | n.d. | n.d. | 60 | n.d. | n.d. | n.d. | n.d. |
| Rb | 20 | 30 | 20 | 20 | 20 | 30 | 30 | 20 | 30 | 20 |
| Sn | n.d. | n.d. | n.d. | n.d. | 30 | n.d. | n.d. | n.d. | n.d. | 30 |
| Sr | 250 | 230 | 270 | 230 | 270 | 200 | 210 | 220 | 230 | 240 |
| V | 230 | 280 | 180 | 240 | 170 | 310 | 240 | 280 | 250 | 210 |
| Zn | 40 | 50 | 30 | 40 | 30 | 50 | 40 | 40 | 40 | 30 |
| Zr | 20 | 50 | 70 | 60 | 40 | 30 | 50 | 70 | 40 | 70 |

Excluded elements (all values <LOD): Cu,Nb,Co,As,Se,Mo,Pd,Ag,Cd,Sb,W,Au,Pb,Bi

**APPENDIX III: WD-XRF Omnian scans data of the drill core samples**

| ID | t1s1 | t1s2 | t1s3 | t1s4 | t1s5 | t1s6 | t1s7 | t1s8 | t1s9 | t1s10 | t1s11 | t1s12 | t2 | t3 | t4 |
|---|---|---|---|---|---|---|---|---|---|---|---|---|---|---|---|
| Depth (m) | 3.90 | 36.00 | 63.35 | 88.95 | 105.35 | 128.30 | 156.00 | 203.00 | 241.55 | 323.20 | 336.70 | 361.60 | 351.50 | 35.00 | 145.70 |
| $SiO_2$ (wt.%) | 50.58 | 50.48 | 51.23 | 53.95 | 55.62 | 48.22 | 49.32 | 56.56 | 56.77 | 50.75 | 51.96 | 59.32 | 72.04 | 43.19 | 51.91 |
| $TiO_2$ | 0.86 | 1.00 | 0.78 | 0.90 | 0.83 | 0.88 | 0.86 | 0.78 | 0.72 | 0.97 | 0.88 | 0.75 | 0.08 | 0.58 | 0.68 |
| $Al_2O_3$ | 16.34 | 15.80 | 18.07 | 14.89 | 15.33 | 15.76 | 16.85 | 16.48 | 16.16 | 15.71 | 17.36 | 16.55 | 13.75 | 8.20 | 18.15 |
| FeOt | 5.82 | 6.93 | 4.46 | 5.43 | 5.53 | 7.46 | 4.71 | 5.57 | 4.33 | 6.53 | 6.61 | 3.50 | 0.72 | 8.87 | 1.35 |
| MnO | 0.11 | 0.11 | 0.07 | 0.11 | 0.10 | 0.16 | 0.11 | 0.09 | 0.06 | 0.09 | 0.13 | 0.10 | 0.02 | 0.17 | 0.04 |
| MgO | 4.09 | 5.40 | 3.63 | 5.15 | 3.98 | 7.45 | 4.90 | 4.80 | 5.65 | 5.39 | 4.09 | 3.36 | 0.35 | 17.73 | 5.33 |
| CaO | 7.03 | 6.18 | 7.29 | 5.93 | 5.62 | 3.78 | 6.27 | 3.39 | 2.22 | 8.09 | 5.56 | 2.69 | 1.20 | 7.30 | 10.59 |
| $Na_2O$ | 3.92 | 3.91 | 4.94 | 3.88 | 3.81 | 3.36 | 4.55 | 4.27 | 4.43 | 4.54 | 4.64 | 5.13 | 4.08 | 0.30 | 4.30 |
| $K_2O$ | 0.93 | 1.96 | 0.55 | 1.51 | 1.52 | 3.90 | 1.53 | 2.30 | 3.75 | 0.68 | 1.76 | 2.75 | 4.23 | 3.81 | 0.92 |
| $P_2O_5$ | 0.25 | 0.25 | 0.25 | 0.22 | 0.21 | 0.18 | 0.19 | 0.18 | 0.19 | 0.27 | 0.20 | 0.22 | 0.05 | 0.17 | 0.26 |
| Sum | 89.93 | 92.02 | 91.27 | 91.96 | 92.55 | 91.15 | 89.29 | 94.40 | 94.28 | 93.02 | 93.19 | 94.37 | 96.53 | 90.30 | 93.52 |
| Cl (ppm) | 110 | 150 | 180 | 140 | 110 | 180 | 100 | 160 | 120 | 150 | 170 | 570 | 190 | 140 | 80 |
| F | 0 | 1220 | 0 | 0 | 0 | 1890 | 1500 | 0 | 2130 | 1600 | 1590 | 1400 | 0 | 1390 | 0 |
| S | 140 | 80 | 40 | 90 | 70 | 80 | 30 | 40 | 40 | 850 | 240 | 70 | 60 | 60 | 50 |
| Ba | 230 | 400 | 170 | 210 | 360 | 370 | 150 | 430 | 260 | 90 | 210 | 130 | 360 | 140 | 200 |
| Co | 0 | 0 | 60 | 0 | 0 | 0 | 0 | 0 | 0 | 0 | 0 | 0 | 0 | 70 | 0 |
| Cr | 180 | 240 | 180 | 290 | 140 | 170 | 180 | 140 | 190 | 270 | 190 | 180 | 0 | 2530 | 170 |
| Cu | 20 | 0 | 30 | 30 | 30 | 30 | 30 | 20 | 20 | 70 | 50 | 20 | 20 | 30 | 30 |
| Ga | 30 | 20 | 30 | 20 | 20 | 20 | 20 | 20 | 20 | 20 | 30 | 20 | 20 | 20 | 20 |
| Nb | 10 | 10 | 10 | 10 | 10 | 10 | 10 | 10 | 10 | 10 | 10 | 10 | 0 | 0 | 10 |
| Ni | 50 | 80 | 40 | 80 | 60 | 60 | 70 | 60 | 70 | 60 | 50 | 40 | 40 | 880 | 60 |
| Pb | 20 | 0 | 20 | 20 | 0 | 30 | 30 | 30 | 20 | 0 | 20 | 0 | 40 | 0 | 0 |
| Rb | 30 | 90 | 0 | 50 | 50 | 180 | 110 | 70 | 230 | 10 | 120 | 240 | 180 | 270 | 40 |
| Sr | 420 | 610 | 450 | 240 | 320 | 210 | 270 | 220 | 120 | 350 | 280 | 140 | 80 | 10 | 320 |
| V | 200 | 220 | 200 | 200 | 160 | 190 | 190 | 150 | 140 | 260 | 180 | 140 | 0 | 150 | 180 |
| Y | 0 | 0 | 20 | 0 | 0 | 0 | 0 | 0 | 0 | 0 | 0 | 0 | 0 | 0 | 0 |
| Zn | 60 | 40 | 40 | 40 | 40 | 130 | 60 | 50 | 100 | 50 | 70 | 100 | 10 | 100 | 30 |
| Zr | 120 | 160 | 140 | 70 | 120 | 90 | 100 | 80 | 100 | 110 | 120 | 80 | 70 | 50 | 90 |

Sample IDs: t1s1–t1s12= amphibolite, t2= granite, t3= actinolite rock, t4= diopside-actinolite skarn

## APPENDIX IV: P-XRF data of the drill core samples

| ID | t1s1 | t1s2 | t1s3 | t1s4 | t1s5 | t1s6 | t1s7 | t1s8 | t1s9 | t1s10 | t1s11 | t1s12 | t2 | t3 | t4 |
|---|---|---|---|---|---|---|---|---|---|---|---|---|---|---|---|
| Depth (m) | 3.90 | 36.00 | 63.35 | 88.95 | 105.35 | 128.30 | 156.00 | 203.00 | 241.55 | 323.20 | 336.70 | 361.60 | 351.50 | 35.00 | 145.70 |
| $SiO_2$ (wt.%) | 64.22 | 55.60 | 54.13 | 57.59 | 64.51 | 59.40 | 55.00 | 63.15 | 60.75 | 55.95 | 57.11 | 63.73 | 77.67 | 47.38 | 57.43 |
| $TiO_2$ | 0.43 | 0.96 | 0.77 | 0.91 | 0.57 | 0.92 | 0.82 | 0.85 | 0.73 | 1.07 | 0.82 | 0.98 | 0.10 | 0.52 | 0.80 |
| $Al_2O_3$ | 13.42 | 13.01 | 12.84 | 11.04 | 11.38 | 12.47 | 14.01 | 12.54 | 12.70 | 12.89 | 12.98 | 12.00 | 9.64 | 5.92 | 13.31 |
| FeOt | 3.64 | 6.67 | 5.61 | 6.40 | 5.01 | 6.15 | 5.01 | 5.25 | 4.70 | 7.55 | 6.43 | 5.21 | 1.17 | 8.55 | 1.54 |
| MnO | 0.06 | 0.11 | 0.08 | 0.15 | 0.09 | 0.10 | 0.11 | 0.06 | 0.07 | 0.11 | 0.13 | 0.15 | 0.00 | 0.17 | 0.04 |
| MgO | 0.53 | 2.60 | 1.87 | 2.55 | 1.77 | 2.35 | 2.07 | 1.84 | 2.61 | 2.36 | 1.98 | 2.44 | 0.45 | 8.83 | 2.47 |
| CaO | 7.43 | 7.05 | 8.38 | 6.42 | 6.38 | 3.55 | 7.12 | 3.40 | 2.47 | 9.32 | 5.91 | 2.61 | 1.09 | 8.25 | 11.76 |
| $K_2O$ | 0.50 | 1.38 | 0.45 | 1.47 | 0.83 | 2.79 | 1.37 | 2.11 | 3.18 | 0.58 | 1.33 | 2.91 | 3.32 | 2.97 | 0.82 |
| $P_2O_5$ | 0.13 | 0.22 | 0.24 | 0.16 | 0.18 | 0.13 | 0.17 | 0.23 | 0.16 | 0.27 | 0.17 | 0.23 | 0.19 | 0.11 | 0.35 |
| Sum | 90.35 | 87.60 | 84.37 | 86.68 | 90.72 | 87.87 | 85.68 | 89.43 | 87.37 | 90.11 | 86.87 | 90.26 | 93.64 | 82.71 | 88.51 |
| Ba (ppm) | 370 | 580 | 340 | 440 | 410 | 510 | 390 | 580 | 440 | 260 | 260 | 300 | 500 | 310 | 400 |
| Cl | 170 | 0 | 0 | 90 | 0 | 0 | 0 | 0 | 0 | 0 | 0 | 0 | 0 | 210 | 0 |
| S | 200 | 0 | 110 | 90 | 150 | 0 | 0 | 0 | 0 | 3820 | 200 | 0 | 0 | 90 | 100 |
| Ag | 100 | 120 | 90 | 110 | 100 | 90 | 110 | 80 | 90 | 110 | 90 | 90 | 70 | 110 | 90 |
| Bi | 0 | 0 | 0 | 0 | 0 | 0 | 10 | 0 | 0 | 10 | 0 | 0 | 10 | 0 | 0 |
| Cr | 170 | 320 | 300 | 370 | 210 | 270 | 290 | 270 | 260 | 420 | 280 | 270 | 40 | 2300 | 300 |
| Cu | 0 | 0 | 0 | 0 | 0 | 0 | 0 | 0 | 0 | 60 | 0 | 0 | 0 | 0 | 0 |
| Nb | 10 | 10 | 10 | 10 | 10 | 10 | 10 | 10 | 10 | 10 | 10 | 10 | 10 | 0 | 10 |
| Ni | 0 | 0 | 0 | 0 | 0 | 0 | 50 | 0 | 0 | 60 | 0 | 0 | 0 | 790 | 0 |
| Pb | 10 | 10 | 10 | 10 | 10 | 10 | 10 | 10 | 30 | 10 | 10 | 10 | 30 | 0 | 10 |
| Pd | 0 | 0 | 0 | 0 | 0 | 0 | 0 | 0 | 0 | 0 | 0 | 0 | 0 | 0 | 10 |
| Rb | 0 | 30 | 0 | 20 | 10 | 70 | 50 | 30 | 110 | 10 | 40 | 150 | 90 | 100 | 30 |
| Sn | 20 | 0 | 20 | 0 | 0 | 0 | 40 | 0 | 30 | 0 | 0 | 0 | 20 | 30 | 0 |
| Sr | 350 | 460 | 310 | 160 | 230 | 160 | 200 | 160 | 90 | 250 | 220 | 90 | 60 | 10 | 220 |
| V | 140 | 310 | 300 | 280 | 220 | 220 | 230 | 200 | 280 | 300 | 280 | 260 | 0 | 290 | 220 |
| W | 0 | 0 | 60 | 0 | 0 | 0 | 0 | 60 | 0 | 0 | 0 | 0 | 0 | 0 | 0 |
| Zn | 10 | 30 | 20 | 40 | 30 | 80 | 60 | 30 | 90 | 40 | 40 | 120 | 20 | 90 | 20 |
| Zr | 70 | 100 | 90 | 10 | 70 | 30 | 70 | 30 | 50 | 80 | 50 | 20 | 60 | 40 | 180 |

Excluded elements (all values <LOD): As, Au, Cd, Co, Mo, Sb, Se

Sample IDs: t1s1–t1s12= amphibolite, t2= granite, t3= actinolite rock, t4= diopside-actinolite skarn

## APPENDIX V: P-XRF data of the whole drill core analyses

| ID | k1 | k2 | k3 | k4 | k5 | k6 | k7 | k8 | k9 | k10 | k11 | k12 | k13 | k14 | k15 |
|---|---|---|---|---|---|---|---|---|---|---|---|---|---|---|---|
| Rock type | Amp | Grt | Diop | Amp | Amp | Grt | Act | Grt | Act | Amp | Grt | Amp | Grt | Grt | Grt |
| Depth (m) | 2.00 | 10.00 | 16.47 | 20.00 | 22.00 | 29.00 | 31.00 | 34.00 | 35.00 | 36.00 | 43.00 | 46.00 | 49.00 | 52.00 | 54.30 |
| $SiO_2$ (wt.%) | 49.71 | 68.95 | 56.27 | 50.78 | 55.87 | 68.04 | 44.99 | 66.68 | 44.99 | 52.59 | 71.66 | 51.21 | 69.36 | 60.71 | 73.04 |
| $TiO_2$ | 0.96 | 0.13 | 0.65 | 0.66 | 0.44 | 0.03 | 0.64 | 0.01 | 0.51 | 0.91 | 0.26 | 1.17 | 0.09 | 0.66 | 0.10 |
| $Al_2O_3$ | 9.89 | 7.37 | 13.33 | 10.58 | 9.81 | 9.03 | 8.67 | 9.76 | 5.13 | 12.05 | 8.75 | 10.92 | 7.97 | 12.65 | 7.67 |
| FeOt | 7.91 | 1.39 | 1.22 | 4.56 | 3.67 | 0.25 | 11.24 | 0.15 | 8.45 | 7.24 | 1.37 | 7.94 | 1.05 | 5.68 | 0.75 |
| MnO | 0.12 | 0.00 | 0.03 | 0.11 | 0.15 | 0.00 | 0.24 | 0.00 | 0.15 | 0.11 | 0.00 | 0.17 | 0.00 | 0.10 | 0.00 |
| MgO | 2.16 | 0.00 | 1.24 | 2.26 | 4.12 | 0.49 | 5.49 | 0.00 | 7.11 | 2.07 | 0.00 | 2.50 | 0.00 | 1.84 | 0.00 |
| CaO | 7.32 | 1.06 | 10.05 | 8.41 | 10.98 | 2.29 | 12.07 | 1.47 | 8.25 | 6.78 | 2.63 | 9.10 | 0.24 | 7.22 | 2.05 |
| $K_2O$ | 1.06 | 3.49 | 1.03 | 0.50 | 0.30 | 0.68 | 0.79 | 1.13 | 2.99 | 1.49 | 0.92 | 0.79 | 3.42 | 0.76 | 0.60 |
| $P_2O_5$ | 0.19 | 0.00 | 0.10 | 0.12 | 0.00 | 0.08 | 0.00 | 0.38 | 0.00 | 0.23 | 0.11 | 0.25 | 0.00 | 0.14 | 0.08 |
| Sum | 79.31 | 82.40 | 83.90 | 77.98 | 85.34 | 80.89 | 84.14 | 79.57 | 77.58 | 83.47 | 85.71 | 84.04 | 82.12 | 89.75 | 84.28 |
| Ba (ppm) | 550 | 740 | 290 | 270 | 350 | 200 | 230 | 290 | 330 | 640 | 510 | 450 | 710 | 430 | 130 |
| Cl | n.d. | n.d. | n.d. | n.d. | n.d. | n.d. | n.d. | n.d. | 140 | n.d. | n.d. | n.d. | n.d. | n.d. | n.d. |
| S | 990 | 220 | 210 | 130 | 130 | 320 | 980 | 320 | n.d. | 270 | 130 | 130 | n.d. | 170 | 100 |
| Bi | n.d. | 20 | n.d. | n.d. | n.d. | 20 | n.d. | n.d. | n.d. | n.d. | n.d. | n.d. | 20 | n.d. | n.d. |
| Cr | 370 | 60 | 170 | 330 | 370 | n.d. | 1120 | 120 | 1600 | 330 | 70 | 460 | 60 | 280 | 80 |
| Cu | n.d. | n.d. | n.d. | n.d. | n.d. | n.d. | n.d. | n.d. | n.d. | n.d. | n.d. | n.d. | n.d. | n.d. | n.d. |
| Nb | n.d. | n.d. | n.d. | n.d. | n.d. | n.d. | n.d. | n.d. | n.d. | n.d. | n.d. | n.d. | n.d. | n.d. | n.d. |
| Ni | n.d. | n.d. | n.d. | n.d. | n.d. | n.d. | 230 | n.d. | 700 | n.d. | n.d. | n.d. | n.d. | n.d. | n.d. |
| Pb | n.d. | 40 | n.d. | n.d. | n.d. | 30 | n.d. | n.d. | n.d. | n.d. | 20 | n.d. | 20 | n.d. | 20 |
| Rb | 20 | 60 | n.d. | n.d. | n.d. | n.d. | n.d. | 20 | 110 | 30 | 20 | n.d. | 60 | n.d. | n.d. |
| Sn | n.d. | n.d. | n.d. | n.d. | 50 | n.d. | n.d. | n.d. | n.d. | n.d. | n.d. | n.d. | n.d. | n.d. | n.d. |
| Sr | 270 | 90 | 330 | 250 | 130 | 90 | 70 | 140 | n.d. | 430 | 160 | 240 | 60 | 290 | 80 |
| V | 290 | n.d. | 120 | 230 | 280 | n.d. | 420 | 50 | 230 | 280 | 50 | 380 | 40 | 240 | 60 |
| W | n.d. | n.d. | n.d. | n.d. | n.d. | n.d. | n.d. | n.d. | n.d. | n.d. | n.d. | n.d. | n.d. | n.d. | n.d. |
| Zn | 50 | 20 | 20 | 40 | 40 | n.d. | 80 | n.d. | 80 | 40 | n.d. | 50 | n.d. | 40 | 20 |
| Zr | 140 | 80 | 80 | 80 | 40 | 20 | 30 | n.d. | 30 | 50 | 110 | 30 | 70 | 60 | 50 |

Excluded elements (all values <LOD): Ag, Au, As, Cd, Co, Mo, Pd, Sb, Se

Rock type names after initial classification. Amp= amphibolite, Grt= granite, Act= actinolite rock, Diop= Diopside-actinolite skarn, Mgm= migmatite

Appendix V continues.

| ID | k15.5 | k16 | k17 | k18 | k19 | k20 | k21 | k22 | k23 | k24 | k25 | k26 | k27 | k28 | k29 |
|---|---|---|---|---|---|---|---|---|---|---|---|---|---|---|---|
| Rock type | Act | Amp | Act | Grt | Act | Mgm | Grt | Mgm | Grt | Diop | Grt | Amp | Grt | Amp | Amp |
| Depth (m) | 59.00 | 61.00 | 64.40 | 66.00 | 68.00 | 70.40 | 76.05 | 78.25 | 81.00 | 82.00 | 83.00 | 84.00 | 85.30 | 88.50 | 94.60 |
| $SiO_2$ wt.% | 46.21 | 53.96 | 46.68 | 66.92 | 50.24 | 53.86 | 68.12 | 54.93 | 74.71 | 54.74 | 67.93 | 59.02 | 73.82 | 55.91 | 54.28 |
| $TiO_2$ | 0.97 | 0.60 | 0.43 | 0.32 | 0.34 | 0.75 | 0.09 | 0.65 | 0.09 | 0.87 | 0.05 | 0.45 | 0.01 | 0.82 | 0.66 |
| $Al_2O_3$ | 13.50 | 13.24 | 6.58 | 10.51 | 9.30 | 11.52 | 10.16 | 11.78 | 7.76 | 11.64 | 7.58 | 10.75 | 8.24 | 11.68 | 11.56 |
| FeOt | 10.29 | 4.17 | 9.77 | 1.80 | 8.39 | 3.93 | 0.56 | 2.22 | 0.94 | 1.33 | 0.34 | 1.79 | 0.19 | 5.85 | 4.65 |
| MnO | 0.19 | 0.05 | 0.22 | 0.00 | 0.23 | 0.08 | 0.00 | 0.06 | 0.00 | 0.05 | 0.00 | 0.08 | 0.00 | 0.13 | 0.09 |
| MgO | 3.88 | 1.58 | 5.50 | 0.85 | 4.91 | 2.24 | 0.60 | 2.17 | 0.44 | 1.73 | 0.00 | 1.32 | 0.39 | 1.93 | 2.22 |
| CaO | 10.15 | 8.29 | 10.73 | 3.22 | 10.71 | 8.54 | 2.57 | 6.72 | 1.27 | 10.13 | 1.32 | 7.15 | 0.37 | 5.86 | 4.63 |
| $K_2O$ | 1.26 | 0.51 | 0.95 | 1.04 | 0.59 | 0.63 | 0.71 | 1.08 | 2.31 | 0.43 | 2.86 | 0.52 | 3.50 | 1.40 | 1.64 |
| $P_2O_5$ | 0.09 | 0.16 | 0.00 | 0.13 | 0.11 | 0.22 | 0.00 | 0.18 | 0.15 | 0.27 | 0.00 | 0.16 | 0.00 | 0.23 | 0.22 |
| Sum | 86.55 | 82.55 | 80.86 | 84.78 | 84.82 | 81.77 | 82.80 | 79.79 | 87.68 | 81.19 | 80.08 | 81.25 | 86.53 | 83.80 | 79.96 |
| Ba ppm | 410 | 260 | 320 | 810 | 270 | 360 | 180 | 260 | 420 | 240 | 330 | 280 | 450 | 310 | 510 |
| Cl | n.d. | n.d. | 130 | n.d. | n.d. | n.d. | n.d. | n.d. | n.d. | n.d. | n.d. | n.d. | n.d. | n.d. | n.d. |
| S | 140 | 110 | n.d. | n.d. | n.d. | n.d. | 340 | 200 | 210 | n.d. | n.d. | 150 | 210 | 150 | n.d. |
| Bi | n.d. | n.d. | n.d. | n.d. | n.d. | n.d. | 30 | n.d. | n.d. | n.d. | n.d. | n.d. | 20 | n.d. | n.d. |
| Cr | 420 | 240 | 1350 | 70 | 1060 | 260 | 140 | 240 | 50 | 190 | 90 | 170 | 130 | 280 | 280 |
| Cu | n.d. | n.d. | n.d. | n.d. | n.d. | n.d. | n.d. | n.d. | n.d. | n.d. | n.d. | n.d. | n.d. | n.d. | n.d. |
| Nb | n.d. | n.d. | n.d. | n.d. | n.d. | n.d. | n.d. | n.d. | n.d. | n.d. | n.d. | n.d. | n.d. | n.d. | n.d. |
| Ni | n.d. | n.d. | 260 | n.d. | 200 | n.d. | n.d. | n.d. | n.d. | n.d. | n.d. | n.d. | n.d. | n.d. | n.d. |
| Pb | n.d. | n.d. | n.d. | n.d. | n.d. | n.d. | n.d. | n.d. | 40 | n.d. | 30 | n.d. | 30 | n.d. | n.d. |
| Rb | 20 | n.d. | 30 | 30 | n.d. | n.d. | n.d. | 30 | 40 | n.d. | 40 | n.d. | 50 | 20 | 60 |
| Sn | n.d. | n.d. | n.d. | n.d. | n.d. | n.d. | n.d. | n.d. | n.d. | n.d. | n.d. | n.d. | n.d. | n.d. | n.d. |
| Sr | 170 | 360 | 60 | 270 | 150 | 250 | 140 | 270 | 60 | 210 | 60 | 140 | 60 | 190 | 120 |
| V | 480 | 290 | 350 | 50 | 300 | 230 | n.d. | 170 | 90 | 180 | n.d. | 170 | n.d. | 290 | 220 |
| W | n.d. | n.d. | n.d. | n.d. | n.d. | n.d. | n.d. | n.d. | n.d. | n.d. | n.d. | n.d. | n.d. | n.d. | n.d. |
| Zn | 90 | 20 | 130 | n.d. | 140 | 20 | n.d. | 40 | n.d. | 20 | n.d. | 30 | n.d. | 50 | 40 |
| Zr | 20 | 70 | n.d. | 190 | n.d. | 70 | 40 | 80 | 20 | 120 | n.d. | 40 | 50 | 100 | 80 |

Excluded elements (all values <LOD): Ag, Au, As, Cd, Co, Mo, Pd, Sb, Se

Rock type names after initial classification. Amp= amphibolite, Grt= granite, Act= actinolite rock, Diop= Diopside-actinolite skarn, Mgm= migmatite

Appendix V continues.

| ID | k30 | k31 | k32 | k34 | k35 | k36 | k37 | k38 | k40 | k42 | k43 | k44 | k45 | k46 | k47 |
|---|---|---|---|---|---|---|---|---|---|---|---|---|---|---|---|
| Rock type | Amp | Grt | Act | Amp | Mgm | Mgm | Mgm | Diop | Diop | Grt | Act | Grt | Grt | Amp | Amp |
| Depth (m) | 95.10 | 98.00 | 99.45 | 105.27 | 106.10 | 109.70 | 111.60 | 113.40 | 118.00 | 124.40 | 125.40 | 125.65 | 127.00 | 127.40 | 130.10 |
| $SiO_2$ (wt.%) | 50.85 | 69.29 | 56.14 | 58.41 | 61.38 | 67.63 | 56.10 | 55.95 | 57.05 | 59.58 | 49.81 | 61.76 | 62.79 | 62.01 | 52.47 |
| $TiO_2$ | 0.64 | 0.30 | 0.73 | 0.77 | 0.48 | 0.31 | 0.47 | 0.32 | 0.44 | 0.58 | 0.39 | 0.28 | 0.50 | 0.81 | 1.29 |
| $Al_2O_3$ | 11.28 | 10.04 | 12.19 | 11.62 | 11.48 | 11.12 | 11.82 | 11.69 | 12.01 | 12.67 | 7.80 | 13.91 | 11.44 | 10.77 | 10.65 |
| FeOt | 8.53 | 1.47 | 7.82 | 5.96 | 2.35 | 1.78 | 2.23 | 1.24 | 1.00 | 1.26 | 8.40 | 1.73 | 2.61 | 6.06 | 8.44 |
| MnO | 0.18 | 0.00 | 0.13 | 0.12 | 0.05 | 0.00 | 0.05 | 0.02 | 0.02 | 0.02 | 0.17 | 0.00 | 0.02 | 0.07 | 0.19 |
| MgO | 3.03 | 0.48 | 2.25 | 1.30 | 1.29 | 0.94 | 1.77 | 1.51 | 1.27 | 1.32 | 4.81 | 0.57 | 0.68 | 2.15 | 2.17 |
| CaO | 10.57 | 3.03 | 5.50 | 6.15 | 7.27 | 3.29 | 7.44 | 9.48 | 8.83 | 8.33 | 10.28 | 1.55 | 3.40 | 2.55 | 5.88 |
| $K_2O$ | 0.55 | 0.97 | 1.00 | 1.35 | 0.50 | 1.17 | 0.56 | 0.43 | 0.52 | 0.48 | 0.62 | 4.35 | 1.42 | 3.07 | 2.10 |
| $P_2O_5$ | 0.14 | 0.68 | 0.22 | 0.21 | 0.18 | 0.16 | 0.15 | 0.11 | 0.16 | 0.00 | 0.19 | 0.15 | 0.19 | 0.08 | 0.18 |
| Sum | 85.77 | 86.28 | 85.98 | 85.89 | 84.97 | 86.40 | 80.60 | 80.74 | 81.30 | 84.26 | 82.47 | 84.30 | 83.06 | 87.57 | 83.38 |
| Ba (ppm) | 300 | 510 | 440 | 560 | 350 | 910 | 340 | 350 | 330 | 300 | 450 | 900 | 730 | 770 | 400 |
| Cl | n.d. | n.d. | 100 | n.d. | n.d. | n.d. | n.d. | n.d. | n.d. | n.d. | n.d. | n.d. | n.d. | n.d. | n.d. |
| S | n.d. | 160 | 770 | n.d. | n.d. | n.d. | n.d. | n.d. | n.d. | n.d. | 250 | n.d. | 180 | 120 | 3200 |
| Bi | n.d. | n.d. | n.d. | n.d. | n.d. | n.d. | n.d. | n.d. | n.d. | n.d. | n.d. | n.d. | n.d. | n.d. | n.d. |
| Cr | 320 | 90 | 270 | 180 | 170 | 70 | 200 | 110 | 150 | 130 | 770 | 120 | 130 | 270 | 400 |
| Cu | n.d. | n.d. | 50 | n.d. | n.d. | n.d. | n.d. | n.d. | n.d. | n.d. | n.d. | n.d. | n.d. | n.d. | 120 |
| Nb | n.d. | n.d. | n.d. | n.d. | n.d. | n.d. | n.d. | n.d. | n.d. | n.d. | n.d. | n.d. | n.d. | n.d. | n.d. |
| Ni | 70 | n.d. | n.d. | n.d. | n.d. | n.d. | n.d. | n.d. | n.d. | n.d. | 250 | n.d. | n.d. | n.d. | n.d. |
| Pb | n.d. | n.d. | n.d. | n.d. | n.d. | n.d. | n.d. | n.d. | n.d. | n.d. | n.d. | n.d. | n.d. | n.d. | n.d. |
| Rb | n.d. | 20 | 30 | 30 | n.d. | 20 | n.d. | n.d. | n.d. | n.d. | n.d. | 130 | 20 | 80 | 40 |
| Sn | n.d. | n.d. | n.d. | n.d. | n.d. | n.d. | n.d. | 30 | n.d. | n.d. | n.d. | n.d. | n.d. | n.d. | n.d. |
| Sr | 250 | 270 | 190 | 240 | 240 | 310 | 240 | 310 | 240 | 210 | 160 | 240 | 310 | 180 | 120 |
| V | 400 | 100 | 300 | 220 | 120 | n.d. | 180 | 120 | 140 | 90 | 270 | 60 | 60 | 260 | 360 |
| W | n.d. | n.d. | n.d. | n.d. | n.d. | n.d. | n.d. | n.d. | n.d. | n.d. | n.d. | n.d. | n.d. | n.d. | n.d. |
| Zn | 70 | 20 | 80 | 40 | 20 | 20 | 30 | n.d. | n.d. | n.d. | 90 | 20 | 20 | 80 | 70 |
| Zr | 30 | 170 | 90 | 80 | 20 | 180 | 120 | 90 | 90 | 150 | 60 | 270 | 250 | 40 | 40 |

Excluded elements (all values <LOD): Ag, Au, As, Cd, Co, Mo, Pd, Sb, Se

Rock type names after initial classification. Amp= amphibolite, Grt= granite, Act= actinolite rock, Diop= Diopside-actinolite skarn, Mgm= migmatite

Appendix V continues.

| ID | k48 | k49 | k50 | k51 | k53 | k54 | k55 | k56 | k57 | k58 | k59 | k60 | k61 | k62 | k63 |
|---|---|---|---|---|---|---|---|---|---|---|---|---|---|---|---|
| Rock type | Grt | Act | Amp | Grt | Grt | Grt | Diop | Diop | Grt | Grt | Mgm | Diop | Grt | Amp | Amp |
| Depth (m) | 132.20 | 134.60 | 136.30 | 138.40 | 141.90 | 143.80 | 145.70 | 147.10 | 148.80 | 150.20 | 151.80 | 152.10 | 154.80 | 157.60 | 158.80 |
| $SiO_2$ (wt.%) | 70.39 | 45.23 | 54.10 | 57.01 | 55.73 | 74.92 | 55.13 | 54.38 | 73.27 | 56.16 | 45.40 | 54.01 | 76.92 | 52.46 | 57.41 |
| $TiO_2$ | 0.49 | 0.86 | 0.96 | 0.53 | 0.72 | 0.21 | 0.90 | 0.71 | 0.37 | 0.76 | 1.11 | 0.16 | 0.04 | 0.87 | 0.48 |
| $Al_2O_3$ | 10.68 | 13.82 | 13.54 | 12.07 | 12.42 | 7.28 | 12.38 | 12.66 | 10.29 | 13.37 | 12.11 | 8.84 | 9.04 | 11.40 | 13.20 |
| FeOt | 2.60 | 9.88 | 5.53 | 3.42 | 1.46 | 1.64 | 1.01 | 2.43 | 2.18 | 1.33 | 9.55 | 3.09 | 0.74 | 6.14 | 1.35 |
| MnO | 0.02 | 0.18 | 0.10 | 0.09 | 0.04 | 0.02 | 0.04 | 0.06 | 0.02 | 0.05 | 0.15 | 0.18 | 0.00 | 0.14 | 0.05 |
| MgO | 0.54 | 3.29 | 2.07 | 2.51 | 2.10 | 0.00 | 2.04 | 2.31 | 0.66 | 1.88 | 4.49 | 2.96 | 0.00 | 2.37 | 1.81 |
| CaO | 3.30 | 11.76 | 6.01 | 6.98 | 9.52 | 1.91 | 11.36 | 9.37 | 2.69 | 8.87 | 5.58 | 14.76 | 1.28 | 6.89 | 9.22 |
| $K_2O$ | 1.36 | 0.81 | 1.53 | 1.33 | 0.46 | 1.00 | 0.66 | 0.53 | 1.20 | 0.45 | 1.76 | 0.50 | 2.59 | 1.14 | 0.45 |
| $P_2O_5$ | 0.13 | 0.00 | 0.19 | 0.27 | 0.27 | 0.00 | 0.16 | 0.35 | 0.17 | 0.00 | 0.22 | 0.00 | 0.14 | 0.16 | 0.00 |
| Sum | 89.51 | 85.84 | 84.03 | 84.22 | 82.74 | 86.97 | 83.67 | 82.79 | 90.85 | 82.87 | 80.37 | 84.49 | 90.76 | 81.55 | 83.97 |
| Ba (ppm) | 610 | 270 | 620 | 460 | 360 | 310 | 320 | 440 | 1010 | 330 | 820 | 310 | 450 | 380 | 300 |
| Cl | n.d. | n.d. | n.d. | n.d. | n.d. | n.d. | n.d. | n.d. | n.d. | n.d. | n.d. | 490 | n.d. | n.d. | 200 |
| S | n.d. | 1940 | n.d. | n.d. | 130 | n.d. | n.d. | n.d. | 120 | n.d. | 140 | 260 | 90 | n.d. | 140 |
| Bi | 20 | n.d. | n.d. | n.d. | n.d. | n.d. | n.d. | n.d. | n.d. | n.d. | n.d. | n.d. | 30 | n.d. | n.d. |
| Cr | 120 | 490 | 320 | 230 | 240 | 60 | 210 | 200 | 90 | 250 | 460 | 310 | 50 | 270 | 220 |
| Cu | n.d. | 200 | n.d. | n.d. | n.d. | n.d. | n.d. | n.d. | n.d. | n.d. | n.d. | n.d. | n.d. | n.d. | n.d. |
| Nb | n.d. | n.d. | n.d. | n.d. | n.d. | n.d. | n.d. | n.d. | n.d. | n.d. | n.d. | n.d. | n.d. | n.d. | n.d. |
| Ni | n.d. | 120 | n.d. | n.d. | n.d. | n.d. | n.d. | n.d. | n.d. | n.d. | n.d. | n.d. | n.d. | n.d. | n.d. |
| Pb | n.d. | n.d. | 20 | n.d. | n.d. | n.d. | n.d. | n.d. | 20 | 20 | n.d. | n.d. | 30 | n.d. | 20 |
| Rb | 30 | n.d. | 30 | 40 | n.d. | 20 | n.d. | n.d. | 30 | n.d. | 70 | n.d. | 40 | 30 | n.d. |
| Sn | n.d. | n.d. | 30 | 40 | n.d. | n.d. | n.d. | n.d. | n.d. | n.d. | n.d. | n.d. | n.d. | n.d. | n.d. |
| Sr | 260 | 170 | 240 | 210 | 250 | 70 | 230 | 290 | 260 | 280 | 130 | 160 | 60 | 210 | 300 |
| V | 150 | 380 | 250 | 210 | 150 | 40 | 150 | 230 | 60 | 170 | 330 | 220 | n.d. | 260 | 150 |
| W | n.d. | n.d. | n.d. | n.d. | n.d. | n.d. | n.d. | n.d. | n.d. | n.d. | n.d. | n.d. | n.d. | n.d. | n.d. |
| Zn | 20 | 170 | 40 | 40 | n.d. | n.d. | n.d. | 40 | 30 | 40 | 120 | 70 | n.d. | 40 | 20 |
| Zr | 320 | 20 | 60 | 40 | 110 | 90 | 50 | 130 | 210 | 130 | 40 | 30 | 60 | 20 | 60 |

Excluded elements (all values <LOD): Ag, Au, As, Cd, Co, Mo, Pd, Sb, Se

Rock type names after initial classification. Amp= amphibolite, Grt= granite, Act= actinolite rock, Diop= Diopside-actinolite skarn, Mgm= migmatite

Appendix V continues.

| ID | k64 | k65 | k66 | k67 | k68 | k69 | k70 | k71 | k72 | k73 | k74 | k75 | k76 | k77 |
|---|---|---|---|---|---|---|---|---|---|---|---|---|---|---|
| Rock type | Amp | Act | Act | Act | Diop | Amp | Act | Grt | Grt | Grt | Grt | Grt | Grt | Grt |
| Depth (m) | 161.40 | 162.15 | 164.00 | 165.00 | 166.00 | 167.60 | 168.30 | 171.00 | 175.40 | 177.00 | 179.70 | 181.50 | 183.20 | 186.10 |
| $SiO_2$ (wt.%) | 50.82 | 45.30 | 45.25 | 51.40 | 57.84 | 51.41 | 51.76 | 59.64 | 53.02 | 56.69 | 58.09 | 59.70 | 59.57 | 49.84 |
| $TiO_2$ | 1.25 | 0.63 | 0.71 | 0.78 | 0.84 | 1.17 | 0.64 | 0.66 | 1.35 | 0.69 | 0.66 | 0.41 | 0.65 | 0.48 |
| $Al_2O_3$ | 12.04 | 8.59 | 8.37 | 14.88 | 11.65 | 12.34 | 12.17 | 14.32 | 11.71 | 11.87 | 13.11 | 12.98 | 13.87 | 13.54 |
| FeOt | 7.78 | 9.67 | 11.24 | 7.49 | 2.31 | 7.35 | 9.14 | 4.78 | 7.52 | 2.43 | 1.96 | 1.30 | 0.84 | 3.82 |
| MnO | 0.15 | 0.21 | 0.23 | 0.15 | 0.09 | 0.11 | 0.19 | 0.08 | 0.11 | 0.05 | 0.04 | 0.03 | 0.02 | 0.09 |
| MgO | 2.60 | 6.64 | 6.44 | 3.14 | 3.54 | 2.63 | 3.95 | 1.20 | 2.16 | 2.31 | 1.78 | 1.58 | 1.63 | 2.37 |
| CaO | 6.14 | 12.62 | 12.25 | 10.89 | 11.25 | 6.38 | 10.72 | 6.57 | 7.00 | 8.47 | 9.13 | 5.32 | 10.34 | 6.52 |
| $K_2O$ | 1.88 | 0.47 | 0.69 | 0.46 | 0.32 | 1.32 | 0.44 | 0.89 | 0.57 | 0.37 | 0.43 | 1.78 | 0.52 | 0.46 |
| $P_2O_5$ | 0.25 | 0.08 | 0.14 | 0.38 | 0.22 | 0.18 | 0.26 | 0.30 | 0.25 | 0.25 | 0.29 | 0.22 | 0.27 | 0.10 |
| Sum | 82.91 | 84.21 | 85.31 | 89.56 | 88.07 | 82.90 | 89.28 | 88.44 | 83.70 | 83.12 | 85.49 | 83.33 | 87.69 | 77.22 |
| Ba (ppm) | 650 | 210 | 260 | 300 | 290 | 500 | 310 | 250 | 470 | 280 | 350 | 280 | 350 | 220 |
| Cl | n.d. | 250 | 140 | n.d. | n.d. | n.d. | n.d. | n.d. | n.d. | n.d. | n.d. | n.d. | n.d. | n.d. |
| S | 310 | n.d. | n.d. | 790 | n.d. | 440 | 320 | 220 | 150 | 160 | 270 | n.d. | 210 | 290 |
| Bi | n.d. | n.d. | n.d. | n.d. | n.d. | n.d. | n.d. | n.d. | n.d. | n.d. | n.d. | n.d. | n.d. | n.d. |
| Cr | 340 | 1160 | 1340 | 440 | 340 | 270 | 360 | 190 | 360 | 280 | 250 | 130 | 150 | 250 |
| Cu | n.d. | n.d. | n.d. | n.d. | n.d. | n.d. | n.d. | n.d. | n.d. | n.d. | n.d. | n.d. | n.d. | n.d. |
| Nb | n.d. | n.d. | n.d. | n.d. | n.d. | n.d. | n.d. | n.d. | n.d. | n.d. | n.d. | n.d. | n.d. | n.d. |
| Ni | n.d. | 330 | 360 | 70 | n.d. | n.d. | n.d. | n.d. | n.d. | n.d. | n.d. | n.d. | n.d. | n.d. |
| Pb | 20 | n.d. | n.d. | n.d. | 20 | n.d. | n.d. | 20 | 20 | 20 | n.d. | n.d. | 20 | n.d. |
| Rb | 40 | n.d. | n.d. | n.d. | n.d. | 30 | n.d. | 20 | n.d. | n.d. | n.d. | 40 | n.d. | 20 |
| Sn | n.d. | n.d. | n.d. | n.d. | n.d. | n.d. | n.d. | n.d. | n.d. | n.d. | n.d. | n.d. | n.d. | 30 |
| Sr | 220 | 80 | 50 | 370 | 240 | 300 | 270 | 330 | 250 | 250 | 320 | 110 | 320 | 120 |
| V | 310 | 410 | 420 | 320 | 270 | 270 | 390 | 210 | 280 | 230 | 190 | 90 | 120 | 160 |
| W | n.d. | n.d. | n.d. | n.d. | n.d. | n.d. | n.d. | n.d. | n.d. | n.d. | n.d. | n.d. | n.d. | n.d. |
| Zn | 80 | 80 | 110 | 60 | 50 | 50 | 70 | 30 | 60 | 30 | n.d. | 20 | 20 | 100 |
| Zr | 100 | 30 | 30 | 40 | 100 | 30 | 40 | n.d. | 240 | 60 | 40 | 70 | 70 | 150 |

Excluded elements (all values <LOD): Ag, Au, As, Cd, Co, Mo, Pd, Sb, Se

Rock type names after initial classification. Amp= amphibolite, Grt= granite, Act= actinolite rock, Diop= Diopside-actinolite skarn, Mgm= migmatite

Appendix V continues.

| ID | k78 | k79 | k80 | k81 | k82 | k83 | k84 | k85 | k86 | k87 | k88 | k89 | k90 | k91 | k92 |
|---|---|---|---|---|---|---|---|---|---|---|---|---|---|---|---|
| Rock type | Amp | Amp | Amp | Amp | Grt | Mgm | Act | Amp | Act | Act | Amp | Act | Mgm | Mgm | Grt |
| Depth (m) | 187.80 | 190.24 | 191.40 | 194.00 | 195.80 | 199.00 | 200.45 | 201.30 | 203.90 | 206.00 | 207.50 | 208.60 | 212.00 | 212.00 | 215.80 |
| $SiO_2$ (wt.%) | 54.16 | 53.65 | 53.90 | 55.34 | 59.24 | 53.64 | 48.37 | 66.34 | 52.18 | 51.55 | 60.48 | 48.83 | 59.91 | 56.16 | 58.59 |
| $TiO_2$ | 0.86 | 0.90 | 1.10 | 1.12 | 0.28 | 0.82 | 0.57 | 0.66 | 0.64 | 0.65 | 0.61 | 0.72 | 0.58 | 0.81 | 0.33 |
| $Al_2O_3$ | 11.47 | 11.68 | 11.50 | 12.56 | 13.14 | 11.91 | 10.12 | 10.60 | 12.46 | 13.26 | 10.75 | 12.55 | 12.15 | 11.19 | 13.23 |
| FeOt | 7.40 | 6.58 | 7.93 | 6.74 | 1.31 | 0.50 | 9.29 | 5.54 | 9.41 | 8.88 | 3.84 | 9.18 | 4.71 | 6.30 | 4.20 |
| MnO | 0.13 | 0.09 | 0.14 | 0.11 | 0.06 | 0.00 | 0.23 | 0.08 | 0.21 | 0.17 | 0.06 | 0.19 | 0.07 | 0.10 | 0.10 |
| MgO | 2.45 | 2.14 | 3.02 | 2.59 | 1.46 | 0.75 | 5.68 | 1.97 | 3.55 | 2.27 | 1.26 | 3.65 | 1.35 | 2.50 | 1.75 |
| CaO | 6.73 | 7.19 | 7.27 | 7.30 | 9.93 | 6.71 | 11.89 | 3.44 | 9.61 | 10.51 | 5.28 | 11.85 | 3.44 | 3.12 | 7.15 |
| $K_2O$ | 1.06 | 1.00 | 0.91 | 0.55 | 0.50 | 0.47 | 0.44 | 1.36 | 0.60 | 0.45 | 1.06 | 0.48 | 1.03 | 1.02 | 1.33 |
| $P_2O_5$ | 0.27 | 0.20 | 0.29 | 0.39 | 0.17 | 0.06 | 0.08 | 0.20 | 0.20 | 0.30 | 0.29 | 0.22 | 0.12 | 0.22 | 0.00 |
| Sum | 84.54 | 83.44 | 86.08 | 86.71 | 86.08 | 74.86 | 86.66 | 90.19 | 88.86 | 88.04 | 83.63 | 87.66 | 83.37 | 81.42 | 86.68 |
| Ba (ppm) | 330 | 380 | 340 | 270 | 310 | 280 | 220 | 450 | 230 | 320 | 480 | 350 | 510 | 500 | 610 |
| Cl | n.d. | n.d. | 110 | n.d. | n.d. | n.d. | 140 | n.d. | n.d. | n.d. | n.d. | n.d. | n.d. | n.d. | n.d. |
| S | 150 | 550 | 280 | 160 | n.d. | 100 | n.d. | 690 | 110 | n.d. | 140 | 2530 | 350 | 180 | 160 |
| Bi | n.d. | n.d. | n.d. | n.d. | n.d. | n.d. | n.d. | n.d. | n.d. | n.d. | n.d. | n.d. | n.d. | n.d. | n.d. |
| Cr | 300 | 320 | 360 | 310 | 120 | 150 | 1340 | 260 | 430 | 340 | 220 | 350 | 160 | 300 | 200 |
| Cu | n.d. | n.d. | n.d. | n.d. | n.d. | n.d. | n.d. | n.d. | n.d. | n.d. | n.d. | 60 | n.d. | n.d. | n.d. |
| Nb | n.d. | n.d. | n.d. | n.d. | n.d. | 20 | n.d. | n.d. | n.d. | n.d. | n.d. | n.d. | n.d. | n.d. | n.d. |
| Ni | 100 | 70 | n.d. | n.d. | n.d. | n.d. | 240 | n.d. | 80 | 100 | n.d. | 70 | n.d. | n.d. | n.d. |
| Pb | 20 | 20 | n.d. | n.d. | 20 | 20 | n.d. | n.d. | n.d. | n.d. | 20 | n.d. | 20 | n.d. | 30 |
| Rb | 30 | 20 | 30 | n.d. | n.d. | n.d. | n.d. | 20 | n.d. | n.d. | n.d. | n.d. | 40 | 30 | 40 |
| Sn | n.d. | n.d. | n.d. | n.d. | n.d. | 30 | n.d. | n.d. | n.d. | n.d. | n.d. | n.d. | n.d. | n.d. | 30 |
| Sr | 210 | 270 | 200 | 190 | 150 | 200 | 50 | 110 | 140 | 230 | 240 | 260 | 230 | 100 | 180 |
| V | 260 | 240 | 320 | 230 | 110 | 90 | 370 | 230 | 390 | 360 | 190 | 440 | 150 | 220 | 180 |
| W | n.d. | n.d. | n.d. | n.d. | n.d. | n.d. | n.d. | n.d. | n.d. | n.d. | n.d. | n.d. | n.d. | n.d. | n.d. |
| Zn | 70 | 40 | 50 | 70 | 20 | n.d. | 100 | 40 | 60 | 60 | 30 | 60 | 60 | 100 | 40 |
| Zr | 140 | 100 | 40 | 90 | 60 | 90 | 40 | 40 | 30 | 30 | 330 | 30 | 20 | 100 | 30 |

Excluded elements (all values <LOD): Ag, Au, As, Cd, Co, Mo, Pd, Sb, Se

Rock type names after initial classification. Amp= amphibolite, Grt= granite, Act= actinolite rock, Diop= Diopside-actinolite skarn, Mgm= migmatite

Appendix V continues.

| ID | k93 | k94 | k95 | k96 | k97 | k98 | k99 | k100 | k101 | k102 | k103 | k104 | k105 | k106 | k107 |
|---|---|---|---|---|---|---|---|---|---|---|---|---|---|---|---|
| Rock type | Amp | Amp | Grt | Act | Amp | Amp | Amp | Grt | Grt | Amp | Grt | Amp | Amp | Act | Diop |
| Depth (m) | 217.50 | 219.60 | 220.80 | 222.00 | 223.00 | 228.45 | 231.40 | 234.00 | 240.00 | 241.20 | 243.30 | 245.60 | 247.50 | 250.30 | 255.00 |
| $SiO_2$ (wt.%) | 57.42 | 49.24 | 54.63 | 44.90 | 48.98 | 69.73 | 58.29 | 74.75 | 60.80 | 61.92 | 76.96 | 50.22 | 57.49 | 42.90 | 60.68 |
| $TiO_2$ | 0.93 | 0.62 | 0.04 | 0.64 | 0.54 | 0.22 | 0.69 | 0.14 | 0.57 | 0.67 | 0.11 | 0.60 | 0.96 | 0.69 | 0.56 |
| $Al_2O_3$ | 11.58 | 14.57 | 13.22 | 9.02 | 14.03 | 8.98 | 10.93 | 8.36 | 11.66 | 11.31 | 9.42 | 14.34 | 10.57 | 10.82 | 12.71 |
| FeOt | 7.91 | 7.67 | 0.67 | 11.56 | 9.14 | 2.02 | 6.40 | 1.04 | 1.68 | 5.11 | 1.14 | 8.91 | 6.00 | 10.20 | 1.02 |
| MnO | 0.16 | 0.14 | 0.00 | 0.22 | 0.19 | 0.03 | 0.11 | 0.00 | 0.05 | 0.12 | 0.00 | 0.20 | 0.13 | 0.20 | 0.05 |
| MgO | 2.22 | 2.36 | 0.77 | 6.97 | 2.89 | 0.00 | 1.74 | 0.00 | 1.97 | 2.02 | 0.00 | 2.90 | 2.25 | 5.78 | 1.17 |
| CaO | 6.70 | 10.71 | 8.58 | 8.69 | 10.85 | 1.39 | 5.17 | 1.87 | 6.98 | 3.86 | 1.15 | 11.62 | 4.12 | 9.69 | 6.67 |
| $K_2O$ | 1.01 | 0.77 | 1.61 | 2.71 | 0.87 | 2.30 | 1.45 | 1.58 | 0.51 | 2.24 | 3.75 | 0.55 | 2.33 | 2.18 | 0.46 |
| $P_2O_5$ | 0.26 | 0.08 | 0.00 | 0.18 | 0.17 | 0.15 | 0.20 | 0.11 | 0.19 | 0.08 | 0.08 | 0.16 | 0.16 | 0.00 | 0.14 |
| Sum | 88.20 | 86.16 | 79.51 | 84.90 | 87.66 | 84.83 | 84.99 | 87.84 | 84.43 | 87.34 | 92.61 | 89.50 | 84.01 | 82.47 | 83.46 |
| Ba (ppm) | 480 | 340 | 470 | 600 | 390 | 580 | 440 | 580 | 250 | 390 | 1030 | 290 | 510 | 300 | 310 |
| Cl | n.d. | 70 | 60 | 140 | n.d. | n.d. | n.d. | n.d. | n.d. | n.d. | n.d. | n.d. | n.d. | 70 | n.d. |
| S | 850 | 180 | n.d. | n.d. | 220 | 100 | 1050 | 80 | 170 | n.d. | 750 | 710 | 480 | 120 | n.d. |
| Bi | n.d. | n.d. | n.d. | n.d. | n.d. | n.d. | n.d. | n.d. | n.d. | n.d. | n.d. | n.d. | n.d. | n.d. | n.d. |
| Cr | 300 | 250 | 40 | 1070 | 260 | 80 | 260 | 40 | 160 | 200 | 110 | 260 | 240 | 680 | 160 |
| Cu | 40 | 110 | n.d. | n.d. | 210 | n.d. | 80 | n.d. | n.d. | n.d. | n.d. | n.d. | n.d. | n.d. | n.d. |
| Nb | n.d. | n.d. | n.d. | n.d. | n.d. | n.d. | n.d. | n.d. | n.d. | n.d. | n.d. | n.d. | n.d. | n.d. | n.d. |
| Ni | n.d. | n.d. | n.d. | 370 | n.d. | n.d. | n.d. | n.d. | n.d. | 70 | n.d. | n.d. | n.d. | 210 | n.d. |
| Pb | 20 | n.d. | n.d. | n.d. | n.d. | 20 | n.d. | 20 | 20 | 20 | 40 | n.d. | 20 | n.d. | 20 |
| Rb | n.d. | n.d. | 40 | 70 | 20 | 30 | 40 | 20 | n.d. | 70 | 50 | n.d. | 50 | 60 | n.d. |
| Sn | n.d. | n.d. | n.d. | n.d. | 30 | n.d. | n.d. | n.d. | n.d. | n.d. | n.d. | n.d. | n.d. | n.d. | n.d. |
| Sr | 210 | 290 | 80 | 30 | 300 | 80 | 210 | 120 | 180 | 80 | 100 | 310 | 160 | 90 | 190 |
| V | 270 | 380 | 90 | 400 | 340 | 50 | 250 | 30 | 120 | 190 | 50 | 340 | 250 | 400 | 150 |
| W | n.d. | n.d. | n.d. | n.d. | n.d. | n.d. | n.d. | n.d. | 90 | n.d. | n.d. | n.d. | n.d. | n.d. | n.d. |
| Zn | 60 | 60 | n.d. | 100 | 80 | 30 | 50 | 20 | 50 | 70 | n.d. | 80 | 60 | 100 | 60 |
| Zr | 150 | 20 | n.d. | 20 | 30 | 130 | 40 | 130 | 190 | 30 | 80 | 30 | 40 | n.d. | 80 |

Excluded elements (all values <LOD): Ag, Au, As, Cd, Co, Mo, Pd, Sb, Se

Rock type names after initial classification. Amp= amphibolite, Grt= granite, Act= actinolite rock, Diop= Diopside-actinolite skarn, Mgm= migmatite

Appendix V continues.

| ID | k108 | k109 | k110.5 | k111 | k112 | k113 | k114 | k115 | k116 | k117 | k118 | k119 | k120 | k121 | k122 |
|---|---|---|---|---|---|---|---|---|---|---|---|---|---|---|---|
| Rock type | Grt | Act | Diop | Diop | Grt | Diop | Diop | Act | Act | Diop | Grt | Diop | Act | Diop | Grt |
| Depth (m) | 256.40 | 263.00 | 264.30 | 267.90 | 269.50 | 271.90 | 274.40 | 278.85 | 279.10 | 282.80 | 286.20 | 288.30 | 294.85 | 295.70 | 297.10 |
| $SiO_2$ (wt.%) | 69.74 | 48.43 | 60.63 | 58.49 | 64.22 | 55.00 | 58.45 | 42.97 | 46.27 | 57.66 | 68.45 | 57.33 | 39.68 | 57.65 | 75.04 |
| $TiO_2$ | 0.40 | 0.66 | 0.54 | 0.60 | 0.04 | 0.64 | 0.31 | 0.54 | 0.67 | 0.57 | 0.30 | 0.37 | 0.88 | 0.45 | 0.02 |
| $Al_2O_3$ | 9.92 | 10.88 | 11.42 | 11.76 | 10.13 | 10.55 | 10.90 | 8.68 | 14.64 | 10.63 | 10.08 | 11.54 | 7.46 | 11.79 | 8.57 |
| FeOt | 0.04 | 9.37 | 2.08 | 1.83 | 0.41 | 1.87 | 0.85 | 11.14 | 8.91 | 1.93 | 0.17 | 0.92 | 11.00 | 2.40 | 0.18 |
| MnO | 0.00 | 0.19 | 0.09 | 0.07 | 0.00 | 0.10 | 0.05 | 0.32 | 0.19 | 0.11 | 0.00 | 0.03 | 0.21 | 0.08 | 0.00 |
| MgO | 0.00 | 5.01 | 1.88 | 1.46 | 0.00 | 1.70 | 1.05 | 5.21 | 1.84 | 2.09 | 0.00 | 0.89 | 4.83 | 1.61 | 0.00 |
| CaO | 3.56 | 13.76 | 7.31 | 6.91 | 2.02 | 6.64 | 7.72 | 12.12 | 10.93 | 6.90 | 2.98 | 9.13 | 10.21 | 6.65 | 0.69 |
| $K_2O$ | 0.34 | 0.51 | 0.56 | 0.52 | 2.26 | 0.54 | 0.50 | 1.06 | 0.64 | 0.60 | 0.71 | 0.87 | 0.37 | 0.41 | 5.17 |
| $P_2O_5$ | 0.10 | 0.00 | 0.19 | 0.26 | 0.00 | 0.10 | 0.14 | 0.14 | 0.49 | 0.00 | 0.00 | 0.09 | 0.08 | 0.16 | 0.11 |
| Sum | 84.10 | 88.81 | 84.70 | 81.91 | 79.08 | 77.15 | 79.97 | 82.19 | 84.58 | 80.48 | 82.70 | 81.17 | 74.70 | 81.20 | 89.77 |
| Ba (ppm) | 330 | 250 | 280 | 280 | 590 | 270 | 290 | 380 | 340 | 300 | 340 | 360 | 220 | 260 | 1800 |
| Cl | n.d. | 270 | 60 | n.d. | n.d. | n.d. | n.d. | 200 | n.d. | n.d. | n.d. | n.d. | 110 | n.d. | n.d. |
| S | n.d. | n.d. | n.d. | 230 | n.d. | 280 | 160 | 120 | 360 | 120 | 170 | 100 | 300 | 180 | n.d. |
| Bi | n.d. | n.d. | n.d. | n.d. | n.d. | n.d. | n.d. | n.d. | n.d. | n.d. | n.d. | n.d. | n.d. | n.d. | n.d. |
| Cr | 40 | 810 | 200 | 120 | 60 | 160 | 130 | 1130 | 210 | 250 | 150 | 150 | 820 | 170 | 40 |
| Cu | n.d. | n.d. | n.d. | n.d. | n.d. | n.d. | n.d. | n.d. | n.d. | n.d. | n.d. | n.d. | n.d. | n.d. | n.d. |
| Nb | n.d. | n.d. | n.d. | n.d. | n.d. | n.d. | n.d. | n.d. | n.d. | n.d. | n.d. | n.d. | n.d. | n.d. | n.d. |
| Ni | n.d. | 190 | n.d. | n.d. | n.d. | n.d. | n.d. | 360 | 100 | n.d. | n.d. | n.d. | 280 | n.d. | n.d. |
| Pb | 20 | n.d. | 20 | 20 | 40 | 20 | n.d. | n.d. | n.d. | n.d. | n.d. | 20 | n.d. | 20 | 30 |
| Rb | n.d. | n.d. | n.d. | n.d. | 30 | n.d. | n.d. | 20 | n.d. | n.d. | n.d. | n.d. | n.d. | n.d. | 60 |
| Sn | n.d. | n.d. | n.d. | n.d. | n.d. | n.d. | n.d. | 40 | n.d. | n.d. | n.d. | n.d. | n.d. | n.d. | n.d. |
| Sr | 190 | 210 | 140 | 200 | 130 | 110 | 170 | 40 | 520 | 160 | 150 | 230 | 100 | 220 | 80 |
| V | n.d. | 430 | 220 | 140 | n.d. | 130 | 140 | 400 | 330 | 200 | 80 | 100 | 420 | 130 | n.d. |
| W | n.d. | n.d. | n.d. | n.d. | n.d. | n.d. | n.d. | n.d. | n.d. | n.d. | n.d. | n.d. | n.d. | n.d. | n.d. |
| Zn | n.d. | 70 | 60 | 40 | n.d. | 230 | 30 | 130 | 70 | 50 | n.d. | 20 | 160 | 30 | n.d. |
| Zr | 70 | 20 | 40 | 20 | 50 | 50 | 70 | 20 | 30 | 80 | 30 | 70 | 60 | 110 | n.d. |

Excluded elements (all values <LOD): Ag, Au, As, Cd, Co, Mo, Pd, Sb, Se

Rock type names after initial classification. Amp= amphibolite, Grt= granite, Act= actinolite rock, Diop= Diopside-actinolite skarn, Mgm= migmatite

Appendix V continues.

| ID | k123 | k124 | k125 | k126 | k127 | k128 | k129 | k130 | k131 | k132 | k133 | k137 | k138 | k139 | k140 |
|---|---|---|---|---|---|---|---|---|---|---|---|---|---|---|---|
| Rock type | Diop | Diop | Amp | Diop | Diop | Diop | Diop | Diop | Act | Act | Amp | Amp | Grt | Amp | Grt |
| Depth (m) | 299.00 | 303.00 | 304.40 | 306.20 | 308.80 | 313.70 | 316.70 | 321.20 | 325.30 | 326.60 | 329.90 | 336.30 | 337.60 | 339.30 | 341.20 |
| $SiO_2$ (wt.%) | 53.71 | 57.46 | 55.48 | 54.55 | 55.39 | 56.36 | 55.42 | 56.59 | 43.55 | 43.06 | 49.23 | 53.42 | 66.53 | 56.92 | 72.17 |
| $TiO_2$ | 0.86 | 0.53 | 0.83 | 0.71 | 0.60 | 0.41 | 0.86 | 0.83 | 0.70 | 0.82 | 0.87 | 0.86 | 0.13 | 0.79 | 0.02 |
| $Al_2O_3$ | 11.56 | 13.02 | 11.15 | 10.16 | 11.65 | 11.75 | 11.65 | 11.34 | 8.40 | 9.08 | 9.41 | 11.24 | 9.87 | 12.58 | 10.40 |
| FeOt | 1.85 | 1.80 | 2.65 | 1.51 | 1.21 | 0.92 | 2.80 | 4.53 | 10.70 | 10.96 | 7.76 | 7.25 | 1.11 | 4.37 | 0.17 |
| MnO | 0.04 | 0.04 | 0.08 | 0.07 | 0.03 | 0.00 | 0.06 | 0.08 | 0.22 | 0.23 | 0.14 | 0.10 | 0.00 | 0.07 | 0.00 |
| MgO | 1.56 | 1.41 | 2.24 | 2.56 | 1.74 | 1.31 | 1.80 | 2.42 | 6.20 | 4.74 | 2.61 | 1.91 | 0.00 | 1.58 | 0.00 |
| CaO | 9.62 | 7.35 | 8.24 | 12.11 | 9.28 | 9.54 | 8.41 | 8.92 | 12.54 | 12.70 | 7.69 | 7.02 | 1.42 | 7.45 | 2.05 |
| $K_2O$ | 0.36 | 0.60 | 0.59 | 0.38 | 0.46 | 0.41 | 0.46 | 0.57 | 0.75 | 0.75 | 0.68 | 0.93 | 3.62 | 0.71 | 2.51 |
| $P_2O_5$ | 0.27 | 0.23 | 0.36 | 0.22 | 0.25 | 0.15 | 0.32 | 0.22 | 0.12 | 0.00 | 0.14 | 0.10 | 0.06 | 0.24 | 0.14 |
| Sum | 79.83 | 82.45 | 81.62 | 82.26 | 80.61 | 80.87 | 81.78 | 85.51 | 83.17 | 82.35 | 78.52 | 82.84 | 82.74 | 84.72 | 87.45 |
| Ba (ppm) | 350 | 280 | 310 | 270 | 210 | 220 | 280 | 280 | 230 | 360 | 280 | 460 | 770 | 350 | 680 |
| Cl | 70 | n.d. | n.d. | 100 | n.d. | n.d. | n.d. | 110 | 110 | 210 | n.d. | n.d. | n.d. | n.d. | n.d. |
| S | 260 | 120 | 160 | n.d. | 270 | 150 | n.d. | n.d. | 280 | 300 | 100 | 340 | 190 | 260 | n.d. |
| Bi | n.d. | n.d. | n.d. | n.d. | n.d. | n.d. | n.d. | n.d. | n.d. | n.d. | n.d. | n.d. | n.d. | n.d. | n.d. |
| Cr | 270 | 190 | 220 | 270 | 150 | 120 | 240 | 320 | 1220 | 1990 | 400 | 270 | 40 | 200 | 120 |
| Cu | n.d. | n.d. | n.d. | n.d. | n.d. | n.d. | n.d. | n.d. | n.d. | n.d. | n.d. | n.d. | n.d. | n.d. | n.d. |
| Nb | n.d. | n.d. | n.d. | n.d. | n.d. | n.d. | n.d. | n.d. | n.d. | n.d. | n.d. | n.d. | n.d. | n.d. | n.d. |
| Ni | n.d. | n.d. | n.d. | n.d. | n.d. | n.d. | n.d. | n.d. | 320 | 240 | n.d. | 80 | n.d. | n.d. | n.d. |
| Pb | 20 | 20 | n.d. | n.d. | 20 | n.d. | n.d. | n.d. | n.d. | n.d. | n.d. | n.d. | 30 | n.d. | 30 |
| Rb | n.d. | n.d. | 20 | n.d. | n.d. | n.d. | n.d. | n.d. | n.d. | n.d. | 20 | 20 | 60 | n.d. | 50 |
| Sn | n.d. | n.d. | 30 | n.d. | n.d. | n.d. | n.d. | n.d. | n.d. | 40 | n.d. | n.d. | n.d. | n.d. | n.d. |
| Sr | 240 | 260 | 230 | 190 | 260 | 250 | 240 | 240 | 50 | 170 | 200 | 290 | 110 | 310 | 100 |
| V | 250 | 130 | 240 | 210 | 140 | 160 | 240 | 270 | 370 | 420 | 280 | 260 | n.d. | 240 | 50 |
| W | n.d. | n.d. | n.d. | n.d. | n.d. | n.d. | n.d. | n.d. | n.d. | n.d. | n.d. | n.d. | n.d. | n.d. | n.d. |
| Zn | 20 | 30 | 40 | 20 | n.d. | n.d. | 20 | 20 | 80 | 90 | 50 | 40 | 20 | 30 | n.d. |
| Zr | 100 | 80 | 80 | 100 | 40 | 70 | 150 | 80 | 30 | 30 | 50 | 30 | 80 | 120 | 40 |

Excluded elements (all values <LOD): Ag, Au, As, Cd, Co, Mo, Pd, Sb, Se

Rock type names after initial classification. Amp= amphibolite, Grt= granite, Act= actinolite rock, Diop= Diopside-actinolite skarn, Mgm= migmatite

Appendix V continues.

| ID | k141 | k142 | k143 | k144 | k145 | k146 | k147 | k148 | k149 | k150 | k151 |
|---|---|---|---|---|---|---|---|---|---|---|---|
| Rock type | Amp | Grt | Diop | Grt | Grt | Amp | Diop | Act | Diop | Act | Diop |
| Depth (m) | 345.00 | 347.77 | 349.40 | 353.00 | 357.80 | 362.40 | 363.30 | 366.00 | 367.00 | 368.00 | 368.70 |
| $SiO_2$ (wt.%) | 56.13 | 79.43 | 58.43 | 71.20 | 70.63 | 57.49 | 58.74 | 45.23 | 57.09 | 45.06 | 58.59 |
| $TiO_2$ | 0.69 | 0.05 | 0.69 | 0.02 | 0.07 | 0.44 | 0.72 | 0.85 | 0.63 | 1.03 | 0.40 |
| $Al_2O_3$ | 12.22 | 8.31 | 11.62 | 11.06 | 10.39 | 10.78 | 12.02 | 10.27 | 10.57 | 11.13 | 13.32 |
| FeOt | 2.83 | 0.54 | 1.56 | 0.23 | 0.60 | 1.52 | 2.72 | 10.97 | 1.21 | 11.73 | 0.69 |
| MnO | 0.06 | 0.00 | 0.05 | 0.00 | 0.00 | 0.02 | 0.06 | 0.22 | 0.04 | 0.24 | 0.00 |
| MgO | 2.15 | 0.39 | 2.06 | 0.00 | 0.00 | 1.96 | 1.64 | 5.30 | 1.58 | 4.90 | 1.09 |
| CaO | 8.42 | 1.06 | 7.68 | 0.83 | 1.49 | 7.38 | 8.13 | 12.42 | 9.71 | 13.08 | 8.74 |
| $K_2O$ | 0.48 | 2.86 | 0.60 | 4.56 | 3.03 | 0.56 | 0.56 | 1.15 | 0.47 | 0.83 | 0.48 |
| $P_2O_5$ | 0.26 | 0.00 | 0.10 | 0.00 | 0.00 | 0.16 | 0.10 | 0.12 | 0.00 | 0.14 | 0.23 |
| Sum | 83.25 | 92.63 | 82.79 | 87.90 | 86.21 | 80.31 | 84.69 | 86.54 | 81.31 | 88.14 | 83.54 |
| Ba (ppm) | 330 | 490 | 230 | 540 | 440 | 350 | 310 | 260 | 280 | 310 | 270 |
| Cl | n.d. | n.d. | n.d. | n.d. | n.d. | 120 | n.d. | 250 | 680 | 930 | 300 |
| S | 280 | 180 | n.d. | n.d. | 220 | 100 | n.d. | 190 | 110 | 420 | 190 |
| Bi | n.d. | n.d. | n.d. | n.d. | n.d. | n.d. | n.d. | n.d. | n.d. | n.d. | n.d. |
| Cr | 230 | 70 | 210 | n.d. | 60 | 210 | 150 | 1140 | 200 | 990 | 110 |
| Cu | n.d. | n.d. | n.d. | n.d. | n.d. | n.d. | n.d. | n.d. | n.d. | n.d. | n.d. |
| Nb | n.d. | n.d. | n.d. | n.d. | n.d. | n.d. | n.d. | n.d. | n.d. | n.d. | n.d. |
| Ni | n.d. | n.d. | n.d. | n.d. | n.d. | n.d. | n.d. | 260 | n.d. | 180 | n.d. |
| Pb | n.d. | 20 | n.d. | 30 | 20 | n.d. | n.d. | n.d. | 20 | n.d. | n.d. |
| Rb | n.d. | 70 | n.d. | 120 | 60 | n.d. | n.d. | 40 | n.d. | n.d. | n.d. |
| Sn | n.d. | n.d. | n.d. | n.d. | n.d. | n.d. | n.d. | n.d. | n.d. | n.d. | n.d. |
| Sr | 220 | 60 | 150 | 60 | 80 | 240 | 240 | 150 | 240 | 210 | 270 |
| V | 260 | n.d. | 160 | n.d. | n.d. | 170 | 180 | 380 | 140 | 490 | 120 |
| W | n.d. | n.d. | n.d. | n.d. | n.d. | n.d. | n.d. | n.d. | n.d. | n.d. | n.d. |
| Zn | n.d. | n.d. | 20 | n.d. | n.d. | n.d. | 20 | 70 | 20 | 80 | n.d. |
| Zr | 90 | 60 | 170 | 20 | 70 | 40 | 100 | 30 | 150 | 30 | 20 |

Excluded elements (all values <LOD): Ag, Au, As, Cd, Co, Mo, Pd, Sb, Se

Rock type names after initial classification. Amp= amphibolite, Grt= granite, Act= actinolite rock, Diop= Diopside-actinolite skarn, Mgm= migmatite

## APPENDIX VI: P-XRF data of the outcrop analyses

| ID | a1p | a1l | a1p | a1p | a1p | a1p | a1l | a1l | a1l | a1l | a2p | a2p | a2p | a2p | a2p |
|---|---|---|---|---|---|---|---|---|---|---|---|---|---|---|---|
| $SiO_2$ (wt.%) | 45.42 | 12.22 | 44.49 | 46.03 | 45.71 | 45.53 | 12.37 | 10.93 | 12.59 | 3.08 | 44.65 | 46.81 | 45.82 | 39.70 | 42.71 |
| $TiO_2$ | 0.53 | 0.34 | 0.53 | 0.73 | 1.16 | 0.74 | 0.30 | 0.36 | 0.27 | 0.21 | 0.56 | 1.08 | 0.62 | 1.01 | 0.66 |
| $Al_2O_3$ | 7.01 | 1.46 | 6.87 | 6.85 | 7.63 | 7.13 | 1.62 | 1.38 | 1.79 | 0.36 | 7.18 | 6.99 | 6.79 | 6.11 | 7.12 |
| FeOt | 1.49 | 2.64 | 2.73 | 1.77 | 1.99 | 2.42 | 2.93 | 3.30 | 2.73 | 2.62 | 1.21 | 2.71 | 2.40 | 1.77 | 1.58 |
| MnO | 0.06 | 0.02 | 0.10 | 0.07 | 0.07 | 0.07 | 0.03 | 0.05 | 0.02 | 0.02 | 0.00 | 0.06 | 0.05 | 0.00 | 0.00 |
| MgO | 0.94 | 0.00 | 1.19 | 1.11 | 1.37 | 0.74 | 0.00 | 0.00 | 0.00 | 0.00 | 0.61 | 1.04 | 0.62 | 0.46 | 0.55 |
| CaO | 4.10 | 1.02 | 4.63 | 4.79 | 4.55 | 3.94 | 1.18 | 1.28 | 0.86 | 1.47 | 3.44 | 4.76 | 3.70 | 3.81 | 3.81 |
| $K_2O$ | 0.94 | 1.45 | 1.01 | 1.01 | 1.00 | 1.23 | 1.51 | 1.56 | 1.57 | 1.11 | 1.37 | 1.09 | 1.02 | 1.32 | 1.43 |
| $P_2O_5$ | 0.07 | 0.56 | 0.14 | 0.13 | 0.23 | 0.14 | 0.62 | 0.51 | 0.52 | 0.35 | 0.30 | 0.22 | 0.21 | 0.16 | 0.23 |
| Sum | 60.56 | 19.71 | 61.69 | 62.48 | 63.72 | 61.94 | 20.55 | 19.38 | 20.35 | 9.23 | 59.31 | 64.78 | 61.24 | 54.35 | 58.09 |
| Ba (ppm) | 280 | 250 | 320 | 280 | 280 | 270 | 220 | 250 | 230 | 220 | 300 | 240 | 290 | 270 | 240 |
| Cl | n.d. | 1320 | 100 | 160 | 110 | n.d. | 1380 | 360 | 320 | 450 | n.d. | n.d. | n.d. | 40 | n.d. |
| S | 1150 | 7440 | 2190 | 1390 | 2040 | 1790 | 7690 | 7800 | 9090 | 5420 | 2170 | 1860 | 2080 | 2480 | 2130 |
| Bi | n.d. | n.d. | n.d. | n.d. | n.d. | n.d. | n.d. | n.d. | n.d. | n.d. | n.d. | n.d. | n.d. | n.d. | n.d. |
| Cr | 160 | 160 | 200 | 180 | 220 | 140 | 190 | 190 | 170 | 170 | 130 | 220 | 160 | 190 | 120 |
| Cu | n.d. | 50 | n.d. | n.d. | n.d. | n.d. | 40 | 30 | 70 | 70 | n.d. | n.d. | n.d. | n.d. | n.d. |
| Ni | n.d. | n.d. | n.d. | n.d. | n.d. | n.d. | n.d. | n.d. | n.d. | n.d. | n.d. | n.d. | n.d. | n.d. | n.d. |
| Pb | 40 | 70 | 50 | 40 | 70 | 50 | 70 | 70 | 80 | 70 | 30 | 40 | 40 | 50 | 40 |
| Rb | n.d. | n.d. | n.d. | n.d. | n.d. | n.d. | n.d. | n.d. | 20 | 30 | n.d. | n.d. | n.d. | n.d. | n.d. |
| Sn | n.d. | n.d. | n.d. | n.d. | n.d. | n.d. | n.d. | n.d. | n.d. | n.d. | n.d. | n.d. | n.d. | n.d. | n.d. |
| Sr | 130 | 130 | 140 | 120 | 150 | 150 | 120 | 100 | 100 | 100 | 230 | 90 | 140 | 210 | 230 |
| V | 140 | 120 | 170 | 190 | 180 | 130 | 130 | 160 | 120 | 100 | 110 | 200 | 140 | 160 | 140 |
| W | n.d. | n.d. | n.d. | n.d. | n.d. | n.d. | n.d. | n.d. | 80 | n.d. | n.d. | n.d. | n.d. | n.d. | n.d. |
| Zn | 30 | 150 | 80 | 30 | 50 | 60 | 170 | 140 | 190 | 130 | n.d. | 90 | 20 | 20 | n.d. |
| Zr | 80 | 100 | 70 | 90 | 190 | 90 | 110 | 70 | 100 | 110 | 60 | 60 | 120 | 100 | 80 |

Excluded elements (all values <LOD): Ag, Au, As, Cd, Co, Mo, Nb, Pd, Sb, Se

First letter in the ID indicates the outcrop. l= poor quality surface, p= good quality surface.

Appendix VI continues.

| ID | a2l | a2l | a2l | a2l | a2l | a3p | a3p | a3p | a3p | a3p | a3l | a3l | a3l | a4p | a4p |
|---|---|---|---|---|---|---|---|---|---|---|---|---|---|---|---|
| $SiO_2$ (wt.%) | 34.77 | 11.44 | 19.56 | 7.91 | 23.06 | 40.95 | 43.81 | 42.83 | 45.55 | 48.03 | 10.28 | 8.50 | 9.28 | 66.05 | 62.44 |
| $TiO_2$ | 0.45 | 0.42 | 0.48 | 0.27 | 0.50 | 0.80 | 1.37 | 0.71 | 1.26 | 0.90 | 0.32 | 0.24 | 0.34 | 0.09 | 0.11 |
| $Al_2O_3$ | 4.81 | 1.43 | 2.48 | 0.99 | 3.12 | 6.59 | 7.46 | 7.16 | 7.85 | 7.96 | 1.08 | 1.03 | 1.34 | 8.66 | 6.33 |
| FeOt | 3.06 | 2.24 | 2.73 | 2.39 | 3.03 | 1.32 | 2.27 | 2.79 | 2.23 | 1.69 | 2.23 | 2.57 | 3.21 | 0.22 | 0.40 |
| MnO | 0.07 | 0.02 | 0.03 | 0.00 | 0.05 | 0.03 | 0.04 | 0.04 | 0.04 | 0.04 | 0.00 | 0.00 | 0.03 | 0.00 | 0.00 |
| MgO | 0.00 | 0.00 | 0.55 | 0.00 | 0.00 | 0.51 | 0.77 | 0.68 | 1.01 | 1.07 | 0.00 | 0.00 | 0.00 | 0.52 | 0.40 |
| CaO | 3.25 | 1.19 | 1.57 | 2.03 | 1.82 | 3.38 | 4.86 | 4.20 | 4.49 | 5.15 | 0.96 | 0.72 | 1.40 | 1.25 | 0.85 |
| $K_2O$ | 1.47 | 1.50 | 1.62 | 1.59 | 1.47 | 1.20 | 1.14 | 1.17 | 0.88 | 1.29 | 1.55 | 1.41 | 1.69 | 2.58 | 3.14 |
| $P_2O_5$ | 0.34 | 0.44 | 0.47 | 1.50 | 0.47 | 0.17 | 0.10 | 0.05 | 0.16 | 0.18 | 0.44 | 0.56 | 0.61 | 0.11 | 0.21 |
| Sum | 48.22 | 18.67 | 29.48 | 16.69 | 33.52 | 54.94 | 61.83 | 59.63 | 63.48 | 66.32 | 16.85 | 15.03 | 17.91 | 79.48 | 73.88 |
| Ba (ppm) | 270 | 300 | 230 | 210 | 320 | 270 | 280 | 300 | 300 | 240 | 270 | 240 | 290 | 580 | 690 |
| Cl | 70 | 270 | 1100 | 300 | 930 | n.d. | n.d. | n.d. | n.d. | n.d. | 840 | 910 | 170 | n.d. | n.d. |
| S | 4780 | 7150 | 6030 | 7000 | 5870 | 2430 | 560 | 580 | 790 | 1300 | 4890 | 5490 | 8950 | 850 | 2550 |
| Bi | n.d. | n.d. | n.d. | n.d. | n.d. | n.d. | n.d. | n.d. | n.d. | n.d. | n.d. | n.d. | n.d. | n.d. | n.d. |
| Cr | 190 | 180 | 160 | 140 | 180 | 90 | 180 | 190 | 160 | 130 | 150 | 170 | 180 | 60 | 60 |
| Cu | n.d. | n.d. | 30 | 50 | n.d. | n.d. | n.d. | n.d. | n.d. | n.d. | 50 | 40 | 40 | n.d. | n.d. |
| Ni | n.d. | n.d. | n.d. | n.d. | n.d. | n.d. | n.d. | n.d. | n.d. | n.d. | n.d. | n.d. | n.d. | n.d. | n.d. |
| Pb | 40 | 50 | 50 | 40 | 60 | 40 | 50 | 40 | 40 | 30 | 50 | 70 | 40 | 30 | 30 |
| Rb | n.d. | 20 | n.d. | 20 | n.d. | n.d. | n.d. | n.d. | n.d. | n.d. | n.d. | n.d. | n.d. | 50 | 50 |
| Sn | n.d. | n.d. | n.d. | n.d. | n.d. | n.d. | n.d. | n.d. | n.d. | n.d. | n.d. | n.d. | n.d. | n.d. | n.d. |
| Sr | 150 | 130 | 210 | 140 | 150 | 200 | 210 | 180 | 210 | 230 | 160 | 130 | 170 | 80 | 70 |
| V | 180 | 130 | 160 | 90 | 170 | 120 | 180 | 230 | 150 | 200 | 110 | 110 | 140 | 50 | n.d. |
| W | n.d. | n.d. | n.d. | n.d. | n.d. | n.d. | n.d. | n.d. | n.d. | n.d. | n.d. | 90 | n.d. | n.d. | n.d. |
| Zn | 50 | 80 | 100 | 80 | 90 | 20 | 40 | 40 | n.d. | 20 | 130 | 170 | 100 | n.d. | n.d. |
| Zr | 200 | 80 | 130 | 100 | 100 | 40 | 30 | 40 | 30 | 170 | 40 | 120 | 80 | 50 | n.d. |

Excluded elements (all values <LOD): Ag, Au, As, Cd, Co, Mo, Nb, Pd, Sb, Se
First letter in the ID indicates the outcrop. l= poor quality surface, p= good quality surface.

Appendix VI continues.

| ID | a4p | a5p | a5p | a5p | a5p | a5l | a5l | a5l | b1p | b1p | b1p | b1p | b1p | b1p | b1p |
|---|---|---|---|---|---|---|---|---|---|---|---|---|---|---|---|
| $SiO_2$ (wt.%) | 62.52 | 47.06 | 57.66 | 48.34 | 66.59 | 19.88 | 25.46 | 12.08 | 47.58 | 52.73 | 57.45 | 54.41 | 53.20 | 59.82 | 57.83 |
| $TiO_2$ | 0.17 | 0.62 | 0.10 | 0.85 | 0.08 | 0.24 | 0.27 | 0.24 | 1.23 | 0.74 | 0.46 | 0.35 | 0.79 | 0.23 | 0.76 |
| $Al_2O_3$ | 6.16 | 8.03 | 6.07 | 8.04 | 7.23 | 2.12 | 2.91 | 1.44 | 10.27 | 10.03 | 4.48 | 7.08 | 9.51 | 8.33 | 9.41 |
| FeOt | 0.72 | 1.10 | 0.28 | 1.17 | 0.21 | 0.84 | 0.95 | 1.19 | 5.58 | 2.07 | 1.98 | 1.92 | 5.52 | 0.79 | 3.22 |
| MnO | 0.00 | 0.03 | 0.00 | 0.03 | 0.00 | 0.00 | 0.00 | 0.00 | 0.12 | 0.06 | 0.00 | 0.00 | 0.10 | 0.00 | 0.03 |
| MgO | 0.36 | 0.61 | 0.35 | 0.79 | 0.00 | 0.00 | 0.00 | 0.00 | 1.95 | 1.20 | 0.40 | 0.00 | 1.40 | 0.66 | 0.00 |
| CaO | 1.26 | 7.51 | 1.12 | 3.42 | 1.09 | 0.96 | 1.19 | 0.65 | 7.68 | 7.27 | 1.46 | 1.92 | 4.26 | 3.54 | 3.44 |
| $K_2O$ | 1.57 | 0.73 | 1.87 | 1.04 | 1.79 | 1.61 | 1.60 | 1.50 | 0.54 | 0.81 | 1.18 | 2.53 | 1.72 | 0.53 | 1.59 |
| $P_2O_5$ | 0.19 | 0.16 | 0.33 | 0.20 | 0.21 | 0.51 | 0.50 | 0.59 | 0.38 | 0.00 | 0.12 | 0.09 | 0.40 | 0.17 | 0.21 |
| Sum | 72.94 | 65.85 | 67.78 | 63.88 | 77.20 | 26.17 | 32.88 | 17.70 | 75.33 | 74.92 | 67.52 | 68.29 | 76.90 | 74.08 | 76.48 |
| Ba (ppm) | 360 | 310 | 680 | 280 | 600 | 630 | 710 | 590 | 280 | 250 | 400 | 640 | 320 | 230 | 810 |
| Cl | n.d. | n.d. | n.d. | n.d. | n.d. | 650 | 230 | 170 | n.d. | n.d. | n.d. | n.d. | 180 | n.d. | n.d. |
| S | 1760 | 920 | 4590 | 1770 | 3350 | 6010 | 7240 | 8140 | 510 | 420 | 500 | 780 | 2310 | 850 | 730 |
| Bi | n.d. | n.d. | n.d. | n.d. | n.d. | n.d. | n.d. | n.d. | n.d. | n.d. | n.d. | n.d. | n.d. | n.d. | n.d. |
| Cr | 60 | 170 | 110 | 150 | 20 | 120 | 140 | 150 | 290 | 160 | 70 | 110 | 220 | n.d. | 60 |
| Cu | n.d. | n.d. | n.d. | n.d. | n.d. | n.d. | n.d. | n.d. | n.d. | n.d. | n.d. | n.d. | n.d. | n.d. | n.d. |
| Ni | n.d. | n.d. | n.d. | n.d. | n.d. | n.d. | n.d. | n.d. | n.d. | n.d. | n.d. | n.d. | n.d. | n.d. | n.d. |
| Pb | 30 | n.d. | 40 | 40 | 40 | 40 | 30 | 50 | n.d. | 20 | 20 | 20 | 20 | 20 | 30 |
| Rb | 30 | n.d. | 30 | n.d. | 20 | 30 | 30 | 30 | n.d. | n.d. | 40 | 50 | 60 | n.d. | 50 |
| Sn | n.d. | n.d. | n.d. | n.d. | n.d. | n.d. | n.d. | n.d. | n.d. | n.d. | n.d. | n.d. | n.d. | n.d. | n.d. |
| Sr | 70 | 240 | 80 | 110 | 90 | 70 | 90 | 60 | 320 | 210 | 140 | 210 | 190 | 150 | 300 |
| V | 50 | 140 | n.d. | 130 | n.d. | 60 | 70 | 80 | 330 | 200 | n.d. | 100 | 200 | 90 | 80 |
| W | n.d. | n.d. | n.d. | n.d. | n.d. | n.d. | n.d. | n.d. | n.d. | n.d. | n.d. | n.d. | n.d. | n.d. | n.d. |
| Zn | n.d. | n.d. | n.d. | n.d. | n.d. | 50 | 60 | 70 | 40 | 20 | 20 | 20 | 50 | n.d. | 50 |
| Zr | 50 | 120 | 30 | 50 | 40 | 40 | 50 | 40 | 20 | 30 | 150 | 190 | 90 | 110 | 300 |

Excluded elements (all values <LOD): Ag, Au, As, Cd, Co, Mo, Nb, Pd, Sb, Se

First letter in the ID indicates the outcrop. l= poor quality surface, p= good quality surface.

Appendix VI continues.

| ID | b1l | b1l | b1l | b1l | b1l | b1l | b1l | c1p | c1l | c2p | c2l | c3p | c3l | c4p | c4l |
|---|---|---|---|---|---|---|---|---|---|---|---|---|---|---|---|
| $SiO_2$ (wt.%) | 17.37 | 20.93 | 16.27 | 14.78 | 12.84 | 14.21 | 18.95 | 44.90 | 26.18 | 50.76 | 28.20 | 47.98 | 20.98 | 49.10 | 31.39 |
| $TiO_2$ | 0.47 | 0.48 | 0.19 | 0.20 | 0.42 | 0.17 | 0.38 | 0.83 | 0.69 | 0.50 | 0.46 | 0.65 | 0.68 | 0.82 | 0.46 |
| $Al_2O_3$ | 2.43 | 2.68 | 1.70 | 1.57 | 1.64 | 1.76 | 2.49 | 7.51 | 3.66 | 8.77 | 3.87 | 7.60 | 2.88 | 8.79 | 4.94 |
| FeOt | 3.85 | 2.58 | 1.07 | 1.36 | 4.51 | 1.13 | 2.39 | 5.44 | 3.60 | 1.56 | 2.32 | 1.30 | 1.80 | 2.98 | 4.63 |
| MnO | 0.05 | 0.08 | 0.00 | 0.00 | 0.06 | 0.02 | 0.00 | 0.12 | 0.06 | 0.02 | 0.04 | 0.05 | 0.05 | 0.07 | 0.09 |
| MgO | 0.00 | 0.00 | 0.00 | 0.00 | 0.00 | 0.00 | 0.00 | 1.28 | 0.00 | 0.41 | 0.00 | 0.59 | 0.00 | 0.65 | 0.58 |
| CaO | 2.00 | 2.97 | 1.10 | 0.97 | 1.80 | 1.42 | 2.06 | 4.62 | 2.41 | 4.75 | 2.42 | 5.21 | 2.66 | 4.49 | 2.42 |
| $K_2O$ | 1.80 | 1.54 | 1.61 | 1.81 | 1.78 | 1.54 | 2.45 | 1.04 | 1.64 | 0.68 | 1.36 | 0.76 | 1.10 | 0.42 | 1.11 |
| $P_2O_5$ | 0.57 | 0.46 | 0.37 | 1.16 | 0.70 | 0.85 | 0.88 | 0.42 | 0.37 | 0.23 | 0.26 | 0.22 | 0.39 | 0.15 | 0.36 |
| Sum | 28.55 | 31.72 | 22.30 | 21.85 | 23.75 | 21.11 | 29.59 | 66.15 | 38.60 | 67.69 | 38.92 | 64.37 | 30.54 | 67.46 | 45.97 |
| Ba (ppm) | 260 | 250 | 1090 | 480 | 240 | 180 | 1620 | 410 | 380 | 250 | 220 | 310 | 300 | 240 | 400 |
| Cl | 1140 | 960 | 900 | 860 | 600 | 320 | 900 | n.d. | 70 | n.d. | 80 | n.d. | 100 | n.d. | 110 |
| S | 10250 | 8300 | 5550 | 10360 | 6880 | 9980 | 7750 | 1460 | 6070 | 950 | 4460 | 1380 | 5710 | 870 | 6360 |
| Bi | n.d. | n.d. | n.d. | n.d. | n.d. | n.d. | n.d. | n.d. | n.d. | n.d. | n.d. | n.d. | n.d. | n.d. | n.d. |
| Cr | 210 | 220 | 110 | 130 | 200 | 100 | 150 | 260 | 200 | 100 | 180 | 150 | 160 | 100 | 180 |
| Cu | 50 | 30 | n.d. | n.d. | n.d. | n.d. | n.d. | n.d. | n.d. | n.d. | n.d. | n.d. | n.d. | n.d. | n.d. |
| Ni | n.d. | n.d. | n.d. | n.d. | n.d. | n.d. | n.d. | n.d. | n.d. | n.d. | n.d. | n.d. | n.d. | n.d. | n.d. |
| Pb | 50 | 60 | 30 | 20 | 40 | 30 | 60 | 20 | 80 | 20 | 50 | n.d. | 30 | 20 | 40 |
| Rb | n.d. | 60 | 40 | 30 | 40 | n.d. | 50 | 20 | 50 | n.d. | n.d. | n.d. | n.d. | n.d. | n.d. |
| Sn | n.d. | n.d. | n.d. | n.d. | n.d. | n.d. | n.d. | n.d. | n.d. | n.d. | n.d. | n.d. | n.d. | n.d. | n.d. |
| Sr | 280 | 190 | 180 | 210 | 170 | 140 | 310 | 150 | 140 | 160 | 160 | 160 | 190 | 180 | 180 |
| V | 160 | 170 | 50 | 50 | 170 | 80 | 130 | 250 | 210 | 100 | 140 | 160 | 150 | 150 | 160 |
| W | n.d. | n.d. | n.d. | n.d. | n.d. | n.d. | n.d. | n.d. | n.d. | n.d. | n.d. | n.d. | n.d. | n.d. | n.d. |
| Zn | 220 | 80 | 70 | 90 | 170 | 100 | 80 | 60 | 60 | 40 | 50 | n.d. | 40 | 40 | 60 |
| Zr | 50 | 40 | 90 | 150 | 80 | 110 | 200 | 100 | 120 | 100 | 100 | 90 | 70 | 80 | 60 |

Excluded elements (all values <LOD): Ag, Au, As, Cd, Co, Mo, Nb, Pd, Sb, Se

First letter in the ID indicates the outcrop. l= poor quality surface, p= good quality surface.

Appendix VI continues.

| ID | c5p | c5l | d1p | d1l | d2p | d2l | dx | e1p | e1l | e1l | e2p | e2l | f1p | f1l | f2p |
|---|---|---|---|---|---|---|---|---|---|---|---|---|---|---|---|
| $SiO_2$ (wt.%) | 52.27 | 37.38 | 47.19 | 11.97 | 63.58 | 31.45 | 73.77 | 52.02 | 32.85 | 36.46 | 48.16 | 21.89 | 53.07 | 38.02 | 61.93 |
| $TiO_2$ | 0.56 | 0.67 | 0.57 | 0.27 | 0.08 | 0.16 | 0.02 | 0.70 | 0.50 | 0.62 | 0.84 | 0.39 | 0.54 | 0.22 | 0.10 |
| $Al_2O_3$ | 8.45 | 5.42 | 6.73 | 1.59 | 5.11 | 2.31 | 9.15 | 7.94 | 4.39 | 4.89 | 7.80 | 2.41 | 9.15 | 8.40 | 8.36 |
| FeOt | 5.24 | 4.28 | 4.11 | 3.01 | 0.56 | 0.83 | 0.05 | 5.31 | 3.82 | 5.11 | 6.20 | 3.20 | 4.67 | 11.23 | 1.56 |
| MnO | 0.12 | 0.11 | 0.07 | 0.02 | 0.00 | 0.00 | 0.00 | 0.05 | 0.03 | 0.06 | 0.14 | 0.05 | 0.08 | 0.05 | 0.05 |
| MgO | 0.91 | 0.60 | 0.48 | 0.00 | 0.00 | 0.00 | 0.00 | 1.06 | 0.00 | 0.88 | 0.99 | 0.00 | 1.21 | 2.33 | 0.60 |
| CaO | 5.50 | 3.40 | 4.51 | 0.99 | 2.70 | 2.02 | 0.09 | 3.94 | 3.84 | 3.26 | 5.21 | 4.09 | 6.30 | 0.64 | 0.22 |
| $K_2O$ | 0.77 | 1.18 | 0.94 | 1.60 | 0.71 | 1.22 | 6.60 | 1.31 | 0.96 | 1.18 | 0.63 | 1.06 | 0.43 | 2.61 | 7.36 |
| $P_2O_5$ | 0.37 | 0.30 | 0.29 | 0.77 | 0.54 | 0.75 | 0.00 | 0.38 | 0.52 | 0.46 | 0.23 | 1.62 | 0.07 | 0.38 | 0.06 |
| Sum | 74.18 | 53.34 | 64.88 | 20.22 | 73.28 | 38.73 | 89.69 | 72.73 | 46.92 | 52.92 | 70.19 | 34.72 | 75.53 | 63.87 | 80.24 |
| Ba (ppm) | 370 | 400 | 360 | 340 | 310 | 230 | 520 | 690 | 490 | 510 | 330 | 380 | 240 | 810 | 410 |
| Cl | n.d. | n.d. | 70 | 990 | n.d. | 640 | n.d. | n.d. | n.d. | 110 | n.d. | 250 | n.d. | n.d. | n.d. |
| S | 2240 | 3350 | 2070 | 5170 | 2210 | 4010 | 1930 | 820 | 5370 | 3830 | 1380 | 8880 | 180 | 950 | 340 |
| Bi | n.d. | n.d. | n.d. | n.d. | n.d. | 20 | n.d. | n.d. | n.d. | n.d. | n.d. | n.d. | n.d. | n.d. | n.d. |
| Cr | 260 | 200 | 140 | 150 | 70 | 150 | n.d. | 140 | 110 | 180 | 200 | 130 | 210 | 280 | 80 |
| Cu | n.d. | n.d. | n.d. | 50 | n.d. | n.d. | n.d. | n.d. | n.d. | n.d. | n.d. | n.d. | n.d. | n.d. | n.d. |
| Ni | n.d. | n.d. | n.d. | n.d. | n.d. | n.d. | n.d. | n.d. | n.d. | n.d. | n.d. | n.d. | n.d. | 80 | n.d. |
| Pb | n.d. | n.d. | 20 | 50 | 20 | 30 | 70 | n.d. | n.d. | n.d. | n.d. | 20 | n.d. | 20 | 60 |
| Rb | n.d. | 20 | 30 | 20 | n.d. | n.d. | 100 | 30 | 20 | 20 | 20 | 30 | n.d. | 70 | 50 |
| Sn | n.d. | n.d. | n.d. | n.d. | n.d. | n.d. | n.d. | n.d. | n.d. | n.d. | n.d. | n.d. | n.d. | n.d. | n.d. |
| Sr | 250 | 180 | 210 | 160 | 190 | 160 | 50 | 190 | 220 | 190 | 230 | 230 | 230 | 70 | 40 |
| V | 210 | 180 | 120 | 120 | n.d. | n.d. | n.d. | 140 | 170 | 160 | 160 | 110 | 180 | 370 | 50 |
| W | n.d. | n.d. | n.d. | n.d. | n.d. | n.d. | n.d. | n.d. | n.d. | n.d. | n.d. | n.d. | n.d. | n.d. | n.d. |
| Zn | 60 | 50 | 120 | 160 | 30 | 30 | n.d. | 60 | 20 | 30 | 30 | 50 | 30 | 60 | 50 |
| Zr | 110 | 90 | 80 | 90 | 90 | 40 | n.d. | 120 | 100 | 100 | 110 | 90 | 120 | 50 | 50 |

Excluded elements (all values <LOD): Ag, Au, As, Cd, Co, Mo, Nb, Pd, Sb, Se

First letter in the ID indicates the outcrop. l= poor quality surface, p= good quality surface.

Appendix VI continues.

| ID | f2p | f3p | f3l | f4p | f5p | f5l | g1l | g2l | g1p | h1l | h2l | h3l | h4l | h5l |
|---|---|---|---|---|---|---|---|---|---|---|---|---|---|---|
| $SiO_2$ (wt.%) | 62.63 | 60.26 | 42.17 | 39.88 | 55.89 | 31.59 | 32.34 | 25.48 | 36.09 | 69.10 | 51.27 | 64.56 | 68.56 | 47.38 |
| $TiO_2$ | 0.10 | 0.04 | 0.12 | 0.90 | 0.61 | 0.57 | 0.47 | 0.48 | 0.72 | 0.15 | 0.19 | 0.16 | 0.09 | 1.26 |
| $Al_2O_3$ | 4.65 | 6.91 | 3.31 | 5.72 | 9.98 | 5.14 | 4.00 | 3.45 | 4.76 | 7.35 | 4.69 | 7.45 | 6.92 | 9.00 |
| FeOt | 0.58 | 0.47 | 0.72 | 4.69 | 6.87 | 5.67 | 3.30 | 4.65 | 4.89 | 1.27 | 1.33 | 1.17 | 0.74 | 7.17 |
| MnO | 0.00 | 0.00 | 0.00 | 0.12 | 0.12 | 0.08 | 0.05 | 0.06 | 0.08 | 0.00 | 0.00 | 0.00 | 0.00 | 0.13 |
| MgO | 0.00 | 0.55 | 0.00 | 0.76 | 1.25 | 0.00 | 0.00 | 0.00 | 0.63 | 0.72 | 0.00 | 0.00 | 0.00 | 1.54 |
| CaO | 1.04 | 0.84 | 1.30 | 3.88 | 4.41 | 3.07 | 3.62 | 6.08 | 3.31 | 0.93 | 1.47 | 1.11 | 1.03 | 5.35 |
| $K_2O$ | 1.02 | 3.87 | 2.20 | 1.86 | 0.56 | 1.26 | 1.17 | 1.49 | 0.92 | 2.91 | 2.31 | 3.00 | 2.68 | 2.38 |
| $P_2O_5$ | 0.25 | 0.38 | 0.38 | 0.68 | 0.26 | 0.31 | 0.41 | 0.45 | 0.33 | 0.11 | 0.45 | 0.21 | 0.06 | 0.36 |
| Sum | 70.27 | 73.32 | 50.21 | 58.50 | 79.95 | 47.70 | 45.36 | 42.15 | 51.71 | 82.54 | 61.72 | 77.65 | 80.07 | 74.57 |
| Ba (ppm) | 140 | 270 | 250 | 540 | 410 | 300 | 410 | 570 | 380 | 480 | 510 | 500 | 480 | 480 |
| Cl | n.d. | n.d. | n.d. | 150 | n.d. | 350 | 210 | 80 | 230 | n.d. | n.d. | n.d. | n.d. | n.d. |
| S | 1930 | 1670 | 3410 | 2760 | 770 | 4350 | 2930 | 3670 | 1960 | 320 | 3360 | 1910 | 520 | 1760 |
| Bi | n.d. | n.d. | n.d. | n.d. | n.d. | n.d. | n.d. | n.d. | n.d. | n.d. | n.d. | n.d. | n.d. | n.d. |
| Cr | 50 | 20 | 80 | 200 | 230 | 210 | 120 | 160 | 190 | 50 | 60 | n.d. | 60 | 290 |
| Cu | n.d. | n.d. | n.d. | n.d. | n.d. | 50 | n.d. | n.d. | n.d. | n.d. | n.d. | n.d. | n.d. | n.d. |
| Ni | n.d. | n.d. | n.d. | n.d. | n.d. | n.d. | n.d. | n.d. | n.d. | n.d. | n.d. | n.d. | n.d. | n.d. |
| Pb | 20 | 30 | 20 | n.d. | n.d. | 20 | n.d. | 20 | n.d. | 40 | 30 | 30 | 20 | n.d. |
| Rb | n.d. | 50 | 40 | 110 | n.d. | n.d. | n.d. | 30 | 20 | 60 | 60 | 60 | 60 | 120 |
| Sn | n.d. | n.d. | n.d. | n.d. | n.d. | n.d. | n.d. | n.d. | n.d. | n.d. | n.d. | n.d. | n.d. | n.d. |
| Sr | 40 | 30 | 40 | 180 | 170 | 140 | 210 | 200 | 210 | 60 | 70 | 80 | 70 | 200 |
| V | 50 | 50 | 30 | 190 | 180 | 190 | 80 | 170 | 160 | 50 | n.d. | n.d. | n.d. | 280 |
| W | n.d. | n.d. | n.d. | n.d. | n.d. | n.d. | n.d. | n.d. | 100 | n.d. | n.d. | n.d. | n.d. | n.d. |
| Zn | n.d. | n.d. | 30 | 120 | 30 | 80 | 40 | 100 | 30 | 20 | 30 | 20 | n.d. | 60 |
| Zr | 40 | 20 | 40 | 110 | 70 | 90 | 100 | 120 | 120 | 70 | 100 | 60 | 50 | 70 |

Excluded elements (all values <LOD): Ag, Au, As, Cd, Co, Mo, Nb, Pd, Sb, Se
First letter in the ID indicates the outcrop. l= poor quality surface, p= good quality surface.

Appendix VI continues.

| ID | h6l | h6p | h6.5p | i1l | i1p | j1l | j2l | j2p | j1p | j3l | j3p | j4p | j4l | j5l | j5p |
|---|---|---|---|---|---|---|---|---|---|---|---|---|---|---|---|
| $SiO_2$ (wt.%) | 42.09 | 52.42 | 55.75 | 26.56 | 47.81 | 66.40 | 57.12 | 52.17 | 63.85 | 40.09 | 45.71 | 43.40 | 32.52 | 49.71 | 59.40 |
| $TiO_2$ | 0.81 | 0.62 | 0.96 | 0.37 | 0.90 | 0.38 | 0.76 | 0.81 | 0.44 | 0.65 | 0.84 | 0.58 | 0.58 | 0.79 | 1.01 |
| $Al_2O_3$ | 7.42 | 7.66 | 7.71 | 3.53 | 7.93 | 7.66 | 9.30 | 9.84 | 9.84 | 5.70 | 7.46 | 10.28 | 4.15 | 7.03 | 11.16 |
| FeOt | 8.16 | 4.93 | 5.36 | 4.42 | 5.82 | 2.14 | 5.15 | 5.78 | 2.83 | 4.98 | 5.46 | 10.14 | 9.64 | 6.50 | 5.67 |
| MnO | 0.09 | 0.09 | 0.06 | 0.11 | 0.12 | 0.02 | 0.11 | 0.11 | 0.03 | 0.12 | 0.10 | 0.20 | 0.20 | 0.11 | 0.06 |
| MgO | 2.59 | 0.62 | 1.49 | 0.00 | 2.25 | 0.00 | 1.36 | 1.73 | 0.47 | 1.04 | 1.37 | 5.02 | 0.00 | 0.76 | 1.34 |
| CaO | 2.41 | 4.83 | 2.92 | 3.76 | 7.37 | 2.22 | 5.35 | 6.17 | 2.41 | 5.92 | 5.36 | 10.62 | 8.97 | 5.55 | 6.14 |
| $K_2O$ | 2.91 | 1.01 | 2.27 | 1.80 | 0.31 | 1.12 | 1.14 | 0.41 | 1.37 | 0.70 | 1.19 | 0.78 | 1.02 | 1.21 | 0.56 |
| $P_2O_5$ | 0.52 | 0.38 | 0.19 | 0.97 | 0.29 | 0.42 | 0.35 | 0.24 | 0.19 | 0.41 | 0.24 | 0.00 | 1.13 | 0.57 | 0.29 |
| Sum | 67.01 | 72.56 | 76.71 | 41.52 | 72.81 | 80.36 | 80.64 | 77.24 | 81.42 | 59.61 | 67.73 | 81.03 | 58.21 | 72.22 | 85.64 |
| Ba (ppm) | 400 | 410 | 380 | 230 | 320 | 700 | 360 | 350 | 820 | 300 | 270 | 330 | 370 | 340 | 280 |
| Cl | n.d. | 120 | n.d. | 490 | 130 | n.d. | n.d. | n.d. | n.d. | n.d. | n.d. | 170 | 470 | 50 | n.d. |
| S | 2610 | 1890 | 170 | 6310 | 100 | 2860 | 3250 | 640 | 170 | 2180 | 340 | 210 | 6310 | 3430 | 100 |
| Bi | n.d. | n.d. | n.d. | n.d. | n.d. | n.d. | n.d. | n.d. | n.d. | n.d. | n.d. | n.d. | n.d. | n.d. | n.d. |
| Cr | 440 | 200 | 220 | 210 | 340 | 60 | 200 | 200 | 50 | 210 | 210 | 610 | 680 | 150 | 150 |
| Cu | 50 | n.d. | n.d. | 70 | n.d. | n.d. | n.d. | n.d. | n.d. | n.d. | n.d. | n.d. | n.d. | n.d. | n.d. |
| Ni | n.d. | n.d. | n.d. | n.d. | n.d. | n.d. | n.d. | n.d. | n.d. | n.d. | n.d. | 210 | 170 | n.d. | n.d. |
| Pb | 20 | n.d. | n.d. | 50 | 20 | 70 | 40 | n.d. | 20 | n.d. | n.d. | n.d. | n.d. | 20 | n.d. |
| Rb | 40 | 20 | 60 | n.d. | n.d. | 20 | 20 | n.d. | 30 | n.d. | n.d. | 20 | 30 | n.d. | n.d. |
| Sn | n.d. | n.d. | n.d. | n.d. | n.d. | n.d. | n.d. | 40 | n.d. | n.d. | n.d. | n.d. | 40 | n.d. | n.d. |
| Sr | 120 | 210 | 150 | 260 | 240 | 220 | 180 | 200 | 240 | 200 | 210 | 120 | 90 | 170 | 220 |
| V | 290 | 170 | 190 | 150 | 290 | 50 | 200 | 200 | 70 | 230 | 160 | 370 | 300 | 300 | 380 |
| W | n.d. | n.d. | n.d. | n.d. | n.d. | n.d. | n.d. | n.d. | n.d. | n.d. | n.d. | n.d. | n.d. | n.d. | n.d. |
| Zn | 210 | 40 | 50 | 150 | 50 | 30 | 50 | 60 | 30 | 40 | 40 | 80 | 300 | 70 | n.d. |
| Zr | 130 | 40 | 90 | 60 | 70 | 190 | 70 | 60 | 330 | 60 | 50 | 20 | n.d. | 90 | 70 |

Excluded elements (all values <LOD): Ag, Au, As, Cd, Co, Mo, Nb, Pd, Sb, Se

First letter in the ID indicates the outcrop. l= poor quality surface, p= good quality surface.

Appendix VI continues.

| ID | j6l | j6p | k1l | k1p | k2p | k2l | k3l | k3p | k4p | k4l |
|---|---|---|---|---|---|---|---|---|---|---|
| $SiO_2$ (wt.%) | 55.78 | 67.29 | 39.52 | 52.93 | 44.58 | 42.10 | 40.24 | 75.10 | 56.72 | 67.60 |
| $TiO_2$ | 0.15 | 0.12 | 0.25 | 1.54 | 1.34 | 1.08 | 0.36 | 0.42 | 0.60 | 0.34 |
| $Al_2O_3$ | 5.39 | 6.99 | 4.10 | 11.97 | 10.35 | 7.51 | 3.36 | 6.18 | 6.37 | 8.71 |
| FeOt | 1.01 | 1.00 | 2.36 | 4.37 | 11.53 | 10.36 | 2.45 | 2.17 | 3.80 | 2.65 |
| MnO | 0.02 | 0.00 | 0.02 | 0.03 | 0.19 | 0.18 | 0.03 | 0.03 | 0.04 | 0.03 |
| MgO | 0.00 | 0.75 | 0.46 | 1.37 | 2.06 | 0.00 | 0.00 | 0.00 | 0.71 | 0.47 |
| CaO | 2.21 | 1.06 | 2.87 | 5.27 | 7.88 | 6.75 | 2.77 | 2.24 | 2.48 | 2.96 |
| $K_2O$ | 1.70 | 2.72 | 0.98 | 1.78 | 0.61 | 0.77 | 1.49 | 1.09 | 1.70 | 1.20 |
| $P_2O_5$ | 0.49 | 0.11 | 0.64 | 0.38 | 0.57 | 0.43 | 0.71 | 0.17 | 0.16 | 0.19 |
| Sum | 66.75 | 80.03 | 51.20 | 79.63 | 79.11 | 69.18 | 51.41 | 87.40 | 72.59 | 84.15 |
| Ba (ppm) | 470 | 350 | 930 | 910 | 320 | 380 | 470 | 550 | 480 | 510 |
| Cl | n.d. | n.d. | 180 | n.d. | n.d. | 470 | 250 | n.d. | n.d. | n.d. |
| S | 4500 | 170 | 5200 | n.d. | 840 | 4600 | 6350 | n.d. | n.d. | 2350 |
| Bi | n.d. | n.d. | n.d. | n.d. | n.d. | n.d. | n.d. | n.d. | n.d. | n.d. |
| Cr | 80 | 40 | 150 | 210 | 240 | 180 | 100 | 110 | 110 | 90 |
| Cu | n.d. | n.d. | n.d. | n.d. | 60 | 70 | 40 | n.d. | n.d. | n.d. |
| Ni | n.d. | n.d. | n.d. | n.d. | n.d. | n.d. | n.d. | n.d. | n.d. | n.d. |
| Pb | 30 | 20 | 60 | n.d. | n.d. | n.d. | 20 | n.d. | n.d. | 20 |
| Rb | 40 | 40 | 30 | 30 | n.d. | n.d. | 30 | 30 | 30 | 30 |
| Sn | n.d. | n.d. | 30 | 40 | 50 | n.d. | n.d. | n.d. | n.d. | n.d. |
| Sr | 70 | 60 | 440 | 430 | 250 | 230 | 150 | 170 | 130 | 150 |
| V | n.d. | 40 | n.d. | 160 | 420 | 370 | 90 | 50 | 130 | 100 |
| W | n.d. | n.d. | n.d. | n.d. | n.d. | n.d. | n.d. | n.d. | n.d. | n.d. |
| Zn | 40 | n.d. | 70 | 50 | 100 | 180 | 100 | 30 | 20 | 60 |
| Zr | 50 | 70 | 260 | 280 | 70 | 70 | 130 | 80 | 110 | 110 |

Excluded elements (all values <LOD): Ag, Au, As, Cd, Co, Mo, Nb, Pd, Sb, Se
First letter in the ID indicates the outcrop. l= poor quality surface, p= good quality surface.

# APPENDIX VII: Geochemical data of the temporally related amphibolite units

Appendix VII. Data from GTK bedrock geochemical database of Finland. Data obtained with WD-XRF with pressed powder pellets and ICP-MS (Rasilainen et al. 2007).

| **WD-XRF** | | | | | | | |
|---|---|---|---|---|---|---|---|
| Point ID | 1 | 2 | 3 | 4 | 5 | 6 | 7 |
| X coordinate | 6670600 | 6667290 | 6679410 | 6678790 | 6684450 | 6721620 | 6701070 |
| Y coordinate | 3338950 | 3353710 | 3367860 | 3375200 | 3386690 | 3415650 | 3435860 |
| Location | Inkoo | Kirkkonummi | Espoo | Espoo | Helsinki | Sääksjärvi | Porvoo |
| Rocktype | Amp. | Amp. | Amp. | Amp. | M. volc. | Amp. | M. volc. |
| $SiO_2$ (wt.%) | 45.40 | 47.10 | 53.00 | 50.70 | 51.40 | 50.10 | 43.00 |
| $TiO_2$ | 2.70 | 0.64 | 0.62 | 2.38 | 0.96 | 1.77 | 2.44 |
| $Al_2O_3$ | 12.10 | 15.60 | 16.70 | 13.80 | 16.70 | 15.90 | 13.00 |
| FeOt | 15.93 | 7.77 | 7.76 | 13.32 | 9.90 | 8.73 | 11.25 |
| MnO | 0.26 | 0.16 | 0.16 | 0.24 | 0.19 | 0.15 | 0.17 |
| MgO | 5.24 | 8.57 | 4.36 | 3.41 | 3.96 | 4.24 | 5.53 |
| CaO | 8.22 | 11.60 | 8.09 | 7.16 | 6.62 | 7.69 | 11.40 |
| $Na_2O$ | 2.19 | 1.74 | 2.75 | 3.06 | 4.77 | 3.63 | 3.62 |
| $K_2O$ | 1.07 | 0.28 | 0.68 | 0.83 | 0.72 | 1.62 | 0.85 |
| $P_2O_5$ | 0.12 | 0.03 | 0.10 | 0.24 | 0.20 | 0.93 | 0.30 |
| Sum | 93.23 | 93.48 | 94.21 | 95.13 | 95.42 | 94.76 | 91.55 |
| Ba (ppm) | 163 | 61.8 | 213 | 179 | 392 | 596 | 459 |
| Cl | 741 | 141 | 261 | 483 | 80.1 | 505 | 146 |
| S | 220 | 737 | 114 | 591 | 78 | 2270 | 1500 |
| Cr | <19 | 491 | 47.1 | 27 | 24 | 27 | 96.1 |
| Cu | 30.1 | 72 | 17 | 33.9 | <17 | 129 | 188 |
| Ga | 22 | 19 | 23.2 | 23.7 | 29 | 29.8 | 31.4 |
| Nb | <7 | <7 | <7 | 7.6 | <7 | 22.5 | 45.9 |
| Ni | <14 | 103 | <14 | 15 | <14 | 38.4 | 122 |
| Pb | 16 | <14 | 22 | 23 | 27 | 16 | 15 |
| Rb | 66.1 | 14.6 | 15.3 | 20.7 | 33.1 | 141 | 29 |
| Sr | 121 | 153 | 272 | 149 | 224 | 1200 | 323 |
| V | 974 | 185 | 184 | 459 | 209 | 221 | 395 |
| Y | 30.6 | 9.1 | 16 | 46.7 | 17.4 | 20.3 | 21.3 |
| Zn | 175 | 77 | 92.3 | 135 | 131 | 141 | 121 |
| Zr | 84.8 | 21 | 70.5 | 194 | 115 | 186 | 195 |
| Mo excluded (all values <LOD) | | | | | | | |
| **ICP-MS** | | | | | | | |
| Ce (ppm) | 21.20 | 4.64 | 21.70 | 34.30 | 34.70 | 95.20 | 64.30 |
| Co | 48.8 | 42.4 | 26.2 | 33.4 | 29.9 | 32.7 | 51.4 |
| Dy | 4.93 | 2.01 | 2.81 | 7.39 | 3.94 | 4.40 | 4.88 |
| Er | 3.18 | 1.13 | 1.53 | 5.06 | 2.09 | 1.66 | 2.29 |
| Eu | 0.97 | 0.64 | 0.81 | 1.77 | 1.39 | 2.50 | 2.07 |
| Gd | 4.23 | 1.84 | 3.06 | 7.06 | 4.27 | 7.77 | 6.49 |
| Hf | 2.18 | 0.63 | 2.00 | 4.60 | 2.94 | 2.91 | 4.50 |
| Ho | 1.05 | 0.44 | 0.58 | 1.77 | 0.73 | 0.73 | 0.87 |
| La | 9.74 | 1.82 | 10.50 | 16.40 | 16.20 | 43.30 | 30.70 |
| Lu | 0.44 | 0.16 | 0.22 | 0.74 | 0.32 | 0.23 | 0.27 |
| Nb | 4.66 | 0.62 | 3.42 | 8.42 | 6.58 | 16.90 | 38.50 |
| Nd | 12.30 | 4.08 | 11.90 | 20.60 | 19.50 | 50.40 | 31.30 |
| Pr | 2.87 | <0.74 | 2.85 | 4.78 | 4.58 | 12.20 | 7.76 |
| Rb | 55.0 | 13.8 | 14.7 | 17.3 | 35.3 | 129.0 | 31.1 |
| Sc | 59.5 | 43.4 | 35.7 | 44.5 | 35.6 | 17.9 | 35.0 |
| Sm | 3.46 | 1.40 | 2.72 | 5.62 | 4.23 | 9.27 | 6.46 |
| Ta | 0.40 | 0.06 | 0.29 | 0.59 | 0.43 | 0.84 | 2.19 |
| Tb | 0.79 | 0.31 | 0.45 | 1.23 | 0.59 | 0.98 | 0.90 |
| Th | 1.34 | 0.24 | 2.37 | 2.01 | 3.04 | 3.69 | 3.44 |
| Tm | 0.48 | 0.21 | 0.26 | 0.74 | 0.32 | 0.25 | 0.32 |
| U | 1.06 | <0.08 | 0.74 | 0.84 | 1.56 | 1.87 | 0.69 |
| V | 911.0 | 177.0 | 177.0 | 413.0 | 193.0 | 195.0 | 354.0 |
| Y | 31.80 | 11.80 | 16.20 | 49.20 | 20.50 | 22.60 | 26.00 |
| Yb | 3.18 | 1.15 | 1.70 | 5.03 | 1.99 | 1.59 | 1.94 |
| Zr | 78.8 | 18 | 64.7 | 177 | 113 | 148 | 170 |

Amp.=amphibolite
M.volc.=mafic volcanite